NTMS New Trends in Medicine Sciences

Volume 1
Issue 1
June
2020

New Trends in Medicine Sciences

Peer-Reviewed Academic Journal

ISSN: 0000-0000
e-ISSN: 0000-0000
https://dergipark.org.tr/tr/pub/ntms

2020 June

New Trends In Medicine Sciences (NTMS) is an internationally recognized, referred, double-blind peer-reviewed, academic, electronic journal and published twice per year. It is aimed to contribute to scientific knowledge of medical sciences by publishing studies in the fields of basic, internal and surgical medical sciences.

E-ISSN:0000-0000

Journal Abbreviation: New Trend Med Sci

Web Page: https://dergipark.org.tr/tr/pub/ntms

Correspondence Adress: ntms.editor@gmail.com

New Trends in Medicine Sciences **Volume 1**

Issue 1

CONTENTS

ISSN:XXXX-XXXX RESEARCH ARTICLE

New Trend Med Sci 2020; 1(1): 1-5 https://dergipark.org.tr/tr/pub/ntms

Role of Hyperoside on Ovarian Tissue Damage Created by Ovarian Torsion Detorsion

Mustafa Can Güler[1], Ayhan Tanyeli[1*]

[1] Department of Physiology, Faculty of Medicine, Atatürk University, 25100, Erzurum, Turkey

Article History
Received 21 May 2020
Accepted 30 May 2020
Published Online 15 June 2020

[*]***Corresponding Author***
Dr Ayhan Tanyeli
Department of Physiology,
Faculty of Medicine,
Atatürk University,
Erzurum, 25240, Turkey,
Phone: +905073631654,
E-mail: ayhan.tanyeli@atauni.edu.tr
ORCID:http://orcid.org/0000-0002-0095-0917

Abstract: Here, hyperoside (HYP) was investigated against ovarian tissue injury induced by bilateral ovarian torsion detorsion (T/D) model. 18 Sprague Dawley female rats were grouped as sham, T/D and T/D+HYP. Sham group, abdominal incision was performed and repaired with no additional intervention. T/D group, T/D model was established. T/D+HYP group, HYP was administered by oral gavage prior to detorsion. Following detorsion, rats were sacrificed and the ovarian tissues were excised. Oxidant parameters elevated and antioxidant values declined in T/D group compared to sham group. HYP treatment decreased oxidant biomarkers and increased antioxidant mediators. After all, HYP prevented ovarian tissue injury generated by T/D model in rats. © 2020 NTMS.

Keywords: Hyperoside, Ovarian Torsion Detorsion, Ovary, Rat.

1. Introduction

Ovarian torsion (O/T) may reduce ovarian reserve through damaging ovarian tissue and therefore it is an gynecological emergency, especially during reproductive period (1). Several clinical conditions lead to O/T which diminishes or blocks ovarian blood flow and results in tissue injury (2). Detorsion leads to ischemia reperfusion (I/R) injury by enhancing reactive oxygen species (ROS) production which aggravates the ischemic injury (3). Early diagnosis has importance for the viability of ovaries and keeping fertility (4, 5).

Antioxidant molecules play role in overcoming the harmful effects of ROS (6). Malondialdehyde (MDA) indicates tissue injury and it is generated as a result of lipid peroxidation. It ruins enzymatic activity and permeability of cell membrane (7).

Total oxidant status (TOS) is a significant parameter on evaluating oxidative damage (8). Total antioxidant status (TAS) reflects whole antioxidant activity.

Therefore, ratio between TOS and TAS determines oxidative balance (9). Different agents have been examined to alleviate or eliminate I/R-induced oxidative injuries in various organs (10-14).

But the role of hyperoside (HYP) against ovarian torsion detorsion (T/D) injury has not been investigated yet. HYP is a flavonoid (15) performs against oxidative stress through its anti-ischemic, anti-inflammatory and antiapoptotic activities (16-18). HYP prevented I/R-induced myocardial injury (19). HYP protected against oxidative damage in lung cells induced by H_2O_2 (20). HYP also performed protection against I/R-induced liver damage (18).

Here, it was aimed to determine potential beneficial effects of HYP against oxidative damage induced by ovarian T/D.

2. Material and Methods

2.1. Experimental Animals and Ethical Approval

This study was carried out with the permission (Protocol number: 07.11.2019-207) of Atatürk University Experimental Animals Local Ethics Committee. The animals were supplied by Atatürk University Experimental Animal Research and Application Center and here was also preferred for the experimental steps. Animals were held in regular cages via appropriate laboratory conditions.

Cite this article as: Güler MC and Tanyeli A. Role of Hyperoside on Ovarian Tissue Damage Created by Ovarian Torsion Detorsion, *New Trend Med Sci* **2020**;1 (1): 1-5.

They were fed with standard pellet feed and water but fasted 12 hours prior to experiment to avoid anesthesia related complications.

2.2. Groups and Torsion Detorsion Model

Rats were immobilized in supine position. Abdominal regions were barbered, cleaned and anesthesia was administered prior to surgical procedure. Povidone-iodine was used for the disinfection step. 60 mg/kg intraperitoneal (i.p.) ketamine (Ketalar®, Pfizer, İstanbul) and 10 mg/kg i.p. xylazine hydrochloride (Rompun®, Bayer, İstanbul) were applied as anesthesia to animals. HYP was obtained from Sigma Aldrich Co. 18 Sprague Dawley female experimental rats were randomized as: Sham group: 1-2 cm incision, a median laparotomy, was performed on abdominal area and then it was repaired. T/D group: Following the incision, as described in sham group, torsion was established by rotating ovaries and related structures in clockwise 360 degrees and they were fixed by microvascular clamps. Following 3 hours, clamps were removed providing blood flow for 3 hours in detorsion phase. Incisions were repaired by silk 3/0 suture. T/D+HYP group: All procedures of T/D group were carried out and 20 mg/kg HYP was given to the rats as i.p. prior to detorsion. After the experiment, rats were sacrificed. Ovarian tissues were excised and held at -80ºC until the biochemical analysis.

2.3. Biochemical Analysis of Ovarian Tissues

Firstly, all ovarian tissue samples were homogenized and then all biochemical analyses were performed. Interleukin-1 beta (IL-1β) and tumor necrosis factor-alpha (TNF-α) were gauged through appropriate kits (Elabscience, Wuhan, China).

MDA level was gauged through a previous described method (21). Superoxide dismutase (SOD) activity was determined via protocol presented by Sun et al (22). Myeloperoxidase (MPO) activity was demonstrated using a foreknown method (23). TAS and TOS values were determined by commercial kits (Rel Assay Diagnostics).

Oxidative Stress Index (OSI) was measured as: OSI=[(TOS, μmol H_2O_2 equivalent/L)/(TAS, mmol Trolox equivalent/L)×10].

2.4. Statistical Analyses

SPSS package program was preferred for the evaluation of the results. One-way ANOVA test was used for data and Tukey test was used for the results that with no distribution. All results were demonstrated as Mean±Standard Deviation (SD) and p value was accepted significant when $p<0.05$ level.

3. Results

Table 1, 2 and figure 1 represent the biochemical results of ovarian tissue samples. MPO activity, TOS, OSI, TNF-α, MDA and IL-1β levels elevated significantly while TAS value and SOD activity diminished in T/D group when it is compared to sham group. HYP treatment decreased oxidant values, pro-inflammatory cytokine levels and increased antioxidant parameters.

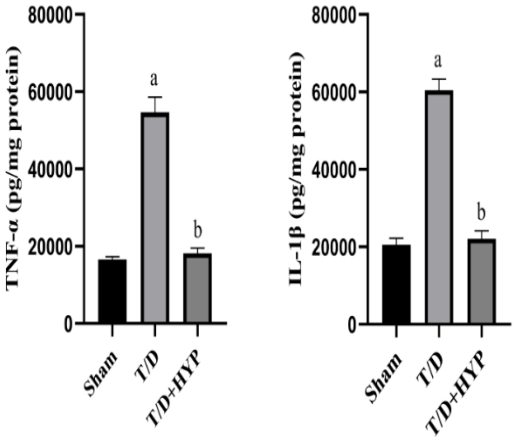

Figure 1: Comparisons of IL-1β and TNF-α levels among sham, T/D and T/D+HYP groups. [a]$p<0.001$ compared to sham group. [b]$p<0.001$ compared to T/D group.

Table 1: Comparisons of Total Antioxidant Status (TAS), Total Oxidant Status (TOS) and Oxidative Stress Index (OSI) levels among sham, T/D and T/D+HYP groups.

Experimental Groups (n=6)	**TAS (mmol/L)**	**TOS (μmol/L)**	**OSI (arbitrary unit)**
Sham	0,73 ± 0,04	5,87 ± 0,81	0,80 ± 0,14
T/D	0,25 ± 0,03[a]	12,17 ± 1,35[a]	4,88 ± 0,68[a]
T/D+HYP	0,72 ± 0,02[b]	6,42 ± 0,77[b]	0,88 ± 0,08[b]

[a]$p<0.001$ compared to sham group. [b]$p<0.001$ compared to T/D group.

Table 2: Comparisons of Superoxide dismutase (SOD), Myeloperoxidase (MPO) activities, and Malondialdehyde (MDA) levels among sham, T/D and T/D+HYP groups.

Experimental Groups (n=6)	**SOD (U/mg protein)**	**MPO (U/g protein)**	**MDA (µmol/g tissue)**
Sham	428,36 ± 29,92	235159,09 ± 20761,28	53,68 ± 4,43
T/D	148,61 ± 7,80[a]	736561,96 ± 55587,92[a]	136,17 ± 12,36[a]
T/D+HYP	408,87 ± 26,12[b]	269082,17 ± 35651,37[b]	66,57 ± 4,30[b]

[a]$p<0.001$ compared to sham group. [b]$p<0.001$ compared to T/D group.

4. Discussion

O/T describes the spinning of ovaries and related structures. During O/T, blood flow is interrupted, ischemia and even necrosis occur in tissues (24). Reperfusion leads to ovarian tissue damage even more than ischemia (25, 26). O/T treatment mainly depends on the protection of ovaries after detorsion (2). Therefore, proactive measures are carried out against tissue injury (27).

I/R injury pathogenesis includes various factors including ROS formation, cytokine release and inflammation (28). It has been proven that oxidative stress causes tissue damage in various animal models (29-32). Various factors including MPO, TOS, TAS and MDA play role in oxidative stress determination. MDA is commonly used to indicate oxidative stress during I/R injury (33-35). Neutrophil infiltration is a part of I/R injury and MPO reflects the neutrophil activity (36). I/R enhances MPO activity in ovarian tissues (37). Neutrophil activation and release of pro-inflammatory cytokines such as TNF-α, IL-1β are enhanced during I/R (38). Exposing to I/R results in increase in TNF-α, IL-1β levels (39, 40). ROS plays role in I/R-related tissue injury (41).

TOS, OSI and TAS values act as oxidative stress indicators and have been used for this purpose in various studies (42, 43). TAS and TOS demonstrate oxidant and antioxidant equilibrium. TAS is an indicator for all antioxidant activity while TOS is limited with ROS (44, 45). SOD catalyzes superoxide free radical conversion into molecular oxygen and superoxide free radical. SOD protects tissues through neutralizing free radicals (46).

HYP prevented H_2O_2-related apoptosis and oxidative stress in granulosa cells by diminishing MDA levels and supporting SOD activity (47). HYP inhibited free radical formation in a previous study (48). Piao et al showed that HYP decreased ROS production besides enhancing antioxidant activity (20). Different agents which performe feature anti-inflammatory, antioxidant and radical scavenging effects have been examined against various I/R injuries (49). In this study, oxidative stress created in ovarian tissues through ovarian T/D model and the potential beneficial properties of HYP were examined against tissue injury. HYP administration was successful on reducing oxidative damage in ovarian tissues caused by ovarian T/D model.

5. Conclusions

HYP is an effective agent against ovarian tissue injury caused by ovarian T/D model via its antioxidant and anti-inflammatory effects. It reduced ovarian tissue injury and became a candidate for therapies against ovarian T/D induced tissue injury.

Conflict of interest statement
None
Financial Support
None

References

1. Bayer AI, Wiskind AK. Adnexal torsion: can the adnexa be saved? *Am J Obstet Gynecol* **1994**; 171(6): 1506-10; 10-11.
2. Oelsner G, Shashar D. Adnexal torsion. *Clin Obstet Gynecol* **2006**; 49(3): 459-463.
3. Erkanli Senturk G, Erkanli K, et al. The protective effect of oxytocin on ischemia/reperfusion injury in rat urinary bladder. *Peptides* **2013**; 40: 82-88.
4. Rey-Bellet Gasser C, Gehri M, Joseph JM, Pauchard JY. Is It Ovarian Torsion? A Systematic Literature Review and Evaluation of Prediction Signs. *Pediatr Emerg Care* **2016**; 32(4): 256-261.
5. Smolinski SE, Kreychman A, Catanzano T. Ovarian Torsion: Multimodality Review of Imaging Characteristics. *J Comput Assist Tomogr* **2015**; 39(6): 922-924.
6. Kalogeris T, Bao Y, Korthuis RJ. Mitochondrial reactive oxygen species: a double edged sword in ischemia/reperfusion vs preconditioning. *Redox Biol* **2014**; 2: 702-714.
7. Rodrigo R, Libuy M, Feliú F, Hasson D. Oxidative stress-related biomarkers in essential hypertension and ischemia-reperfusion myocardial damage. *Dis Markers* **2013**; 35(6): 773-790.
8. Aycicek A, Ipek A. Maternal active or passive smoking causes oxidative stress in cord blood. *Eur J Pedatr* **2008**; 167(1): 81-85.
9. Akcilar R, Akcilar A, Savran B, et al. Effects of ukrain in rats with intestinal ischemia and reperfusion. *J Surg Res* **2015**; 195(1): 67-73.
10. Eraslan E, Tanyeli A, Polat E, Polat E. 8-Br-cADPR, a TRPM2 ion channel antagonist, inhibits renal ischemia-reperfusion injury. *J Cell Physiol* **2019**; 234(4): 4572-4581.
11. Eraslan E, Tanyeli A, Polat E, Yetim Z. Evodiamine alleviates kidney ischemia reperfusion injury in

rats: A biochemical and histopathological study. *J Cell Biochem* **2019**; 120(10): 17159-17166.
12. Ozturk D, Erdogan DG, Tanyeli A, Çomaklı S, Baylan H, Polat E. The protective effects of urapidil on lung tissue after intestinal ischemia-reperfusion injury. *Turk J Biochem* **2019**; 44(4): 539.
13. Tanyeli A, Guler M, Eraslan E, et al. Barbaloin attenuates ischemia reperfusion-induced oxidative renal injury via antioxidant and anti-inflammatory effects. *Med Sci* **2020**; 9(1): 246-250.
14. Dogan C, Halici Z, Topcu A, et al. Effects of amlodipine on ischaemia/reperfusion injury in the rat testis. *Andrologia* **2016**; 48(4): 441-452.
15. Zou YP, Lu YH, Wei DZ. Antioxidant activity of a flavonoid-rich extract of Hypericum perforatum L. in vitro. *J Agr Food Chem* **2004**; 52(16): 5032-5039.
16. Conforti F, Statti GA, Tundis R, Menichini F, Houghton P. Antioxidant activity of methanolic extract of Hypericum triquetrifolium Turra aerial part. *Fitoterapia* **2002**; 73(6): 479-483.
17. Schettler V, Methe H, Staschinsky D, Schuff-Werner P, Muller GA, Wieland E. Review: the oxidant/antioxidant balance during regular low density lipoprotein apheresis. *Ther Apher* **1999**; 3(3): 219-26.
18. Shi YP, Qiu XX, Dai MJ, Zhang XB, Jin GX. Hyperoside Attenuates Hepatic Ischemia-Reperfusion Injury by Suppressing Oxidative Stress and Inhibiting Apoptosis in Rats. *Transpl P* **2019**; 51(6): 2051-2059.
19. Xiao R, Xiang AL, Pang HB, Liu KQ. Hyperoside protects against hypoxia/reoxygenation induced injury in cardiomyocytes by suppressing the Bnip3 expression. *Gene* **2017**; 629: 86-91.
20. Piao MJ, Kang KA, Zhang R, et al. Hyperoside prevents oxidative damage induced by hydrogen peroxide in lung fibroblast cells via an antioxidant effect. *Bba-Gen Subjects* **2008**; 1780(12): 1448-1457.
21. Ohkawa H, Ohishi N, Yagi K. Assay for Lipid Peroxides in Animal-Tissues by Thiobarbituric Acid Reaction. *Anal Biochem* **1979**; 95(2): 351-358.
22. Sun Y, Oberley LW, Li Y. A Simple Method for Clinical Assay of Superoxide-Dismutase. *Clin Chem* **1988**; 34(3): 497-500.
23. Bradley PP, Priebat DA, Christensen RD, Rothstein G. Measurement of cutaneous inflammation: estimation of neutrophil content with an enzyme marker. *J Invest Dermatol* **1982**; 78(3): 206-209.
24. Hibbard LT. Adnexal torsion. *Am J Obstet Gynecol* **1985**; 152(4): 456-61.
25. Sak ME, Soydinc HE, Sak S, et al. The protective effect of curcumin on ischemia-reperfusion injury in rat ovary. *Int J Surg* **2013**; 11(9): 967-970.
26. Ozkisacik S, Yazici M, Gursoy H, Culhaci N. Does gradual detorsion protect the ovary against ischemia-reperfusion injury in rats? *Pediatr Surg Int* **2014**; 30(4): 437-440.
27. Ozler A, Turgut A, Soydinç HE, et al. The biochemical and histologic effects of adnexal torsion and early surgical intervention to unwind detorsion on ovarian reserve: an experimental study. *Reprod Sci* **2013**; 20(11): 1349-1355.
28. Yaman Tunc S, Agacayak E, Goruk NY, et al. Protective effects of honokiol on ischemia/reperfusion injury of rat ovary: an experimental study. *Drug Des Devel Ther* **2016**; 10: 1077-1083.
29. Tanyeli A, Güzel G. Investigation into the Biochemical Effects of Barbaloin on Renal Tissue in Cecal Ligation and Puncture-Induced Polymicrobial Sepsis Model in Rats. S*out Clin Istanb Eurasia* **2019**; 30: 285-289.
30. Tanyeli A, Güzel D. Alliin mitigates Cecal Ligation Puncture (CLP)-induced lung injury through antioxidant and antiinflammatory effects. *Turk J Sci* **2019**; 4(2): 46-59.
31. Ekinci Akdemir FN, Tanyeli A. The Antioxidant Effect of Fraxin against Acute Organ Damage in Polymicrobial Sepsis Model induced by Cecal Ligation and Puncture. *Turk J Sci* **2019**; 4(1): 22-29.
32. Tanyeli A, Eraslan E, Guler MC, Ozbek Sebin S, Demet Celebi D, Ozgeris FB, Toktay E. Investigation of biochemical and histopathological effects of tarantula cubensis D6 on lung tissue in cecal ligation and puncture-induced polymicrobial sepsis model in rats. *Med Sci* **2019**; 8(3): 644-650.
33. Ergenoglu M, Erbaş O, Akdemir A, et al. Attenuation of ischemia/reperfusion-induced ovarian damage in rats: does edaravone offer protection? *Eur Surg Res* **2013**; 51(1-2): 21-32.
34. Yildirim N, Yigitturk G, Sahingoz Yildirim AG, et al. Octreotide protects ovary against ischemia-reperfusion injury in rats: Evaluation of histological and biochemical parameters. *J Obstet Gynaecol Res* **2015**; 41(10): 1591-1597.
35. Akdemir A, Erbas O, Gode F, et al. Protective effect of oxytocin on ovarian ischemia-reperfusion injury in rats. *Peptides* **2014**; 55: 126-130.
36. Zhang Y, Zhu J, Guo L, et al. Cholecystokinin protects mouse liver against ischemia and reperfusion injury. *Int Immunopharmacol* **2017**; 48: 180-186.
37. Meister A. Glutathione deficiency produced by inhibition of its synthesis, and its reversal; applications in research and therapy. *Pharmacol Therapeut* 1991; 51(2): 155-194.
38. Raup-Konsavage WM, Gao T, Cooper TK, Morris SM, Jr, Reeves WB, Awad AS. Arginase-2 mediates renal ischemia-reperfusion injury. *Am J physiol Renal* **2017**; 313(2): 522-534.
39. Sengul O, Ferah I, Polat B, et al. Blockade of endothelin receptors with bosentan limits ischaemia/reperfusion-induced injury in rat ovaries. *Eur J Obstet Gynecol Reprod Biol* **2013**; 170(2): 458-463.

40. Lutz J, Thürmel K, Heemann U. Anti-inflammatory treatment strategies for ischemia/reperfusion injury in transplantation. *J Inflamm (Lond)* **2010**; 7:27.
41. Murphy E, Steenbergen C. Mechanisms underlying acute protection from cardiac ischemia-reperfusion injury. *Physiol Rev* **2008**; 88(2): 581-609.
42. Kumas M, Altintas O, Karatas E, Kocyigit A. Protective Effect of Ischemic Preconditioning on Myocardium Against Remote Tissue Injury Following Transient Focal Cerebral Ischemia in Diabetic Rats. *Arq Bras Cardiol* **2017**; 109(6): 516-526.
43. Soylu Karapinar O, Pinar N, Özcan O, Özgür T, Dolapçıoğlu K. Protective effect of alpha-lipoic acid in methotrexate-induced ovarian oxidative injury and decreased ovarian reserve in rats. *Gynecol Endocrinol* **2017**; 33(8): 653-659.
44. Rabus M, Demirbag R, Sezen Y, et al. Plasma and tissue oxidative stress index in patients with rheumatic and degenerative heart valve disease. *Turk Cardiol Assoc* **2008**; 36(8): 536-540.
45. Erel O. A new automated colorimetric method for measuring total oxidant status. *Clin Biochem* **2005**; 38(12): 1103-1111.
46. Arosio B, Gagliano N, Fusaro LM, et al. Aloe-Emodin quinone pretreatment reduces acute liver injury induced by carbon tetrachloride. *Pharmacol Toxicol* **2000**; 87(5): 229-233.
47. Wang XX, Fan GM, Wei FM, Bu Y, Huang WH. Hyperoside protects rat ovarian granulosa cells against hydrogen peroxide-induced injury by sonic hedgehog signaling pathway. *Chem-Biol Interact* **2019**; 310.
48. Liu ZY, Tao XY, Zhang CW, Lu YH, Wei DZ. Protective effects of hyperoside (quercetin-3-o-galactoside) to PC12 cells against cytotoxicity induced by hydrogen peroxide and tert-butyl hydroperoxide. *Biomed Pharmacother* **2005**; 59(9): 481-490.
49. Tanyeli A, Ekinci Akdemir FN, Eraslan E, Guler MC, Sebin S, Gülçin I. Role of p-Coumaric acid in Alleviating of the Intestinal Ischemia/Reperfusion Injury. *Kocaeli Med J* **2020**; 9: 166-173.
50. Topdagi O, Tanyeli A, Ekinci Akdemir FN, Eraslan E, Guler MC, Comakli S. Preventive effects of fraxin on ischemia/reperfusion-induced acute kidney injury in rats. *Life Sci* **2020**; 242: 117217.
51. Guzel D and Tanyeli A. Investigation of Chlorogenic Acid (Cga) as An Antioxidant in Renal Ischemia-Reperfusion Injury: An Experimental Study. *Sakarya Med J* **2018**; 8(2): 410-415.
52. Güzel D and Tanyeli A. Investigation of Oxidative Damage of Lung Tissue in Experimental Renal Ischemia Reperfusion Model and The Protective Effects of Chlorogenic Acid (CGA). *Sakarya Med J* **2018**; 8(2): 260-265.
53. Topdağı Ö, Tanyeli A, Ekinci Akdemir FN, Güzel Erdoğan D, Güler MC, Eraslan E. Higenamine decreases testicular damage injured by ischemia reperfusion: A biochemical study. *Turk J Sci* **2019**; 4(2): 92-99.

Authors' ORCID
Mustafa Can Güler
http://orcid.org/0000-0001-8588-1035
Ayhan Tanyeli
http://orcid.org/0000-0002-0095-0917

https://dergipark.org.tr/tr/pub/ntms

ISSN:XXXX-XXXX RESEARCH ARTICLE

New Trend Med Sci 2020; 1(1): 6-13 https://dergipark.org.tr/tr/pub/ntms

Diffusion Tensor Imaging of Metastatic Axillary Lymph Nodes

Irmak Durur-Subasi[1,2,3*], Fatih Alper[3], Pınar Tuncel-Eyi[2], Adem Karaman[3], Veysel Esdur[3], Elif Demirci[4], Baki Hekimoğlu[2]

[1] Department of Radiology, Faculty of Medicine, İstanbul Medipol University, Istanbul, Turkey
[2] Clinic of Radiology, Diskapi Yildirim Beyazit Training and Research Hospital, University of Health Sciences, Ankara, Turkey
[3] Department of Radiology, Faculty of Medicine, Atatürk University Erzurum, Turkey
[4] Department of Pathology, Faculty of Medicine, Atatürk University, Erzurum, Turkey

Article History
Received 24 May 2020
Accepted 03 June 2020
Published Online 15 June 2020

[*]***Corresponding Author***
Irmak Durur-Subasi MD, PhD,
Istanbul Medipol University
Faculty of Medicine
Department of Radiology
Istanbul, Turkey
E-mail: irmakdurur@yahoo.com
Phone: +905334603846
Fax: +902124607070
ORCID: http://orcid.org/0000-0003-3122-4499

Abstract: It was aimed to investigate whether the fractional anisotropy (FA) differs for the benign and metastatic axillary lymph nodes (LNs). 58 women with benign (n=33) and metastatic (n=25) axillary LNs who underwent diffusion-weighted and tensor imaging with a 3T scanner were enrolled. Apparent diffusion coefficient (ADC) and FA, cortex thickness, long and short axes were measured retrospectively and compared statistically. Observer reliabilities were also assessed in terms of intra and inter-reviewer variability. Metastatic LNs showed significantly lower ADC and FA values and greater cortex thickness, long and short axes. ROC test showed the area under the curve values of 0.876 for ADC, 0.661 for FA, and 0.960 for cortex thickness. Cortex thickness had excellent sensitivity, specificity, and accuracy. A cutoff value of 3.5 mm for cortex thickness had 92% sensitivity, 94% specificity, 92% positive predictive value (PV), 93% negative PV, and 93% accuracy. A cutoff value of 0.774×10^{-3} mm^2/s for ADC had 84% sensitivity, 82% specificity, 79% positive PV, 90% negative PV, and 84% accuracy. A cutoff value of 0.423×10^{-3} mm^2/s for FA had 64% sensitivity, 76% specificity, 67% positive PV, 71% negative PV, and 71% accuracy. High intra- and inter-observer reliabilities were seen. Among the parameters assessed by our study, cortex thickness had superior accuracy. ADC and FA showed a respectable diagnostic performance, especially the first one having a high negative PV and the second one relatively high specificity. © 2020 NTMS.

Keywords: Axilla, Apparent Diffusion Coefficient, Diffusion Tensor Imaging, Fractional Anisotropy, Lymph Nodes, Magnetic Resonance Imaging.

1. Introduction

Diagnosing axillary lymph node (LN) involvement is important in breast carcinoma management because LN status changes treatment decisions (1,2). Although sentinel biopsy is generally done in invasive breast cancer, axilla dissection continues to be performed in patients with invasive, high-grade carcinomas (1,3).

Magnetic resonance imaging (MRI) with its superior latitudinal resolution and tissue categorization capacity has the uppermost sensitivity for the discovery of breast carcinoma (4,5).

On the other hand, its moderate specificity leads to the search for additional supportive tools.

Cite this article as: Durur-Subasi I, Alper F, Tuncer P, Karaman A, Esdur V, Demirci E, Hekimoğlu B. Diffusion tensor imaging of metastatic axillary lymph nodes. *New Trend Med Sci* **2020**;1 (1): 6-13.

Diffusion tensor and diffusion-weighted imaging (DTI and DWI) are two advanced MRI tools and are currently active research areas with this point of view (6-10).
Although many studies have been conducted on breast DWI, few studies have reported on DTI for breast and no DTI study for axilla (11-16). DTI applies extra gradients to identify the amount of diffusion and allows the evaluation of the extent of anisotropic diffusion in concerned tissue, referred to as the full diffusion tensor (11). Fractional anisotropy (FA) deals with the amount of anisotropy, while the apparent diffusion coefficient (ADC) is the directionally averaged diffusivity (17).
According to our knowledge, DTI has not been previously used to evaluate axillary LNs.
In this study, we studied the importance of the FA parameter for benign and metastatic axillary LNs.

2. Patients and Methods

The institutional ethics committee of our university hospital appropriated the retrospectively designed procedure, and informed-consent was surrendered (2301-13/1).

2.1. Patients

We reviewed our archives and identified 58 women with benign (n=33) and metastatic (n=25) axillary LNs between July 2013 and October 2015. Axillary LNs of patients with Breast Imaging-Reporting and Data System (BI-RADS) category 1-2 results on MRI, no suspicious findings on conventional imaging, no change in findings over 2 years, and histopathological evidence of benign breast pathology were involved in the benign group. Patients with breast carcinoma and pathologically proven ipsilateral metastatic LNs were included in the metastatic group. When several nodes were detected, the biggest one was measured.
Exclusion criteria were previous chemotherapy for breast carcinoma, incomplete examination, or un-diagnosable images (e.g. due to artifacts or distortions, or lack of coil cover).

2.2. Breast MRI

Breast MRI was acquired by a 3-Tesla scanner (Skyra; Siemens, Germany) and a dedicated coil with patients in the prone position. A standard protocol was used: coronal short time inversion recovery (STIR), sagittal fat-suppressed, turbo-spin echo T2-weighted imaging, turbo-spin echo T1-weighted imaging, single-shot echo-planar imaging (as DWI) and dynamic pre- and post-contrast fat-suppressed, fast low-angle shot (FLASH) three-dimensional images were acquired.

2.3. DWI and DTI

DWI and DTI were acquired with the following parameters: TR=4000-ms, TE=60-ms, slice thickness=4.0-mm, FOV=380-mm, averages=4, interslice gap=0 and scan time=3.37-min. Diffusion gradients were applied in 6 directions with b=50, 400, and 800 s/mm^2 in all cases.

2.4. Interpretations

Breast MRI, DWI, and DTI data were post-processed on the MRI console using the Neuro3D toolbox (Leonardo, Siemens Healthcare, Erlangen, Germany). The cortex thickness, greatest long and short axes of the LNs was measured on the post-contrast T1-weighted image. The DWI and DTI parameters were calculated by tracing a free-hand region of interest (ROI) on the cortex of the LNs on ADC and FA map by a simultaneous display with T1-WI. The two-dimensional ROI was cautiously positioned on the LN to include the cortex and exclude the necrotic and cystic components, axillary fat, or hilum. The ROI size was variable depending on the anatomy and size of the LN. ROI calculations were done by a radiologist with 15-year-experienced (AK) who was blinded to the patients' history and histological results at least three times. Intraobserver consistency was evaluated by the same radiologist at a time interval of two weeks, and the same information was used with a second radiologist with 5 years of experience (VE) to assess inter-observer reliability.

2.5. Statistics

The statistics were done by IBM SPSS Statistics for Windows, Version 21.0. Distribution normality was determined by the Shapiro-Wilk test. The cortex thickness, long and short axes, ADCs, and FAs were compared by independent samples *t*-test between the benign and metastatic lesions. Receiver operating characteristic (ROC) curve analysis was performed to define the cutoff points and diagnostic performances. Intraobserver agreement was calculated by the Pearson correlation coefficient and interobserver agreement by Kendall's coefficient of concordance (the mean value of the first observer compared with the second observer's measurement). All tests were two-tailed and a p-value under 0.05 was accepted as a statistical significance level.

3. Results

A total of 33 female (mean age=41±7 (32-50) years) were enrolled in the benign group and 25 female patients (mean age=50±13 (26-80) years) with pathologically proven metastatic axillary involvement comprised the metastatic group (Figures 1, 2).
For the benign group, the mean long axis was 16±5-mm (between 9-31-mm) and the mean short axis was 9±3-mm (between 5-17-mm). For the metastatic group, the mean long axis was 26±21-mm (between 10-95-mm) and the mean short axis was 22±17-mm (between 8-78-mm).
Statistical analyses showed significant changes in ADC (P=0.00), and FA values (P=0.04) cortex thickness (P<0.00), long (P=0.00) and short axes (P=0.00), (Table 1). The metastatic group had a significantly greater size and cortex thickness, lower ADC and FA values (Figures 3, 4).
ROC analysis showed the area under the curve value of 0.876 for ADC and 0.661 for FA values, 0.960 for

cortex thickness, 0.687 for long axis, 0.848 for short axis (Figures 5, 6; Table 2). A cutoff value of 3.5 mm for cortex thickness had 92% sensitivity, 94% specificity, 92% positive predictive value (PV), 93% negative PV and 93% accuracy. A cutoff value of $0.774x10^{-3}$ mm^2/s for ADC had 84% sensitivity, 82% specificity, 79% positive PV, 90% negative PV and 84% accuracy. A cutoff value of 0.423 $x10^{-3}$ mm^2/s for FA had 64% sensitivity, 76% specificity, 67% positive PV, 71% negative and 71% accuracy (Figure 7).

High intra- and inter-observer agreements were seen for ADC (R=0.917, P=0.00 and R=0.761, P=0.00) and FA values (R=0.876, P=0.00 and R=0.700, P=0.00), cortex thickness (R=0.910, P=0.00 and R=0.850, P=0.00), for long axis (R=0.956, P=0.00 and R=0.887, P=0.00), short axis (R=0.970, P=0.00 and R=0.910, P=0.00).

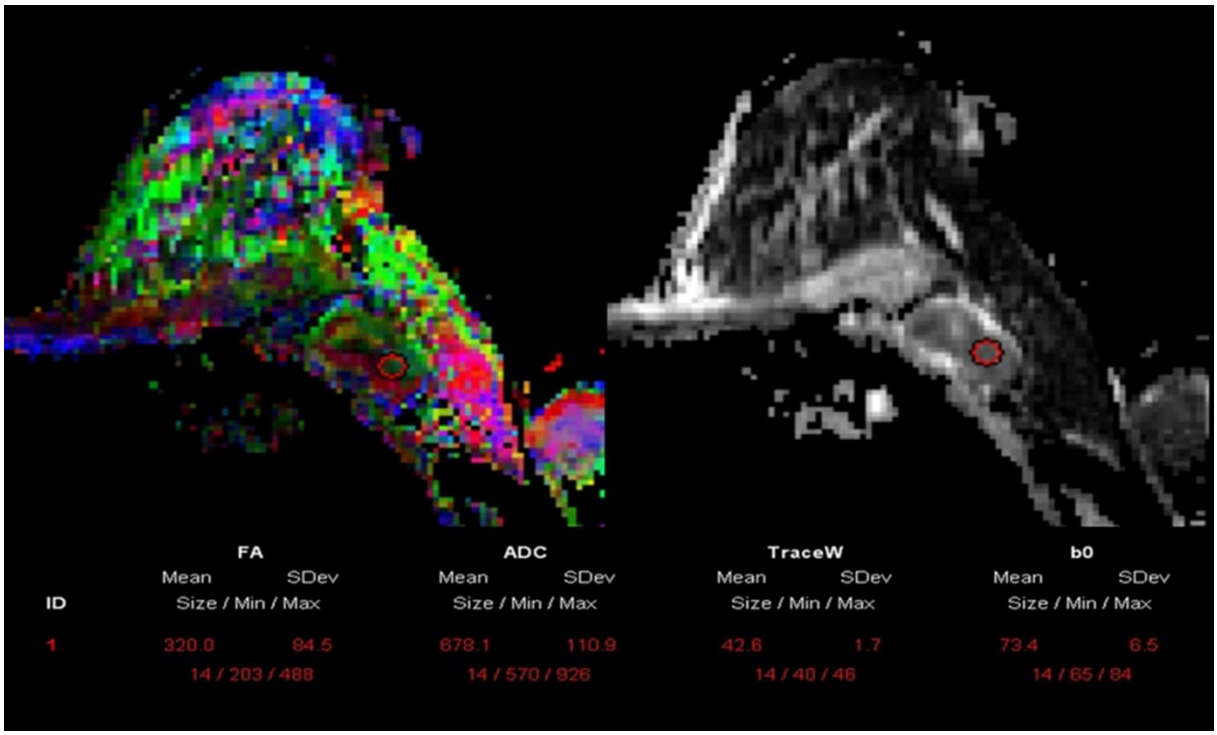

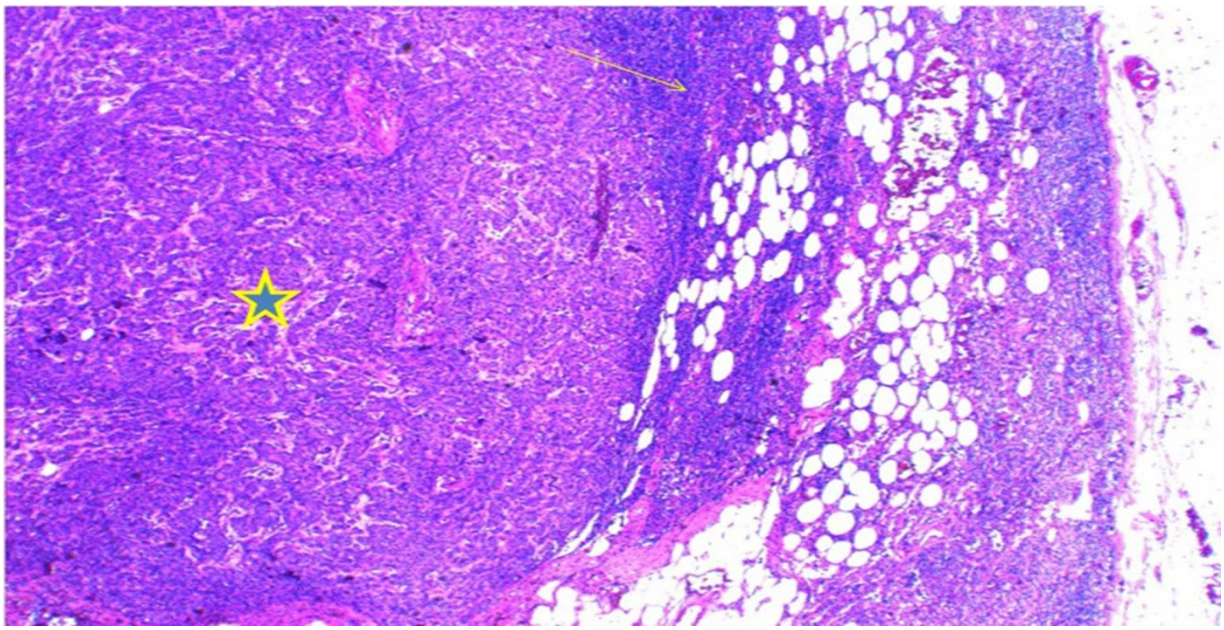

Figure 1: A case of metastatic axillary involvement on the left. Thickened cortex, round configuration and hilar obliteration can be seen (a). Pathology specimen shows lymphoid tissue (arrow) and metastasis (star) (b).

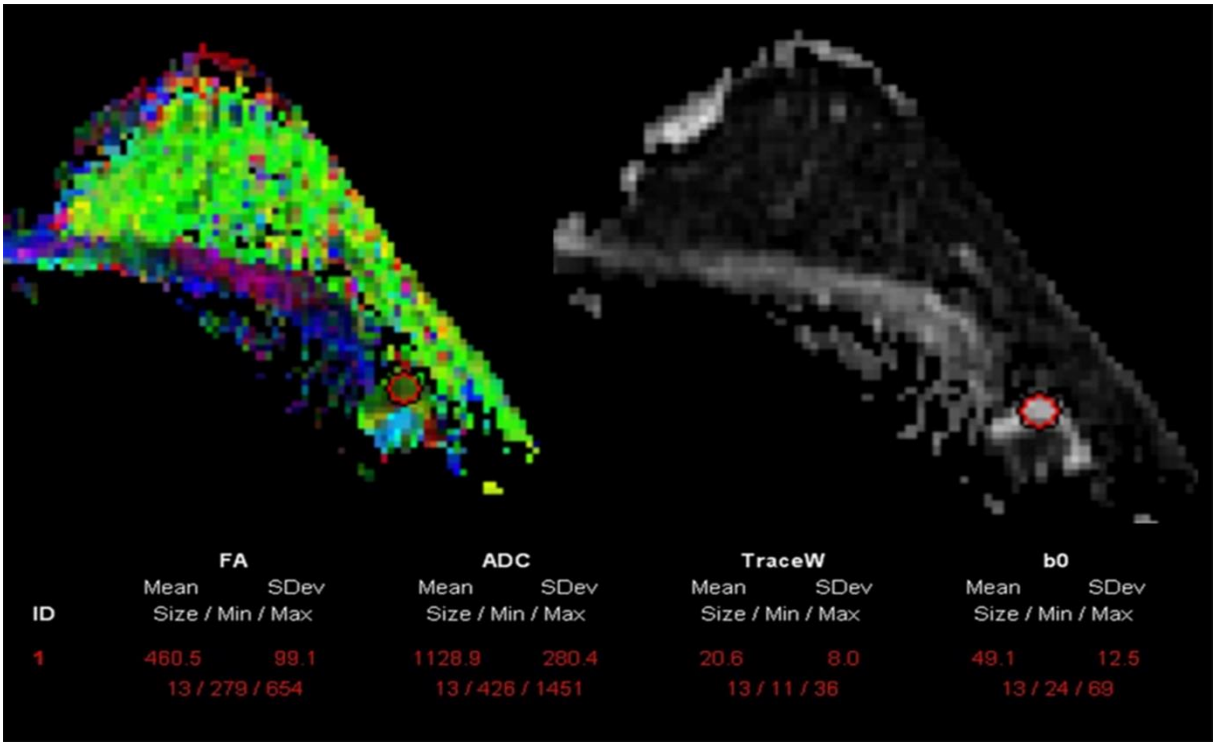

Figure 2: A benign lymph node with a thin cortex is visible in the left axilla.

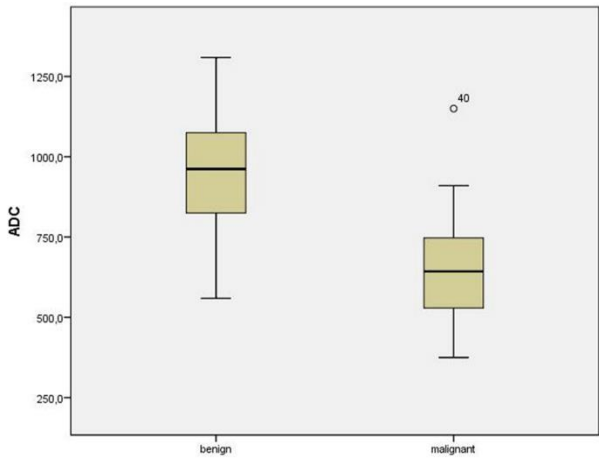

Figure 3: Box plot shows ADC values of benign and metastatic lymph nodes. Boxes symbolize interquartile range divided at the median; whiskers show range of all values. Circles and diamonds represent outliers. Metastatic nodes show lower ADC values.

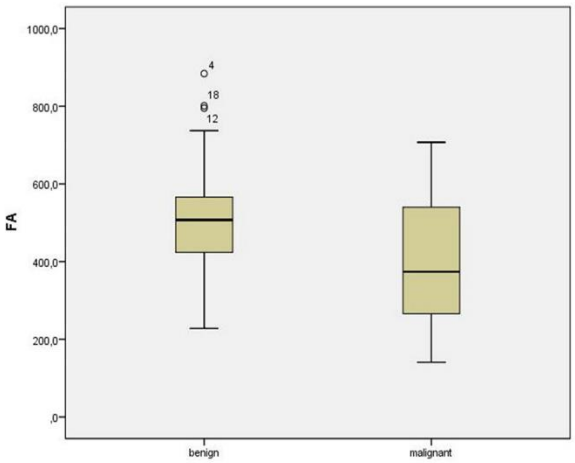

Figure 4: Box plot shows FA values of benign and metastatic lymph nodes. Boxes symbolize interquartile range divided at the median; whiskers show range of all values. Circles and diamonds represent outliers. Metastatic nodes show lower FA values.

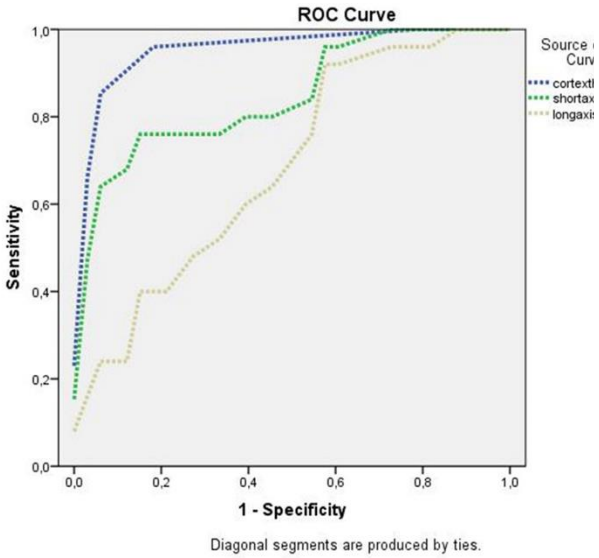

Figure 5: In receiver operating characteristic (ROC) curve analysis, cortex thickness has the highest area under the curve (AUC) value.

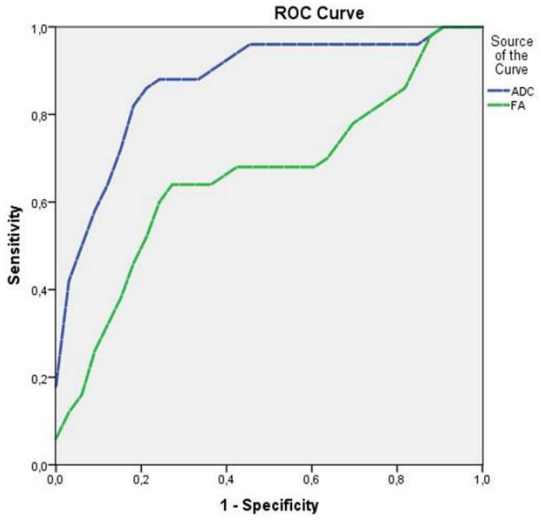

Figure 6: Receiver operating characteristic (ROC) curve analysis shows a high area under the curve (AUC) value of ADC.

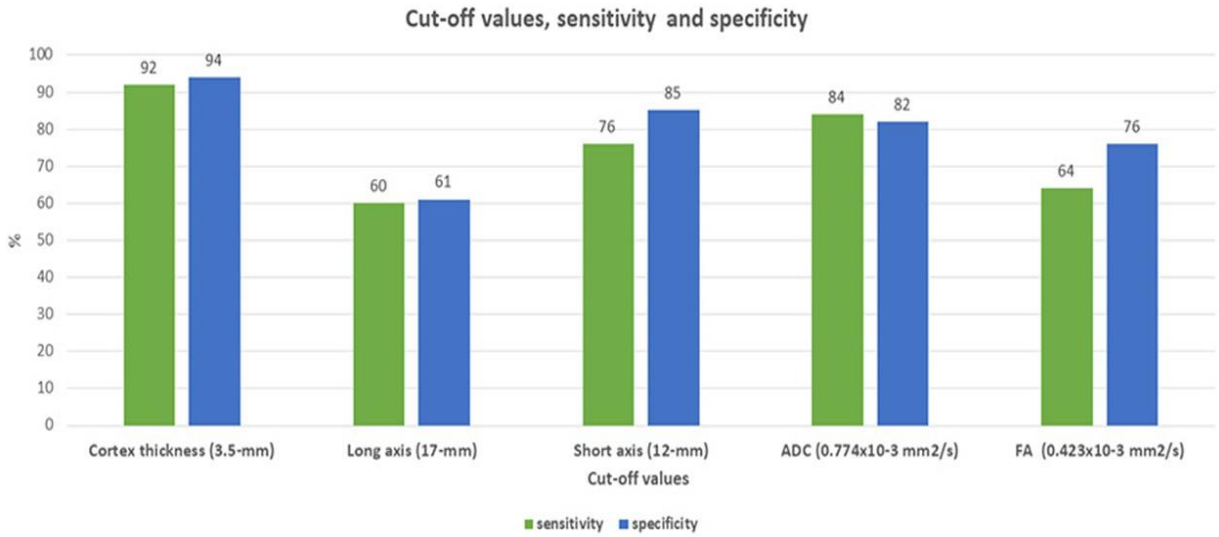

Figure 7: Graphic shows cutoff values obtained by ROC analysis and sensitivity and specificity combinations.

4. Discussion

In this study, we evaluated ADC and FA values, cortex thickness, short-long axes of benign and metastatic axillary LNs. Metastatic LNs showed significantly greater cortex thickness and short-long axes, lower ADC and FA values. Cortex thickness had an excellent diagnostic performance. ADC value had a relatively good diagnostic performance with especially a high negative PV of 90%. FA had a moderate diagnostic performance with remarkable specificity.

Staging axilla by LN dissection is highly accurate. However, due to morbidities such as lymphedema and paresthesia following this procedure, the development of non-invasive, image-based methods for detecting axillary LN metastasis is an active research area. There is no characteristic finding on dynamic MRI with high specificity for the distinction between benign and metastatic LNs (18).

Although several studies have suggested that DWI has some utility in axillary LN assessment (19), there is a paucity of data in the English literature concerning DTI parameters of axillary LNs.

ADC values obtained by DWI were reported as useful in discriminating benign and metastatic LNs by some authors, but not others (20-22). Rautiainen et al. imaged 56 axillae (121 LNs) and concluded that metastatic axillary LNs consumed significantly lower ADC values ($P<0.001$). According to their results, mean ADC as obtained by 3-T was $0.663\text{-}0.676 \times 10^{-3}$ mm^2/s for metastatic LNs and $1.100\text{-}1.225 \times 10^{-3}$ mm^2/s for benign ones (maximum *b* value of 800 s/mm^2) (21).

Yamaguchi et al. evaluated pathologically proven axillary LNs with and without metastasis and determined a mean ADC value of 0.746×10^{-3} mm^2/s for metastatic LNs and 1.033×10^{-3} mm^2/s for non-metastatic LNs (maximum *b* value of 800 s/mm^2) ($P<0.001$). They reported 85% sensitivity and 81% specificity by a cutoff ADC value of $0.852x10^{-3}$ mm^2/s to differentiate metastatic from non-metastatic LNs (23).

In contrast, Kamitani et al. studied axillary LNs with and without metastasis on a 1.5-T system and concluded that the ADC of metastatic nodes was considerably higher than that of benign LNs (1.08×10^{-3} mm^2/s vs. 0.92×10^{-3} mm^2/s, maximum *b* value of 1000 s/mm^2, $P=0.004$) (24). According to our results, benign LNs had higher mean ADC values than metastatic ones (0.965×10^{-3} mm^2/s vs. 0.669×10^{-3} mm^2/s) and the difference was statistically significant (maximum *b* value of 800 s/mm^2).

Additionally, ROC analysis showed that an ADC cutoff of $0.774x10^{-3}$ mm^2/s had high sensitivity and specificity. Especially negative PV was better.

DWI is reported to provide information about tissue microenvironments such as perfusion, flow effects, cell density, proliferation rate, nucleus size, intracellular macromolecules, nucleus/cytoplasm ratio and extracellular matrix volume (25-31). ADC values are considered to represent the cellular or extracellular elements of the tissue, while FA values are believed to reflect tissue organization (14). The lower FA values reported representing more organized tissues.

Table 1: Differences of size, diffusion tensor imaging (DTI) and diffusion-weighted imaging (DWI) parameters of axillary lymph nodes.

Variable(s)	Group	N	Mean	Standard Deviation	P values
Cortex thickness (mm)	Benign	33	2.2	1.3	0.00*
	Metastatic	25	10.8	9.1	
Long axis (mm)	Benign	33	16	5	0.00*
	Metastatic	25	26	21	
Short axis (mm)	Benign	33	9	3	0.00*
	Metastatic	25	22	17	
ADC value ($x10^{-3}$ mm^2/s)	Benign	33	0.965	0.186	0.00*
	Metastatic	25	0.669	0.183	
FA value ($x10^{-3}$ mm^2/s)	Benign	33	0.481	0.153	0.04*
	Metastatic	25	0.394	0.151	

Table 2: ROC analysis results, performance of benign-metastatic discrimination of variables.

Variable(s)	Area under curve	95% Confidence Interval	
		Lower Bound	Upper Bound
Cortex thickness	0.960	0.910	1,000
Long axis	0.687	0.551	0.822
Short axis	0.848	0.745	0.951
ADC	0.876	0.783	0.970
FA	0.661	0.514	0.808

DTI studies of breast imaging are limited in number. Partridge et al. reported in their study that anisotropy was reduced in metastatic tumors than the normal parenchyma, but FA did not allow significant discrimination (13). In another study, it is reported that the breast parenchyma showed mainly anterior-posterior diffusion, whereas breast lesions had no principal diffusion direction (14). The metastatic tumors displayed a lower ADC and higher FA and ADC was more distinctive. Cakir et al. studied ADC and FA in 30 malignant and 25 benign lesions as well as normal breast parenchyma. They reported that FA was not discriminative for benign and malignant lesions (11). Tagliafico et al. measured ADC and FA values of normal breast tissue at 3.0 T and concluded that ADC values obtained with DTI are more reproducible than FA (15). Jiang et al. studied DTI of breast lesions and concluded ADC and FA values are statistically different between benign and malignant lesions and associated with cellularity. To their results, ADC was useful to estimate the grade (32). Our study showed a better diagnostic performance of ADC than FA, and the

first one was considerably different for benign and metastatic LNs much more. So ADC was more reproducible than FA.

A limitation of the present study is its retrospective design. Secondly, there may be potential population bias because the axilla was not fully covered by the coil during DWI/DTI for every patient examined in our department. The number of patients was also limited. For the benign group, diagnostic confirmation was based on clinical, radiologic and follow-up data but there was no histopathological analysis and some benign LNs too small for ROI placement were not evaluated. In the metastatic group, histopathological results were available, but no marking procedure had been performed. Additionally, no normalization was used for parameters.

5. Conclusions

In conclusion, to our understanding, this is the first study using DTI to evaluate axillary LNs. Metastatic LNs presented significantly greater cortex thickness and short-long axes, lower ADC and FA values. ADC value had a relatively better diagnostic performance than FA.

Institutional review board (IRB) statement

IRB approved the study.

Informed consent statement

No informed consent due to retrospective design.

Conflict of interest statement

No conflict of interests.

Funding statement

No funding received.

References

1. Fornasa F, Nesoti MV, Bovo C, et al. Diffusion-weighted magnetic resonance imaging in the characterization of axillary lymph nodes in patients with breast cancer. *J Magn Reson Imaging* **2012**; 36: 858-864.
2. Silverstein MJ, Skinner KA, Lomis TJ. Predicting axillary nodal positivity in 2282 patients with breast carcinoma. *World J Surg* **2001**; 25:767–772.
3. Mansel RE, Fallowfield L, Kissin M etal. Randomized multicenter trial of sentinel node biopsy versus standard axillary treatment in operable breast cancer: the ALMANAC trial. *J Natl Cancer Inst* **2006**; 98:599–609.
4. Durur-Subasi I, Durur-Karakaya A, Alper F etal. Breast lesions with high signal intensity on T1-weighted MR images. *Jpn J Radiol* **2013**; 31: 653-661.
5. Durur-Subasi I, Alper F, Akcay MN, et al. Magnetic resonance imaging findings of breast juvenile papillomatosis. *Jpn J Radiol* **2013**; 31: 419-423.
6. Durur-Subasi I, Durur-Karakaya A, Karaman A, et al. Is the necrosis/wall ADC ratio useful for the differentiation of benign and malignant breast lesions? *Br J Radiol* **2017**; 90: 20160803.
7. Durur-Subasi I, Durur-Karakaya A, Karaman A et al. Value of MRI sequences for prediction of invasive breast carcinoma size. *J Med Imaging Radiat Oncol* **2014**; 58: 565-568.
8. Durur-Karakaya A, Seker M, Durur-Subasi I. Diffusion-Weighted Imaging in Ectopic Pregnancy: Ring of Restriction Sign. *Br J Radiol* **2017**; 90: 20170528.
9. Pinker K, Helbich TH, Morris EA. The potential of multiparametric MRI of the breast. *Br J Radiol* **2017**; 90: 20160715.
10. Guvenc I, Akay S, Ince S et al. Apparent diffusion coefficient value in invasive ductal carcinoma at 3.0 Tesla: is it correlated with prognostic factors? *Br J Radiol* **2016**; 89: 20150614.
11. Cakir O, Arslan A, Inan N et al. Comparison of the diagnostic performances of diffusion parameters in diffusion weighted imaging and diffusion tensor imaging of breast lesions. *Eur J Radiol* **2013**; 82: 801–806.
12. Eyal E, Shapiro-Feinberg M, Furman-Haran E et al. Parametric diffusion tensor imaging of the breast. *Invest Radiol* **2012**; 47: 284-291.
13. Partridge SC, Ziadloo A, Murthy R et al. Diffusion tensor MRI: preliminary anisotropy measures and mapping of breast tumors. *J Magn Reson Imaging* **2010**; 31: 339-347.
14. Baltzer PA, Schäfer A, Dietzel M et al. Diffusion tensor magnetic resonance imaging of the breast: a pilot study. *Eur Radiol* **2011**; 21: 1-10.
15. Tagliafico A, Rescinito G, Monetti F etal. Diffusion tensor magnetic resonance imaging of the normal breast: reproducibility of DTI-derived fractional anisotropy and apparent diffusion coefficient at 3.0 T. *Radiol Med* **2012**; 117: 992-1003.
16. Kim JY, Kim JJ, Kim S, Choo KS, Kim A, Kang T, Park H. Diffusion tensor magnetic resonance imaging of breast cancer: associations between diffusion metrics and histological prognostic factors. *Eur Radiol* **2018**; 28: 3185-3193.
17. Jaimes C, Darge K, Khrichenko D, et al. Diffusion tensor imaging and tractography of the kidney in children: feasibility and preliminary experience. *Pediatr Radiol* **2014**; 44: 30-41.
18. Partridge SC, Nissan N, Rahbar H, et al. Diffusion-weighted breast MRI: Clinical applications and emerging techniques. *J Magn Reson Imaging* **2017**; 45: 337-355.
19. Kim SH, Shin HJ, Shin KC et al. Diagnostic Performance of Fused Diffusion-Weighted Imaging Using T1-Weighted Imaging for Axillary Nodal Staging in Patients With Early Breast Cancer. *Clin Breast Cancer* **2017**; 17:154–63.
20. Xing H, Song CL, Li WJ. Meta analysis of lymph node metastasis of breast cancer patients: clinical value of DWI and ADC value. *Eur J Radiol* **2016**; 85: 1132-1137.
21. Rautiainen S, Könönen M, Sironen R et al. Preoperative axillary staging with 3.0-T breast MRI: clinical value of diffusion imaging and

apparent diffusion coefficient. *PLoS One* **2015**; 10: 0122516.
22. Rahbar H, Conlin JL, Parsian S, et al. Suspicious axillary lymph nodes identified on clinical breast MRI in patients newly diagnosed with breast cancer: can quantitative features improve discrimination of malignant from benign? *Acad Radiol* **2015**; 22: 430-438.
23. Yamaguchi K, Schacht D, Nakazono T, et al. Diffusion weighted images of metastatic as compared with nonmetastatic axillary lymph nodes in patients with newly diagnosed breast cancer. *J Magn Reson Imaging* **2015**; 42: 771-778.
24. Kamitani T, Hatakenaka M, Yabuuchi H et al. Detection of axillary node metastasis using diffusion-weighted MRI in breast cancer. *Clin Imaging* **2013**; 37: 56-61.
25. Karaman A, Durur-Subasi I, Alper F, et al. Is it better to include necrosis in apparent diffusion coefficient (ADC) measurements? The necrosis/wall ADC ratio to differentiate malignant and benign necrotic lung lesions: Preliminary results. *J Magn Reson Imaging* **2017**; 46:1001-1006.
26. Iannicelli E, Di Pietropaolo M, Pilozzi E et al. Value of diffusion-weighted MRI and apparent diffusion coefficient measurements for predicting the response of locally advanced rectal cancer to neoadjuvant chemoradiotherapy. *Abdom Radiol (NY)* **2016**; 41: 1906-1917.
27. Nesbakken A, Nygaard K, Westerheim O, et al, Local recurrence after mesorectal excision for rectal cancer. *Eur J Surg Oncol* **2002**; 28: 126-134.
28. Kapiteijn E, Marijnen CA, Nagtegaal ID et al. Preoperative radiotherapy combined with total mesorectal excision for resectable rectal cancer. *N Engl J Med* **2001**; 345: 638-646.
29. Henzler T, Schmid-Bindert G, Schoenberg SO, et al. Diffusion and perfusion MRI of the lung and mediastinum. *Eur J Radiol* **2010**; 76: 329-336.
30. Durur-Subasi I. DW-MRI of the breast: a pictorial review. *Insights Imaging*. **2019**; 10(1): 61.
31. Durur-Subasi I. Diagnostic and Interventional Radiology in Idiopathic Granulomatous Mastitis. *Eurasian J Med*. **2019**; 51(3): 293-297.
32. Jiang R, Ma Z, Dong H, et al. Diffusion tensor imaging of breast lesions: evaluation of apparent diffusion coefficient and fractional anisotropy and tissue cellularity. *Br J Radiol* **2016**; 89: 20160076.

Authors' ORCID
Irmak Durur Subasi
http://orcid.org/ 0000-0003-3122-4499
Fatih Alper
http://orcid.org/0000-0002-9483-8861
Pınar Tuncel-Eyi
http://orcid.org/0000-0002-2417-8546
Adem Karaman
http://orcid.org/0000-0002-3091-0609
Veysel Esdur
http://orcid.org/0000-0001-6729-3600
Elif Demirci
http://orcid.org/0000-0002-6660-3870
Baki Hekimoğlu
http://orcid.org/0000-0002-1824-5853

https://dergipark.org.tr/tr/pub/ntms

ISSN:XXXX-XXXX RESEARCH ARTICLE

New Trend Med Sci 2020; 1(1): 14-19 https://dergipark.org.tr/tr/pub/ntms

Short-Mid Term Results of Open Reduction and Simultaneous Single Stage Pemberton Pericapsular Osteotomy in Patients with Bilateral Developmental Hip Dysplasia

Muhammed Çağatay Engin[1*], Kemal Zencirli[2], Mehmet Köse[1], Naci Ezirmik[1]

[1] Department of Orthopedics and Traumatology, Research Hospital, Atatürk University, Erzurum, Turkey
[2] Department of Orthopedics and Traumatology, Kozluk State Hospital, Ministry of Health, Batman, Turkey

Article History
Received 31 May 2020
Accepted 08 June 2020
Published Online 15 June 2020

[*]***Corresponding Author***
Dr Muhammed Çağatay Engin
Department of Orthopaedics and Traumatology,
Faculty of Medicine,
Atatürk University,
Erzurum, Turkey
Phone: +90532 330 19 49
E-mail:mcagatayengin@hotmail.com
ORCID:http://orcid.org/0000-0002-9302-9587

Abstract: In this study, we aimed to publish the data on the clinical-radiological outcomes and perioperative analysis of PPO applied simultaneously in patients with bilateral developmental hip dysplasia compared with the literature. In the study, which was retrospectively analyzed, 75 patients (150 hips) who were followed up for at least 1 year between 2010-2018 were included in the study. Preoperative radiological Asetabular Index (AI) measurement and the International Hip Dysplasia Institute (IHDI) classification, postoperative radiological AI measurement and Severin classification, clinically McKay criteria, for osteonecrosis Kalamchi-MacEwen classification were used. In the perioperative analysis, the duration of anesthesia exposure, hospital stay, and total cost were evaluated. Sixty-seven patients were girls and 8 patients were boys. The mean follow-up times were 31.65±16.2 (12-60) months and the age of surgery was 21.4 (18-36). There was no statistically significant difference between the mean follow-up times and surgical ages between both genders (p=0.681). A statistically significant difference between the mean corrected AI (p=0.509), intraoperative bleeding amount (p=0.431), hospital stay time (p=0.909), anesthesia exposure (p=0.368) and cost (p=0.531) between both sex no difference was found. It was statistically significant for the right and left hips in pre-postoperative AI (p<0.001). Clinical and radiological results were found in similar rates to the literature. Compared with the literature, clinical and radiological results were found in similar rates in patients who underwent simultaneous PPO. In addition, simultaneous PPO reduces anesthesia exposure time, hospital stay and total cost. Simultaneous procedure seems to be advantageous for surgeons who have sufficient experience in PPO or who have started using this technique routinely. © 2020 NTMS.

K***eywords***: Pemberton, Simultaneous Surgery, Developmental Hip Dysplasia.

1. Introduction

Developmental hip dysplasia (DDH) is a pathological condition that is common in children and infants. It is frequently seen unilaterally, and approximately 20% bilaterally (1, 2).

Early diagnosed DDH patients (less than 12 months) are mostly treated via conservative methods (bracing, casting) and particularly in walking age or not benefited from conservative therapy are treated surgically.

Cite this article as: Engin MÇ, Zencirli K, Köse M, Ezirmik N. Short-Mid Term Results of Open Reduction and Simultaneous Single Stage Pemberton Pericapsular Osteotomy in Patients with Bilateral Developmental Hip Dysplasia. *New Trend Med Sci* **2020**;1 (1): 14-19.

Although there are many surgical methods for patients with DDH in walking age, pemberton pericapsular osteotomy (PPO) is one of the most common used surgical procedures (4). PPO is an incomplete osteotomy technique that reshapes the acetabulum and provides concentric reduction of the femoral head (5). And for this reason, forming a relatively stable pelvis has brought to mind the possibility of simultaneous bilateral technique.

Since PPO is an incomplete osteotomy technique, providing natural stability after the graft may allow surgery to be performed simultaneously bilaterally (6, 7). Although the literature is inadequate, whether concurrent or sequential surgery to the patients with bilateral DDH is often controversial.

In this study, we aimed to publish the data on clinical, radiological and perioperative analysis of the patients whom PPO applied simultaneously with bilateral DDH and compared with the literature.

2. Material and Methods

Patients with bilateral DDH who underwent PPO between 2010 and 2018 years were included to the study and they were retrospectively analyzed. Patient criteria; 18-36 months old, no neurological and congenital disease, no previous surgical treatment, no femoral osteotomy during surgery. 75 patients (150 hips) met these criteria and followed for at least 1 year were included in the study.

Anesthesia exposure time includes the time from the beginning of anesthesia to the end of it. Pelvipedal plastering is also within this period. The cost is the fee that the institution has incurred for any expenses (anesthesia premedication, blood tests, consultations, etc.) during discharge. The amount of intraoperative bleeding was recorded as a parameter obtained from the follow-up of the anesthesia team.

Patients who underwent PPO were used to measure the Acetabular Index (AI) preoperatively and the International Hip Dysplasia Institute (IHDI) classification (Figure 1). Tönnis classification is widely used in the literature. However, since the IHDI classification does not require the presence of ossific nucleus is a more reliable classification compared to the classification of Tönnis (8).

PPO patients were evaluated postoperatively with AI measurement and Severin classification (Table 1) for radiological assessment, McKay classification (Table 2) for clinical assessment, and Kalamchi-MacEwen classification (table 3) for osteonecrosis (9-11).

2.1. Surgical Technique and Patient Follow Up

The classical Smith-Peterson anterior iliofemoral surgical approach was used and if necessary, iliopsoas tenotomy was performed over the pelvic rim. Ligamentum teres were cleared and the transverse acetabular ligament was loosened. Fibrous adipose tissues in the acetabular fossa were cleared, but limbus was preserved. Pemberton type iliac osteotomy was performed in all cases. Pelvipedal plaster was generally applied in a safe position with 35-40° abduction, 30-45° flexion, 0-10° internal rotation, and 35-45° knee flexion.

After applying pelvipedal plaster for 2 months, abduction orthosis was applied for another month. Plaster cover was opened in the incision area for wound care on the first postoperative day. Patients were called for 2-month follow-up in the first 1-year period, and an anterior posterior (AP) radiograph was requested at each control (Figure 2). Encouraging advice was given to walking. Preoperative traction was not used in any patient.

2.2. Statistical Analyses

Statistical Analysis Data was analyzed using the Statistical Package for Social Sciences (SPSS) version 20 statistical analysis program (IBM Corp; Armonk, NY, USA). Data were presented as mean, standard deviation, minimum, maximum and percentage. The significance of AI change was analyzed with the Wilcoxon test, using mean gender follow-up time and surgical age, corrected AI amount, intraoperative bleeding amount, hospital discharge time, anesthesia exposure and cost difference with Mann-Whitney U test. If $p<0.05$, the differences were considered significant.

3. Results

67 of the patients were female and 8 were male. The mean follow-up times were 31.65±16.2 (12-60) months and the age of surgery was 21.4 (18-36). There was no statistically significant difference between the mean follow-up times and surgical ages between both genders ($p=0.681$).

A statistically significant difference between the mean corrected AI ($p=0.509$), intraoperative bleeding amount ($p=0.431$), hospital discharge time ($p=0.909$), anesthesia exposure ($p=0.368$) and cost ($p=0.531$) between both sexes. No difference was found.

Right-left preoperative AI and postoperative AI of the patients were given in table 4. It was found statistically significant for the right and left hips in pre-postoperative AI ($p<0.001$). In the same table, intraoperative bleeding amount, hospital discharge time, anesthesia exposure and cost were given together with mean and standard deviation values.

Number (rate) according to the preoperative IHDI and postoperative Kalamchi-MacEwen, Severin and McKay classification were given in table 5.

Deep infection was not detected in any patient. Superficial infection was detected in four patients. All patients showed improvement with antibiotherapy. There was no need for additional surgery.

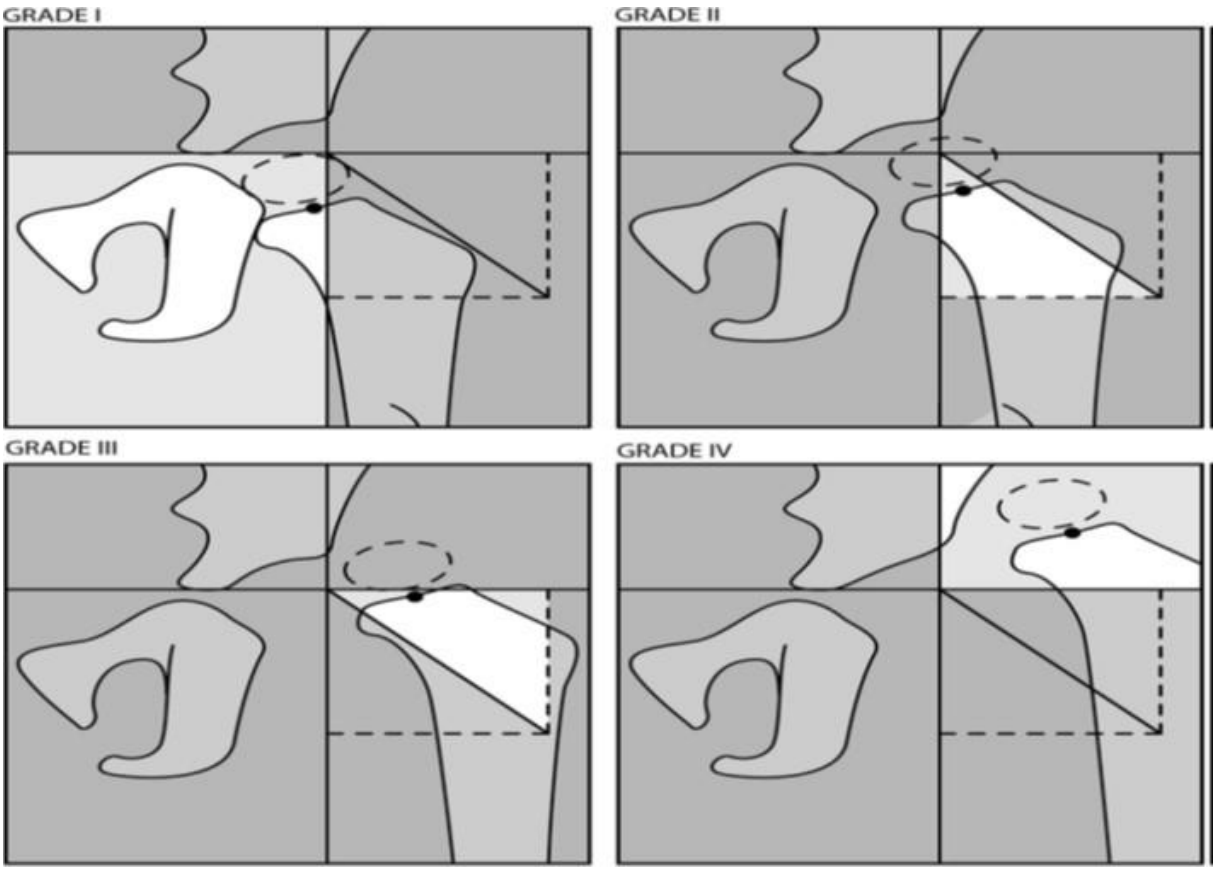

Figure 1: The standard Perkins (P) line is drawn perpendicular to the superolateral edge of the acetabulum. An additional 45 degrees cross line (D-line) is then drawn from the combination of Hilgenreiner's line (H-line) and P-line. The H-line is a single line drawn bilaterally from the top of the triradiate cartilage. The relationship of the H-point with these 3 lines determines the IHDI rating. The IHDI grade I is at the hip, H point at the P line or medial. In the IHDI grade II hip, the H-point is lateral to the P line or medial of the D-line. In the IHDI grade III hip, the H-point is lateral to the D-line and below the H-line. Finally, the H-point on the IHDI grade IV hip is above the H-line.

Figure 2: Respectively; Pelvis radiographs of the patient before the operation, immediately after the operation and 4th year.

Table 1: Severin's Radiological Classification.

Degree	Description
I (excellent)	Normal view
II (good)	Mild deformity in the acetabulum or femoral head and neck
III (moderate)	Dysplasia or mid degree deformity in acetabulum-femoral head and neck or both
IV (worse)	Subluxation of the femoral head
V (worse)	Joint of the femoral head with the wrong acetabulum
VI (worse)	Redislocation

Table 2*:* McKay Clinical Classification.

Degree	Description
I (excellent)	Pain-free, stable hip, no limping, full range of motion, negative Tredelenburg sign
II II (good)	Pain-free, stable hip, normal or slightly limp, slightly reduced range of motion
III (moderate)	Slight or painless claudication, stable hip, moderate stiffness, positive Trendelenburg sign
IV (worse)	Pain and instability in both hips, positive Trendelenburg sign

Table 3*:* Kalamchi-MacEwen Osteonecrosis Classification.

Degree	Description
I	Changes affecting the ossific nucleus
II	Lateral physical damage
III	Central physical damage
IV	Total damage to fizis and femoral head
V	Unclassifiable

Table 4: Preoperative AI, Postoperative AI, Intraoperative Bleeding Amount, Hospital Discharge Time, Anesthesia Exposure and Cost Means and Standard Deviations.

	Mean±Standard Deviation	
Preoperatif AI	39,92±5,22 (right)	40,75±5,37 (left)
Postoperatif AI	12,68±4,58 (right)	13,37±5,10 (left)
Intraoperative Bleeding Amount/cc	80,07±17,13	
Hospital Discharge Time/Day	4,96±1,25	
Anesthesia Exposure/Min	200,13±50,5	
Cost /TL	2642,60±407,39	

Table 5: Preoperative IHDI and postoperative Kalamchi-MacEwen number according to Severin and McKay classification (rate).

	IHDI		Kalamchi-MacEwen		Severin		McKay	
	Right	Left	Right	Left	Right	Left	Right	Left
			49 (65.3)-no AVN	52 (69.3)-no AVN				
I	2 (2.7)	2 (2.7)	20 (26.7)	18 (24.0)	47 (62.7)	49 (65.3)	56 (74.7)	56 (74.7)
II	41 (54.7)	41 (54.7)	3 (4.0)	-	26 (34.7)	23 (32.0)	13 (17.3)	15 (20.0)
III	20 (26.7)	20 (26.7)	3 (4.0)	5 (6.7)	2 (2.7)	2 (2.7)	6 (8.0)	4 (5.3)
IV	12 (16.0)	12 (16.0)						

4. Discussion

PPO is a surgical technique described by Pemberton in 1965, which he first described with his name (5). PPO provides anterior (anterolateral) covering especially in the acetabulum and reduces concentrate femoral head reduction by reducing the acetabulum volume. It is an incomplete osteotomy technique since it uses triradiate cartilage as a hinge. PPO has become popular over time because it does not create pelvic instability, does not cause leg length difference and does not require fixation after osteotomy (4).

In the literature, many positive results have been reported in patients with unilateral DDH related to PPO. However, there are different opinions in bilateral cases. There is a lot of literature information about the positive results of PPO (4, 12, 13).

It has been reported in the literature that PPO significantly improves on acetabular index (AI). Alsiddiky et al. (14) 22.36 degrees in the right hip, 22.64 degrees in the left hip, Subaşı et al. (15).

On the other hand, they achieved an average correction of 16.7 degrees in patients who underwent sequential surgery. Agus et al. (1) average 10.2 degrees, Baki et al. (16) achieved an average of 31.2 degrees of improvement. In our study, an average of 27.3 degrees in the right hip and 27.4 degrees in the left hip were obtained. An AI value was obtained among the correction amounts specified in the literature.

Since PPO does not create pelvic instability, especially in patients with bilateral DDH, it allows simultaneous bilateral operation. Zorer et al. (7) reported significant data in favor of simultaneous acetabular index, cost effectiveness, duration of anesthesia, and length of hospital stay among patients with bilateral and unilateral DDH to whom they applied PPO. In this study, the average length of hospital stay was determined as 4.1 days. Agus et al. found this time to be an average of 5 days (1). The mean discharge times of the patients who underwent simultaneous PPO in our case series were 4.9 days. The reasonable discharge times we have obtained show us that the simultaneous operation of patients with bilateral DDH does not prolong hospital stay.

Agus et al. (1) compared bilateral simultaneous open reduction and unilateral pelvic osteotomy for DDH treatment in patients over the walking age after approximately 55 months of follow-up. They could not find a significant difference between the two groups in terms of results in clinical, radiology and corrected AI between the two groups. In the studies of Alsiddiky (14), Baki (16) and Subaşı (15), the results of open reduction and pelvic osteotomy in which they performed sequential single-session and bilateral single-session were excellent (14-16). In our study, where we presented our concurrent PPO results, we used the results of the 4 studies mentioned above as a control group.

One of the worst complications associated with DDH treatment is osteonecrosis or avascular necrosis (AVN). Multiple theories about the cause of AVN are explained. The general common idea is that with increasing age, the risk of developing postoperative AVN is increased. The average incidence of AVN after open reduction and pelvic osteotomy ranges from 7 to 22% (1, 19, 21).

In our study, AVN developed in 11 (7.3%) of 150 hips. Since type 1 is accepted as the variant of the normal in the literature, the sum of type 2 type 3 and type 4 has been evaluated as avascular necrosis.

The relatively low AVN rates we achieved; we believe that our patient age range in our case series is related to our age range (18-36 months).

5. Conclusions

Our study revealed that simultaneous bilateral open reduction and pelvic osteotomy demonstrated very limited and treatable complications for children with 18-36 months of bilateral DDH. In addition, the need for equipment and hospitalization costs decreased when a single operation was performed. We believe that this procedure will cause less problems for families in terms of psycho-social aspects.

Conflict of interest statement
None

References

1. Agus H, Bozoglan M, Kalenderer Ö, Kazımoğlu C, Onvural B, Akan İ. How are outcomes affected by performing a one-stage combined procedure simultaneously in bilateral developmental hip dysplasia? *Int Orthop* **2014**; 38(6): 1219-1224.
2. Murphy RF, Kim Y-J. Surgical management of pediatric developmental dysplasia of the hip. *J Am Acad Orthop Surg* **2016**; 24(9): 615-624.
3. Schwend RM, Shaw BA, Segal LS. Evaluation and treatment of developmental hip dysplasia in the newborn and infant. *Pediatr Clin* **2014**; 61(6): 1095-1107.
4. Aydin A, Kalali F, Yildiz V, Ezirmik N, Aydin P, Dostbil A. The results of Pemberton's pericapsular osteotomy in patients with developmental hip dysplasia. *Acta Orthop Traumato* **2012**; 46(1): 35-41.
5. Pemberton PA. Pericapsular osteotomy of the ilium for treatment of congenital subluxation and dislocation of the hip. *JBJS* **1965**; 47(1): 65-86.
6. Gillingham BL, Sanchez AA, Wenger DR. Pelvic osteotomies for the treatment of hip dysplasia in children and young adults. *J Am Acad Orthop Surg* **1999**; 7(5): 325-337.
7. Zorer G, Bagatur AE. Single-stage bilateral Pemberton's pericapsular osteotomy in bilateral developmental dysplasia of the hip. *Acta Orthop Traumato* **2002**; 36(4): 288-294.
8. Narayanan U, Mulpuri K, Sankar WN, Clarke NM, Hosalkar H, Price CT, et al. Reliability of a new radiographic classification for developmental dysplasia of the hip. *J Pediatr Orthop* **2015**; 35(5): 478.
9. Severin E. Congenital dislocation of the hip: development of the joint after closed reduction. *JBJS* **1950**; 32(3): 507-518.
10. Mckay DW. A comparison of the innominate and the pericapsular osteotomy in the treatment of congenital dislocation of the hip. *Clin Orthop Rel Res* **1974** ;98: 124-132.
11. Kalamchi A, MacEwen GD. Avascular necrosis following treatment of congenital dislocation of the hip. *JBJS* **1980**; 62(6): 876-888.
12. Wu K-W, Wang T-M, Huang S-C, Kuo KN, Chen C-W. Analysis of osteonecrosis following Pemberton acetabuloplasty in developmental dysplasia of the hip: long-term results. *JBJS* **2010**; 92(11): 2083-2094.
13. Wang T-M, Wu K-W, Shih S-F, Huang S-C, Kuo KN. Outcomes of open reduction for developmental dysplasia of the hip: does bilateral dysplasia have a poorer outcome? *JBJS* **2013**; 95(12): 1081-1086.

14. Alsiddiky A, Alatassi R, Alqarni MM, Bakerman K. Simultaneous bilateral single-stage combined open reduction and pelvic osteotomy for the treatment of developmental dysplasia of the hip. *J Pediatr Orthop* **2020**.

15. Subasi M, Arslan H, Cebesoy O, Buyukbebeci O, Kapukaya A. Outcome in unilateral or bilateral DDH treated with one-stage combined procedure. *Clin Orthop Rel Res* **2008**; 466(4): 830-836.

16. Baki ME, Baki C, Aydin H, Ari B, Özcan M. Single-stage medial open reduction and Pemberton acetabuloplasty in developmental dysplasia of the hip. *J Pediatr Orthop*. **2016**; 25(6): 504.

17. Wilder RT, Flick RP, Sprung J, Katusic SK, Barbaresi WJ, Mickelson C, et al. Early exposure to anesthesia and learning disabilities in a population-based birth cohort. Anesthesiology: *ASA* **2009**; 110(4): 796-804.

18. Schneuer FJ, Bentley JP, Davidson AJ, Holland AJ, Badawi N, Martin AJ, et al. The impact of general anesthesia on child development and school performance: a population-based study. *Pediatr Anesth* **2018**; 28(6): 528-536.

19. Ezirmik N, Yildiz K. Advantages of single-stage surgical treatment with salter innominate osteotomy and Pemberton pericapsular osteotomy for developmental dysplasia of both hips. *J Int Med Res* **2012**; 40(2): 748-755.

20. Zorer G, Bagatur A. Single-stage bilateral Pemberton's pericapsular osteotomy in bilateral developmental dysplasia of the hip. *Acta orthop traumatol* **2002**; 36(4): 288-294.

21. Ochoa O, Seringe R, Soudrie B, Zeller R. Salter's single-stage bilateral pelvic osteotomy. *SOFCOT* **1991**; 77(6): 412-418.

22. Aghayev E, Beck A, Staub LP, Dietrich D, Melloh M, Orljanski W, et al. Simultaneous bilateral hip replacement reveals superior outcome and fewer complications than two-stage procedures: a prospective study including 1819 patients and 5801 follow-ups from a total joint replacement registry. *BMC Musculoskelet Disord* **2010**; 11(1): 245.

23. Parvizi J, Tarity TD, Sheikh E, Sharkey PF, Hozack WJ, Rothman RH. Bilateral total hip arthroplasty: one-stage versus two-stage procedures. *Clin Orthop Rel Res* **2006**; 453: 137-141.

24. Lorenze M, Huo MH, Zatorski LE, Keggi KJ. A comparison of the cost effectiveness of one-stage versus two-stage bilateral total hip replacement. *Orthop* **1998**; 21(12): 1249-1252.

25. Berend KR, Lombardi Jr AV, Adams JB. Simultaneous vs staged cementless bilateral total hip arthroplasty: perioperative risk comparison. *J Arthroplasty* **2007**; 22(6): 111-115.

Authors' ORCID

Muhammed Çağatay Engin
http://orcid.org/ 0000-0002-9302-9587

NTMS New Trends in Medicine Sciences

https://dergipark.org.tr/tr/pub/ntms

ISSN:XXXX-XXXX RESEARCH ARTICLE

New Trends in Medicine Sciences

New Trend Med Sci 2020; 1(1): 20-24 https://dergipark.org.tr/tr/pub/ntms

The Examination Results of Lymph Nodes in a Tertiary Health Center

Sevilay Özmen[1*], Sare Şipal[1], Elif Demirci[1], Esra Çınar Tanrıverdi[2], Zülal Özkurt[3], Remzi Arslan[1], Onur Ceylan[1]

[1] Department of Pathology, School of Medicine, Atatürk University, Erzurum, Turkey
[2] Department of Medical Education, School of Medicine, Atatürk University, Erzurum, Turkey
[3] Department of Infectious Diseases, School of Medicine, Atatürk University, Erzurum, Turkey

Article History
Received 31 May 2020
Accepted 03 June 2020
Published Online 15 June 2020

[*]***Corresponding Author***
Dr Sevilay Özmen
Department of Patology,
School of Medicine,
Atatürk University,
Erzurum, Turkey
Phone: +905337254072
E-mail: ertekozmen@gmail.com
ORCID:http://orcid.org/0000-0002-1973-6101

Abstract: Lymphadenopathy is the rapid or slow growth of lymph nodes. The differential diagnosis of lymphadenopathy frequently encountered in internal diseases, and department of otorhinolaryngology, has a wide range. The growth of lymph nodes is a common finding during physical examination and most of them are benign. They usually develop due to infectious, neoplastic or autoimmune diseases. Localization of lymphadenopathies may also provide important clues in diagnosis. Lymphoma, toxoplasma, rubella, tuberculous lymphadenitis in cervical lymphadenopathies; gastrointestinal system malignancies or lymphoma in supraclavicular lymphadenopathies; in patients with axillary lymphadenopathies, infections such as lymphoma, brucellosis and cat scratch fever disease are common. To review the diagnostic data of lymphadenopathies in the pathology department of the Faculty of Medicine of Atatürk University. The diagnostic results of lymph node excisions in Atatürk University Faculty of Medicine Pathology Department were retrospectively analyzed, categorized, and the number of cases was determined according to the ages. Of the 1658 patients, 835 (52.7%) were reactive lymphadenitis, 462 (29.1%) were malignant tumor metastasis positive lymph node and 165 (10.4%) were lymphoid malignancy, 122 (7.7%) Non-Hodgkin lymphoma, 41 (2.5%) were reported as Hodgkin lymphoma and 2 (0.1%) as plasma cell dyscrasias. 96 (6.0%) of the cases were diagnosed as necrotizing granulomatous lymphadenitis and 27 (1.7%) were diagnosed as non-necrotizing granulomatous lymphadenitis. No histomorphological details of the lymph node were found in 73 specimens (4.6%) that were sent as lymph node excision. Most of the cases were excised from the cervical region and the second line was axillary region. Lymphadenopathies may be the first manifestation of infections and various cancers. In these patients, delayed diagnosis may cause significant medical problems and should be excised without delay for histopathological diagnosis.

Keywords: Lymphadenomegaly, Granulomatous Lymphadenitis, Histopathological Diagnosis.

Cite this article as: Özmen S, Şipal S, Demirci E, Çınar Tanrıverdi E, Özkurt Z, Arslan R, Ceylan O. The Examination Results of Lymph Nodes in a Tertiary Health Center, *New Trend Med Sci* **2020**;1 (1): 20-24.

1. Introduction

The word lymph means “clean water” in Latin. Nutrients, electrolytes, immunoglobulins and some proteins are transported to the tissues by the lymphatic system. It acts like an immune control system for tissues (1,2). The lymphatic system has a complex structure and is associated with the circulatory system, hematopoietic system, and the immune system. The lymph fluid drained in the tissues enters the lymph nodes through lymph canaliculi and the circulatory system through the ductus thoracicus (3,4). The lymphatic system is primarily responsible for fulfilling cellular needs, ensuring the transfer of fat from the gastrointestinal tract, and forming an immune response. Lymph nodes are small stations mostly located on the intermammary cleft, usually in the lymphatic canaliculi located in the head and neck region in our body (5). Lymphatic fluid has a place in transporting essential nutrients such as proteins and especially lipids taken from the gastrointestinal tract by enterocytes (6). Immunoglobulins and proteins associated with the immune system are also present in the lymphatic fluid (2,4). The structure of the lymphatic system in the abdomen and thorax is dense and complex compared to other regions and lymphatic flow is quite slow. The flow is very slow especially in the lower extremities. There is no muscle tissue in lymphatic vessels. Of the 300-600 lymph nodes in the human body, approximately half of them are located in the head and neck region. In addition to growing in systemic diseases, lymph nodes can grow locally in diseases localized to anatomical regions with lymph flow drained to a particular node. This growth is called “lymphadenomegaly” or “lymphadenopathy” (LAP) (7,8).

LAP may be the first symptom in most diseases. In physical examination, LAPs show certain distinctive features in terms of etiology. Small lymph nodes in the suboccipital region in children and in the inguinal region in adults can be palpated without any pathology. Cervical lymphadenopathies usually develop as a result of infections and careful physical examination can easily identify the underlying cause. However, growth in supraclavicular, scalene, axillary and epitrochlear lymph nodes is generally pathological, and more detailed examination is required to determine the etiology. LAPs that do not regress or continue to grow after treatment or follow-up should be examined histopathologically (9,10). Excisional biopsy of the lymph node is accepted as the “gold standard” in the diagnosis of LAP (11).

2. Material and Methods

The pathological results of lymph node excisions examined in our tertiary center between 2010 and 2017 were retrospectively scanned from archival records. The data were categorized as total number of cases by age groups and histopathological results by mean age.

3. Results

A total of 1658 lymph node resections were sent to our clinic for histopathological examination from different clinics of our university between 2010 and 2017. Histopathological examinations of lymph node resections revealed that 835 cases (52.7%) were reactive lymphadenitis, 462 cases (29.1%) were malignant tumor metastasis positive lymph node, and 165 cases (10.4%) were lymphoid malignancy. 122 (7.7%) of these malignancies were reported as Non-Hodgkin Lymphoma, 41 (2.5%) as Hodgkin Lymphoma, and 2 (0.1%) as plasma cell dyscrasia (Table 1). 96 (6.0%) of the cases were necrotizing granulomatous lymphadenitis and 27 (1.7%) were non-necrotizing granulomatous lymphadenitis. No histomorphology details of lymph node were found in 73 (4.6%) lymph node excisions sent to out clinic, and most of these were reported as ‘fibrous tissue’ and ‘fibrolipomatous tissue’. Most of our cases were excised from the cervical region, followed by the axillary region. The distribution of the patients with lymphadenopathy according to age is shown in Figure 1 and the distribution of their diagnoses according to average age is shown in Figure 2.

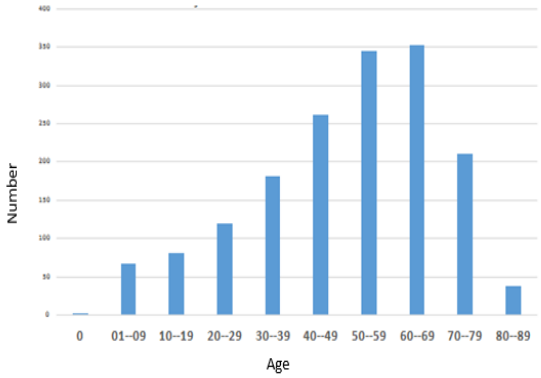

Figure 1: Age distribution of patients with lymphadenopathy.

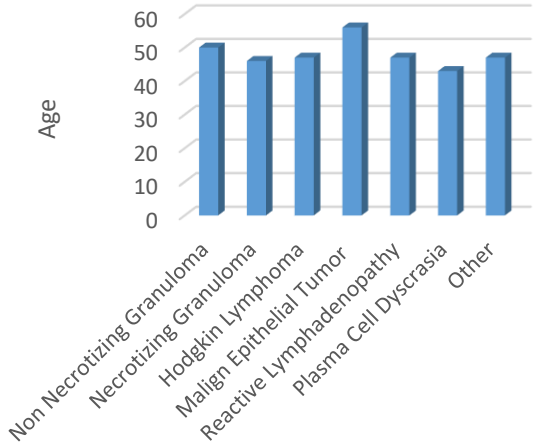

Figure 2: Average age of lymphadenopathy diagnoses.

Table 1: Classification of lymphadenopathies according to histopathological diagnosis.

Diagnosis	Number (n)	Percentage (%)
Reactive Lymphadenopathy	**835**	**52.7**
Malignancy	**627**	**39.5**
Malignant Tumor Metastasis	462	29.1
Lymphoid Malignancy	165	10.4
Non-Hodgkin Lymphoma	122	7.7
Hodgkin Lymphoma	41	2.5
Plasma Cell Dyscrasia	2	0.1
Granulomatous Lymphadenopathies	**123**	**7.8**
Necrotizing	96	6.0
Non-necrotizing	27	1.7
Total	**1585**	**100**

4. Discussion

LAP is a common reason for patients to consult a physician and it is coincidentally identified during physical examination conducted for other reasons. LAP may be a symptom accompanying many rare and common diseases. LAP is usually seen in the course of systemic infections. However, it may constitute one of the findings of primary lymphoid malignancies or other malignant conditions or may develop secondary to a significant systemic disease. Various causes such as autoimmune, infectious and malignant diseases are considered in differential diagnosis, histopathological diagnosis with excisional biopsy is therefore highly important (12,13).

In the present study, the age range in which LAP requiring excision was more frequent was also investigated to assist the clinicians. LAP not responding to initial treatments and requiring excisional biopsy was seen in all age groups, but it was most commonly seen in the 50-70 age group. While LAP is also a common clinical symptom in childhood and adolescence, most cases are due to infections and resolve spontaneously or by various treatments. However, excisional biopsy should be performed for diagnosis in the presence of LAP not responding to a treatment, not regressing spontaneously, being protracted, solid and immobile, or when detected in an area such as the supraclavicular region.

In the present study, the mean age of malignant cases was 56 for malignant epithelial tumors, 49 for Non-Hodgkin Lymphoma, 47 for Hodgkin Lymphoma, and 43 for plasma cell dyscrasias. These results were similar to those of Darnal and Desforges (14,15).

Darnal et al. reported that malignant cases with a rate of 47% were most common in adults (14). Reactive lymphadenitis was the most common condition in the present study.

In a study by Gül et al., male: female ratio of Non-Hodgkin Lymphoma and Hodgkin Lymphoma was reported to be 2.67:1 and 2.5:1, respectively (16). These rates are similar to those reported by Darnal and Desforges and the findings of our study (14,15).

In the study of Mohan et al., malignancy rate was 25.8%, after non-specific lymphadenitis and tuberculosis lymphadenitis. It was stated that the number of cases with metastatic lymph node was higher than cases with lymphoma (11). In the present study, calcified granulomatous lymphadenitis was the second most common condition (29.9%).

In the study of Öksüz et al., 192 pediatric cases undergoing lymph node biopsy were included and benign causes were detected in 139 (72%) and malignant causes were detected in 53 (28%) cases (17). Even though the pediatric age group was included in that study, there are similarities in terms of histopathological results. However, it is seen that reactive LAP diagnosis was more frequent compared to our study.

In a Nigerian study conducted by Adesuva et al. on 126 patients who underwent lymph node biopsy, tuberculosis lymphadenitis, reactive changes, and malignancy were reported in 48%, 25%, and 24% of the cases, respectively (18). In the present study, reactive lymphadenitis (52.7%) was the most common condition.

Malignancy followed reactive lymph nodes with a frequency of 39.5%, and malignant tumor metastasis was the most common form of malignancy (29.1%). Öksüz et al. reported that malignancy rate increases with age. In the present study, it was seen that malignant cases peaked between the ages of 40-60 (17).

Limitations

There are certain limitations of this study. Since our unit is a regional, tertiary reference hospital, excisions of long-term lymph nodes that cannot be diagnosed in general polyclinics and family health centers or do not respond to non-specific treatments are sent to our pathology laboratory for histopathological examination. Therefore, our histopathological results may not reflect overall LAP results of the region. Also, due to the retrospective nature of this study, we did not have the opportunity to access more comprehensive data other than the information in the archival records.

5. Conclusions

Since regional epidemiological distribution, incidence and prevalence of diseases vary, interregional differences are highly normal. Although this study does not represent the overall population of our region due to its limitations, the histopathological results of the pathology laboratory of our hospital are important as they reiterate the different causes of LAP. Reactive LAP is the most common cause of LAP in our region, followed by malignant diseases. Contrary to expectation, granulomatous diseases are less common, and tuberculosis takes the first place among them.

Considering that lymphadenopathies may be the first finding in the course of various infections and cancers, excision and histopathological diagnosis should be performed as early as possible.

Conflict of interest statement

None

Financial Support

There is no financial support organization.

References

1. Baytan B, Güneş A.M, Günay Ü. Çocukluk Çağında Lenfadenomegaliler. *Güncel Pediatri* **2006**; 2: 49-51.

2. Newman K, Hayes-Jordan AA. Lymph Node Disorders. In: Grosfeld JL, O'Neil JA, Fonkalsrud EW, Coran

3. Grosfeld J, Oneil J, Coran A, Fonkalsrud E, (eds). Pediatric Surgery, Mosby Elsevier, Philadelphia, USA, 6 th ed. **2006**: 844-849.

4. Akyüz C. Lenfadenopatili çocuğa yaklaşım. *İstanbul Üniversitesi Cerrahpaşa Tıp Fakültesi Sürekli Tıp Eğitimi Sempozyumu* **2006**; 49: 17-28.

5. Lanzkowsky P. Lymphadenopathy and Splenomegaly. In: Philip Lanzkowsky (ed). Manual of Pediatric Hematology and Oncology, Elsevier Academic Pres. New York, USA, 5th ed. **2011**;463-468

6. Nolder AR. Paediatric cervical lymphadenopathy: When to biopsy. *Curr Opin Otolaryngol Head Neck Surg* **2013**; 21: 567-70.

7. Şen M. Çocukluk çağı lenfadenopatilerinin değerlendirilmesi. Selçuk Üniversitesi, Uzmanlık Tezi, **2009**.

8. Leung AK, Robson WL. Childhood cervical lymphadenopathy. *J Pediatr Health Care* **2004**; 18: 3-7.

9. Oguz A. Çocukluk çağındaki periferal lenfadenopatiler. *Sürekli Tıp Egitim Dergisi* **1993**; 2: 335-339

10. Sibanda EN, Stanczuk G. Lymph node pathology in Zimbabwe: A review of 2194 specimens. *Q J Med* **1993**; 86: 811- 817.

11. Adeniji KA, Anjorin AS. Peripheral lymphadenopathy in Nigeria. *Afr J Med Med Sci* **2000**; 29: 233-237.

12. Mohan A, Reddy MK, Phaneendra BV, et al. Aetiology of peripheral lymphadenopathy in adults: Analysis of 1724 cases seen at a tertiary care teaching hospital in southern India. *Natl Med J India* **2007**; 20: 78-80.

13. Cianchetti M, Mancuso AA, Amdur RJ, Werning JW, Kirwan J, Morris CG et all. Diagnostic evaluation of squamous cell carcinoma metastatic to cervical lymph nodes from an unknown head and neck primary site. *Laryngoscope* **2009**; 119(12): 2348-2354.

14. Dilber M, Erişen I, Yerci Ö, Coşkun H, Basut O, Onart S, Hızalan İ. Tiroid dışı baş boyun kitlelerinde ince iğne aspirasyon sitolojisi sonuçlarımız. *Türk Otolarengeloji Arşivi*, **2005**; 43: 86-93.

15. Darnal HK, Karim N, Kamini K, et al. The profile of lymphadenopathy in adults and children. *Med J Malaysia* **2005**; 60:590-598.

16. Desforges]F, Rutherford C], Piro A. Hodgkin's Disease. N Engl J Med 1979; 301: 1212-1222.

17. Gül M. Aliosmanoğlu İ, Türkoğlu A, Dal S, Taş İ, Baç B. Erişkin çağı periferik lenfadenopatileri. Eksizyonel Biyopsi Uygulanan 67 Hastanın Sonuçları. *Dicle Med J* **2013**; 40(2); 245-249.

18. Öksüz RYÇ, Dağdemir A, Acar S, Elli M, Öksüz M. Çocukluk çağı periferik lenfadenomegalili olguların retrospektif değerlendirilmesi. *OMÜ Tıp Derg* **2008**; 25: 94–101.

19. Adesuwa Olu-Eddo N, Egbagbe EE. Peripheral lymphadenopathy in Nigerian children. *Niger J Clin Pract* **2006**; 9: 134-138.

Authors' ORCID

Sevilay Özmen
http://orcid.org/0000-0002-1973-6101
Sare Şipal
http://orcid.org/0000-0002-5369-5251
Elif Demirci
https://orcid.org/0000-0002-6660-3870
Esra Çınar Tanrıverdi

https://orcid.org/0000-0001-8857-3986
Zülal Bozkurt
https://orcid.org/0000-0001-5554-8768
Remzi Arslan
https://orcid.org/0000-0002-3198-4706
Onur Ceylan
https://orcid.org/0000-0003-2768-5524

https://dergipark.org.tr/tr/pub/ntms

ISSN:XXXX-XXXX RESEARCH ARTICLE

New Trend Med Sci 2020; 1(1): 25-28 https://dergipark.org.tr/tr/pub/ntms

A Patient Safety Approach for Imaging-Guided Breast Interventions: Red Rules for Prevention of Hematoma

Irmak Durur-Subasi[1,2*], Fatih Alper[1], Mufide Nuran Akcay[3]

[1] Department of Radiology, Faculty of Medicine, Istanbul Medipol University, Istanbul, Turkey
[2] Department of Radiology, Faculty of Medicine, Atatürk University, Erzurum, Turkey
[3] Department of General Surgery, Faculty of Medicine, Atatürk University, Erzurum, Turkey

Article History
Received 25 May 2020
Accepted 01 June 2020
Published Online 15 June 2020

[*]***Corresponding Author***
Irmak Durur-Subasi MD, PhD,
Istanbul Medipol University
Faculty of Medicine
Department of Radiology
Istanbul, Turkey
E-mail: irmakdurur@yahoo.com
Phone: +905334603846
Fax: +902124607070
ORCID:http://orcid.org/0000-0003-3122-4499

Abstract: It was aimed to present the safety program and red rules we use to prevent hematoma complications in imaging-guided breast interventions. Patients who underwent breast intervention between January 2011 and January 2013 were included in the study. Based on the patient records, procedure-related features and hematoma complications were investigated retrospectively. A total of 173 patients had breast intervention. In the records, it was understood that hematoma developed in 3 cases, these were approximately 1-1.5 cm in diameter, and 2 of them developed after a core biopsy and one the vacuum biopsy. A successful interventional procedure not only provides proper diagnosis but also prevents possible complications. The most important complication in breast interventions is the hematoma. For the prevention, some points to be applied before, during, and after the procedure may be useful. Before the procedure, bleeding diathesis, drugs should be questioned, and INR and platelet levels should be checked. During the procedure, the biopsy region should be evaluated with Doppler ultrasonography. Interventions should be performed in a non-traumatic manner. The needle should be entered by holding itself, not the handle of the needle. Among the samples, compression can be made to the biopsy region with an ultrasound probe. After the procedures, the patient should be turned into the prone position, and passive compression should be performed on the biopsy site with her body weight for 10 minutes. In mammography, after the intervention, active compression should be made for 10 minutes with the compression plate of the device, and passive compression should be continued as in ultrasonography. A pressure bandage can be applied while closing the biopsy site. As a result, red lines in breast interventions can be determined as the investigation of the patient's bleeding diathesis, evaluation of the vascularity of the biopsy region, and compression.

Keywords: Patient safety, Breast interventions, Compression.

1. Introduction

Recently, safety (error prevention) programs have been a successful tool for minimizing the error in the industry (1).

This program includes error prevention training, determination of the “red rules,” an applied safety coaching program, and an element to include patients and families in safety.

Cite this article as: Durur-Subasi I, Alper F, Akcay MN. A Patient Safety Approach for Imaging-Guided Breast Interventions: Red Rules for Prevention of Hematoma. *New Trend Med Sci* **2020**;1 (1): 25-28.

Red rules, when not obeyed, have the most severe results or pose the highest risk to safety (1).
The breast interventions must be applied in a safety program to prevent errors. We tried to describe our safety program in terms of the formation of red rules for providing hemostasis in imaging-guided breast biopsies.

2. Patient and Methods

Between January 2011 and January 2013, the patients who underwent breast intervention by one radiologist (IDS) were included in the study by a retrospective viewpoint. The local ethical committee confirmed the study and informed consent was waived. Information on lesion laterality, lesion location, type of the intervention, and thickness of the needle, number of sampling and complication of hematoma were obtained from records.

3. Results

Between January 2011 and January 2013 one hundred and seventy-three patients who underwent breast intervention in our tertiary center were included in the study. Except for one man, the rest 172 patients were women. The patients were between 19–87 years (Mean±Standard Deviation of 48±14 years).
Of the lesions, 98 (56.6%) were at the left breast, and 74 (42.8%) right. One patient had bilateral lesions (0.6%). Seventy lesions (40.5%) were at the upper outer quadrant, 35 (20.2%) at the upper inner quadrant, 28 (16.2%) at the subareolar region, 17 (9.8%) at the lower outer quadrant and 16 (9.2%) at the lower inner quadrant. The location of the seven lesions had not been recorded.
Breast needle biopsies are carried out under image guidance with either ultrasound or using a prone stereotactic mammography table. Of the 173 breast interventions, 141 (81.5%) were core biopsy, 13 (7.5%) fine-needle aspiration (FNA), 12 (6.9%) hook wire insertion and 7 (4%) vacuum biopsy.
During core biopsy, 16 and 18 gauge needles were used respectively for 137 (79.2) and 4 (2.3%) procedures. Fine needles were 21, 24, and 27-gauge (respectively 2, 10, and 1 procedure). Marking hook wires were 20-gauge (12 patients, 6.9%). Vacuum biopsies were performed by 11-gauge needles (7 patients, 4%).
Of the patients, 88 had 2 number of sampling during the intervention (50.9%). 28 (16.2) had one, 28 (16.2%) had 3, 17 (9.8%) had 4, 5 (2.9%) had 5 and 7 (4%) had 12 number of sampling. Twelve-samplings were performed during vacuum biopsies.
All of the methods except FNAs were performed under local anesthesia in the outpatient setting. During FNA local anesthesia was not applied.
The monitorization of hematoma formation has been done both during and after the procedure by sonography. It was learned from the records that 3 patients had been determined to have a hematoma (1.7%). All of them resorbed at about 3-4 weeks after the intervention. One patient underwent a vacuum and 2 patients' core biopsies. All three hematomas were approximately 1-1,5-cm. Additionally, the patient was informed about the admission to the hospital if her breast swelled significantly and became red. There was no applicant with such a complaint.

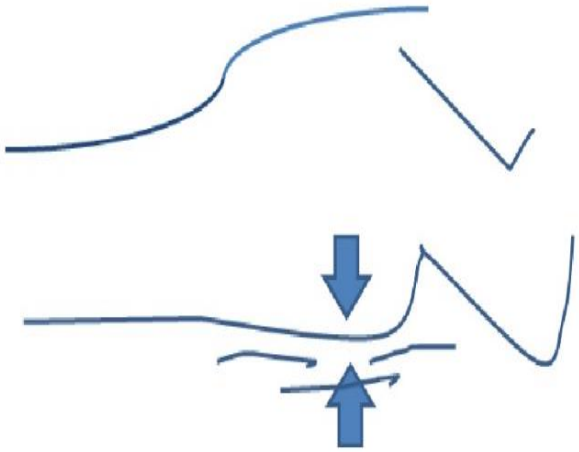

Figure 1: In the prone position; a passive breast compression is applied.

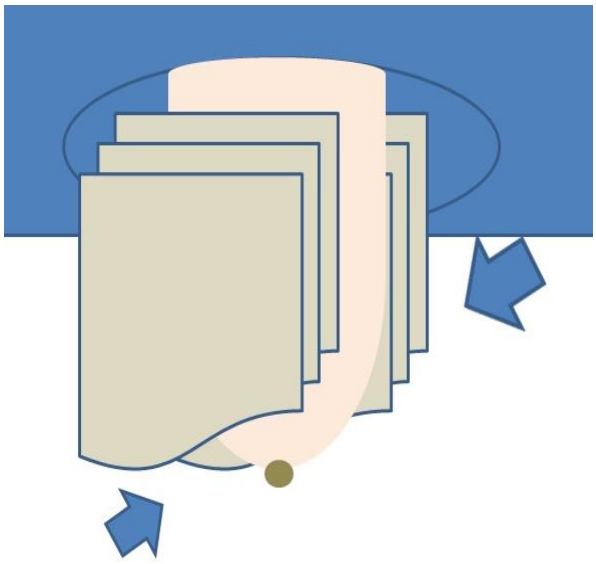

Figure 2: Mammography plates of prone table can be used for active compression, immediately after the intervention.

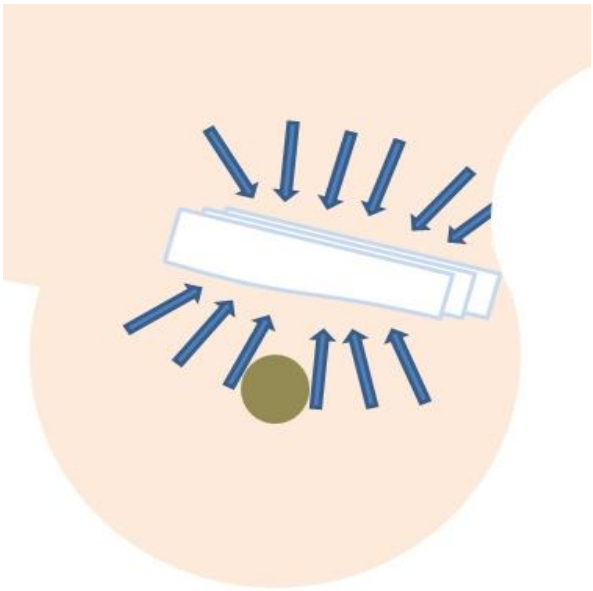

Figure 3: After the procedure, pressure bandage is being applied.

4. Discussion

In this study, breast interventions, those carried out in a 2-year-period by a single radiologist at a tertiary center, were reviewed and hematoma complication rates were evaluated. The hematoma was a rare complication in this group.

Recently many hospitals and health care organizations have recognized the importance of prevention of medical errors resulting from behavior-based events and started to apply patient safety programs (2). A manifestation of this consciousness during medical school training is "primum non-nocere" with the common expression.

All women with breast abnormalities are assessed using the triple diagnostic method. Clinical and imaging assessment should be carried out prior to needle biopsy. Therefore, interventional methods of the breast are relatively frequent. This relatively frequent procedure requires a safety program. We tried to call attention to this fact.

Red rules are rules about critical actions. Red rules, when broken, have the most severe consequences or pose the highest risk to safety. When a red rule is broken the process has to be stopped in every condition in every hand (1). The red rules should be a few in number, clear, and unforgettable (3). Red rules for breast interventions are discussed in this paper.

Imaging-guided needle biopsy is a skilled technique and requires diagnostic, interventional, and ultrasound skills (4). The success of the intervention is not only measured by obtaining a specimen, large enough to provide an adequate pathological assessment. Also, factors related to patient safety, and no procedure related-complication may be a criterion. Before any invasive procedures, some information should be taken from the patient. Bleeding diathesis should be questioned; use of drugs, such as acetylsalicylic acid or warfarin, should be queried. If so with the consultation of a related physician the drug is discontinued before the intervention. Duration of discontinuation is one week for aspirin and 3 days for warfarin. Also before the intervention INR (international normalized ratio) level and platelet count should be checked.

Informed consent is required for any procedure, but written consent is not essential for diagnostic breast needle sampling procedures. It is up to the policy of the hospital. The main risks associated with breast biopsy are bleeding and hematoma formation, post-procedure pain, or discomfort (5). The core biopsy of the breast is a commonly performed procedure. Serious complications are rare. The most common problem is bleeding, which is usually easy to control at the time of the procedure. The bleeding rate has been reported as 1-3.9% for vacuum-assisted biopsies. Rarer complications include infection and abscess formation, pneumothorax, milk fistula formation, cosmetic deformity, and seeding of the tumor along the biopsy tract (6-7).

During the procedure, firstly the vascular assessment of the region of interest is done. This control process may be performed by color Doppler sonography. At mammography, a prominent vasculature must not be seen in the region of interest, too. Passes have to be made in a non-traumatic manner as much as possible. The entrance has to be performed by keeping the needle itself not the stem. After the acquisition of each core sample, the needle has to be re-inserted for further samples. During these subsequent passes specimens composed of blood are experienced due to the destruction of the breast and focal minimal hemorrhage (8). Between each of the sampling, we offer compression by the ultrasound probe.

According to our clinical ceremony, after a sonography-guided intervention, the patient is turned around herself and in the prone position; a passive breast compression is applied for about 10 minutes (Figure 1). In mammography, immediately after the intervention, the biopsy site is compressed against the compression plate of the device (active compression) for about 10 minutes (Figure 2) and then passive compression in the prone position is applied for 5 minutes to provide hemostasis, too.

After the procedure, pressure bandage can be applied if required (Figure 3). Although unconditionally abide by the rules, we encountered a 1.7% rate of bleeding. None of them did require surgery and at follow-up they all resorbed.

5. Conclusions

As a result, for hemostasis during breast interventions, questioning of the patients in terms of bleeding diathesis and drug usage, evaluation of the vascularity of the region before the process, and compression are the red rules. In our opinion, with adherence to these red rules, reasonable complication rates may be seen.

Conflict of interest statement
The author(s) declare(s) that there is no conflict of interests regarding the publication of this article.

References

1. Dickerson JM, BL Koch, JM Adams, MA Goodfriend, and LF Donnelly. Safety coaches in radiology: decreasing human error and minimizing patient harm. *Pediatr Radiol* **2010**; 40:1545-1551.
2. Frush KS. Fundamentals of a patient safety program. *Pediatric radiology* **2008**; 38: 685-689.
3. Grissinger M. Some Red Rules Shouldn't Rule In Hospitals. *P.T* **2012**; 37: 4-5.
4. Denton ER, S Ryan, T Beaconfield, and MJ Michell. Image-guided breast biopsy: analysis of pain and discomfort related to technique. *Breast* **1999**; 8: 257-260
5. O'Flynn EA, AR Wilson, MJ Michell. Image-guided breast biopsy: state-of-the-art. *Clin Radiol* **2010**; 65: 259-270.
6. Burbank F. Stereotactic breast biopsy: comparison of 14- and 11-gauge Mammotome probe performance and complication rate. *Am Surg* **1997**; 63: 988–995.
7. Parker SH, Klaus AJ. Performing breast biopsy with a directional, vacuum-assisted biopsy instrument. *Radiographics* **1997**; 17: 1233–1252.
8. Helbich TH, W Matzek, and MH Fuchsjager. Stereotactic and ultrasound-guided breast biopsy. *Euro Radiol* **2004**; 14:383-393.

Authors' ORCID
Irmak Durur Subasi
http://orcid.org/ 0000-0003-3122-4499
Fatih Alper
http://orcid.org/0000-0002-9483-8861
Mufide Nuran Akcay
http://orcid.org/0000-0001-8470-1741

https://dergipark.org.tr/tr/pub/ntms

ISSN:XXXX-XXXX RESEARCH ARTICLE

New Trends in Medicine Sciences

New Trend Med Sci 2020; 1(1): 29-34 https://dergipark.org.tr/tr/pub/ntms

Role of 6-Shogaol Against Ovarian Torsion Detorsion-Induced Reproductive Organ Damage

Mustafa Can Güler[1], Ayhan Tanyeli[1*], Ersen Eraslan[2], Fazile Nur Ekinci Akdemir[3]

[1] Department of Physiology, Faculty of Medicine, Atatürk University, Erzurum, Turkey
[2] Department of Physiology, Faculty of Medicine, Bozok University, Yozgat, Turkey
[3] Department of Nutrition and Dietetics, High School of Health, Ağrı İbrahim Çeçen University, Ağrı, Turkey

Article History
Received 30 May 2020
Accepted 01 June 2020
Published Online 15 June 2020

[*]***Corresponding Author***
Dr Ayhan Tanyeli
Department of Physiology,
Faculty of Medicine,
Atatürk University,
Erzurum, 25240, Turkey,
Phone: +905073631654,
E-mail: ayhan.tanyeli@atauni.edu.tr
ORCID:http://orcid.org/0000-0002-0095-0917

Abstract: 6-Shogaol (SHO) was examined on ovarian torsion detorsion (T/D) rat model to find out the potential beneficial results exist or not. 4 groups were composed to establish the experimental step. Sprague-Dawley female rats were used in the experiment. Each group included 8 rats and 32 rats were examined totally. Groups were designed as: Sham, T/D, T/D+Dimethyl sulfoxide (DMSO) and T/D+SHO groups. Sham group: Only abdominal incision was performed and closed without any additional process. T/D group: 3 hours torsion and 3 hours detorsion process were established following the abdominal incision. T/D+DMSO group: 0.3 ml of DMSO was given as intraperitoneal 30 minutes before detorsion. T/D+SHO group: SHO was administered as intraperitoneal 30 minutes prior to detorsion. At the end of the experiment, high doses of anesthesia were preferred for the euthanasia of the rats and the ovarian tissues were excised in order to obtain samples. Oxidative and pro-inflammatuar biomarkers such as MPO activity, OSI, IL-1β, MDA, TNF-α and TOS levels elevated significantly but TAS and SOD levels diminished in T/D group compared to sham group. On the other hand, SHO administration provided a decrease in oxidant and pro-inflammatuar parameters and elevated TAS and SOD levels, antioxidant mediators. Consequently, SHO demonstrated beneficial activity by protecting the ovarian tissues against ovarian injury induced by experimental T/D rat model.

Keywords: 6-Shogaol, Torsion Detorsion, Ovary, Rat.

1. Introduction

Ovarian torsion (O/T) is described as the partial or total rotation of the ovary and/or fallopian tube around the vascular axis (1). It is a gynecological emergency and frequently observed in reproductive years, especially in mid-20s (2). Reperfusion damage might be greater than ischemic harm which is also called ischemia reperfusion (I/R) injury (3). Ovarian torsion detorsion (T/D) reduced ovarian reserve levels and just surgical interventions are inadequate to cope with the loss in ovarian reserves (4).

Thereby, studies performed recently aimed to struggle against ovarian damage induced by ovarian T/D. In the main, molecules with anti-inflammatory and antioxidant features were examined (5-7).

Detorsion increases oxygen levels in ovarian tissues due to enhanced vascular reperfusion. Elevation in oxygen levels increase reactive oxygen species (ROS) production and thus causes tissue injury (8-10). ROS are detrimental to tissues because of lipid peroxidation.

Cite this article as: Güler MC, Tanyeli A, Eraslan E, Ekinci Akdemir FN. Role of 6-Shogaol Against Ovarian Torsion Detorsion-Induced Reproductive Organ Damage. *New Trend Med Sci* **2020**;1 (1): 29-34.

They play role in lipid peroxidation and thus, malondialdehyde (MDA) formation. MDA is a harmful molecule for cells (11). Total oxidant status (TOS) shows the oxidant activity while total antioxidant status (TAS) reflects the antioxidant actions (12). Interleukin-1 beta (IL-1β), tumor necrosis factor-alpha (TNF-α) and the other pro-inflammatory cytokines were found related with ischemic tissue injury in several studies (13, 14). Myeloperoxidase (MPO) exists in neutrophils and plays role in hydroxyl radical formation (15).
Various molecules have been used to cope with several organ injuries induced by I/R (16-20), but 6-Shogaol (SHO) has not been examined yet. SHO has been noted with a variety of properties such as anti-inflammatory (21) and antioxidative (22) features. SHO alleviated neuro-inflammation and eased cognitive deficits in an animal dementia model (23). Here, it was aimed to evaluate the possible beneficial effects of SHO against ovarian tissue injury.

2. Material and Methods

2.1. Experimental Animals and Ethical Approval

Atatürk University Experimental Animal Ethics Committee was the competent authority to confirm the study (07.11.2019/205). Atatürk University Experimental Animals Research and Application Center was preferred to follow out the experimental protocols and the animal care. They were housed in laboratory conditions including 12/12-h light and dark cycles, humidity of 55±5%, polypropylene-individual cages and a constant temperature of 22±2 °C. Standard rat feed and tap water were free to reach. The rats were fasted 12 hours prior to experiment but allowed to drink water.

2.2. Pre-operative Preparation

As a single species, 32 Sprague-Dawley female rats, each weighing 240-270 g were used to carry out the experiment. They were fastened up in supine position. For each rat, hair was removed from abdominal surgical site and surgical space was cleaned with povidone-iodine. 10 mg/kg i.p. xylazine hydrochloride (Rompun®, Bayer, İstanbul) and 60 mg/kg i.p. ketamine (Ketalar®, Pfizer, Istanbul) were used as anesthetic. SHO and Dimethyl sulfoxide (DMSO) were obtained from Sigma Aldrich Corporation.

2.3. Groups and Experimental Procedure

The rats were grouped randomly (4 groups, n=8). Sham group: Following the pre-operative preparations, abdominal area was incised and closed with 3-0 silk suture. T/D group: Surgical procedure was performed as in sham group and T/D model was carried out as described in a previous study (24). The ovaries, fallopian tubes and vascular structures were spun in clockwise 360 degrees and fixed via atraumatic clamps for 3 hours to block blood flow (torsion period). Following 3 hours, the clamps were removed to provide blood circulation for 3 hours (detorsion period). T/D+DMSO group: Exactly same steps were followed with T/D group but DMSO was given 0.3 ml intraperitoneally (i.p.) to the rats 30 minutes prior to detorsion. T/D+SHO group: Procedures in T/D group were applied but 20 mg/kg SHO was administered i.p. to the rats 30 minutes before detorsion period (25). When the experiment is over, ovarian tissues were excised and cleaned by washing and kept frozen until the analysis.

2.4. Biochemical Measurements

MDA assessment was performed due to lipid peroxidation determining by the methods of Ohkawa et al (26). Superoxide dismutase (SOD) activity determination depends on the protocol described by Sun et al (27). MPO activity is gauged using a method belongs to Bradley et al (28). TAS and TOS values were gauged via appropriate kits (Rel Assay Diagnostics). TOS to TAS ratio was used as the oxidative stress index (OSI). IL-1β and TNF-α levels were measured by commercially available kits (Elabscience, Wuhan, China).

2.5. Statistical Analyses

SPPS (version 20.0, for windows) programme was preferred for the data evaluation. One-way ANOVA test was used for data. For multiple comparisons, Tukey HSD test was performed. The results were demonstrated as Mean±Standard Deviation (SD). It was accepted as statistically significant when p value was below 0.05.

3. Results

No animal death has occurred as a result of surgical interventions in the experimental groups. Biochemical results were demonstrated in Table 1, Figure 1 and 2. MDA, TOS, MPO and OSI levels elevated but TAS and SOD values declined in T/D and T/D+DMSO groups compared to sham group. SHO administration significantly reduced the oxidative parameters and elevated antioxidant mediators (Table 1 and Figure 1, $p<0.001$). In addition, in the presented study, it was found that pro-inflammatory cytokine levels (TNF-α and IL-1β) in the tissue increased significantly due to T/D, while this cytokine levels decreased especially in the SHO treatment group ($p<0.001$, Figure 2).

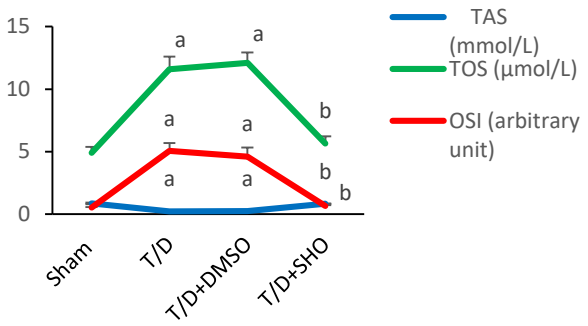

Figure 1: Mean±SD results of TAS, TOS and OSI levels belonging to all experimental groups. Green "a" demonstrates increase in TOS activity, red "a" shows elevation in OSI value and blue "a" means decrease in TAS level of T/D and T/D+DMSO groups. Green "b" reflects decrease in TOS activity, red "b" signs decline in OSI level and blue "b" shows elevation in TAS value of T/D+SHO group.

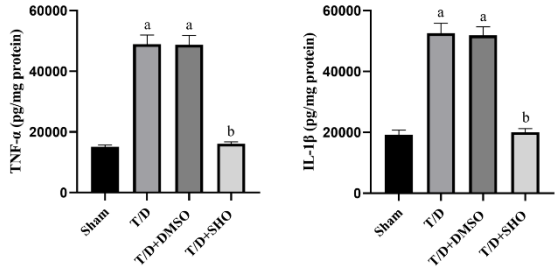

Figure 2: Mean±SD results of TNF-α and IL-1β level(s) belonging to all experimental groups. [a]p<0.001 compared to sham group. [b]p<0.001 compared to T/D group.

Table 1: Mean±SD results of SOD, MPO activities and MDA levels belonging to all experimental groups.

	Sham	T/D	T/D+DMSO	T/D+SHO
SOD (U/mg protein)	403,42±40,79	157,72±8,08[a]	161,08±8,86[a]	397,36±27,75[b]
MPO (U/g protein)	221667,60±16872,18	622968,94±50354,88[a]	647563,92±41799,52[a]	243475,92±23078,63[b]
MDA (µmol/g tissue)	58,07±2,38	129,04±11,49[a]	129,68±6,40[a]	64,78±4,68[b]

[a]p<0.001 compared to sham group. [b]p<0.001 compared to T/D group.

4. Discussion

O/T is the interruption of arterial supply due to the twisting of ovary and sometimes fallopian tube (29). Women, particularly in first three decades, expose to O/T which prevents blood flow and results in ovarian tissue injury (30). Women in reproductive age are more affected and thus, early intervention is crucial for the maintaining of fertility. Thereby, coping with torsion via applying detorsion is more valuable than applying the adnexectomy process (31). Detorsion is performed to able to restore blood flow to ovaries but on the other hand, it may lead to a much more damage than the ischemia did (32). This increased damage is related with high free oxygen radical levels which are generated due to excessive oxygen supply during reperfusion (33) and it is called as I/R injury (3).

Various studies have been carried out but a thoroughly mechanism for I/R still remains unclear. Nevertheless, free oxygen radicals have been linked to I/R injury (34). ROS leads to cell membrane, mitochondrial and DNA damage through lipid peroxidation and also induces cytokine generation (35). It has been presented oxidative stress related tissue injury in different experimental animal models (36-39). Ovarian I/R pathophysiology includes several factors and especially inflammation, oxidative stress and free oxygen radicals play a main role (40). MDA value raises during oxidative stress and high MDA levels point out lipid peroxidation (3).

MDA ruins membrane permeability and separates the cells (41). ROS occurs as a part of aerobic metabolism and it is scavenged by antioxidant system components including SOD (42). Antioxidant enzymes including SOD prevent oxidative stress (43). TAS and TOS are beneficial parameters on considering I/R injury (44). TAS and TOS have negative correlation between each other (12, 45). MPO is produced by neutrophils and plays role in hydroxyl radical generation (15). IL-1β and TNF-α are the samples of pro-inflammatory cytokines and show up in the beginning of inflammation. They induce neutrophil infiltration and release of free radicals (46, 47).

Various molecules which have antioxidant and anti-inflammatory effects were examined in different tissues to observe possible beneficial effects against I/R injuries (48-52). Ginger (Zingiber officinale rhizome) is a widespread medicinal herb preferred in traditional medicine especially for cough, asthma and cold (53). SHO, with high levels in ginger, performs anti-inflammatory and antioxidant features (54). SHO has been found effective against Alzheimer's disease, cerebral ischemia, sepsis-induced neuro-inflammation and Parkinson's disease (55, 56).

In several studies, SHO performed beneficial activities against inflammation, neuronal damage and even cancer (23, 56, 57-59).

Here, SHO was examined in ovarian T/D model in order to determine the potential beneficial effects against ovarian injury. In T/D and T/D+DMSO groups, TAS and SOD values diminished while OSI, MDA, TNF-α, MPO, TOS and IL-1β levels elevated compared to sham group. SHO treatment reversed these parameters. And in the light of these data, SHO reduced tissue injury in ovarian T/D rat model.

5. Conclusions

SHO attenued T/D-induced ovarian tissue injury. SHO succeed the amelioration activity through its antioxidant and anti-inflammatory features. As a natural herb derived agent, SHO may be a new potential molecule as to be evaluated in T/D related ovarian tissue injuries.

Conflict of interest statement
None
Financial Support
There is no financial support organization.

References

1. Tuncer AA, Bozkurt MF, Koken T, et al. The Protective Effects of Alpha-Lipoic Acid and Coenzyme Q10 Combination on Ovarian Ischemia-Reperfusion Injury: An Experimental Study. *Adv Med* **2016**; 2016 (8 pages) doi: 10.1155/2016/3415046
2. Sasaki KJ, Miller CE. Adnexal torsion: review of the literature. *J Minim Invasive Gynecol* **2014;** 21: 196-202
3. Carden DL, Granger DN. Pathophysiology of ischaemia-reperfusion injury. *J Pathol* **2000;** 190: 255-266
4. Ozler A, Turgut A, Soydinç HE, et al. The biochemical and histologic effects of adnexal torsion and early surgical intervention to unwind detorsion on ovarian reserve: an experimental study. *Reprod Sci* **2013;** 20: 1349-1355
5. Behroozi-Lak T, Zarei L, Moloody-Tapeh M, et al. Protective effects of intraperitoneal administration of nimodipine on ischemia-reperfusion injury in ovaries: Histological and biochemical assessments in a rat model. *J Pediatr Surg* **2017;** 52: 602-608
6. Kurt RK, Dogan AC, Dogan M, et al. Protective effect of colchicine on ovarian ischemia-reperfusion injury: an experimental study. *Reprod Sci* **2015**; 22: 545-550
7. Gungor AN, Turkon H, Albayrak A, et al. Does Omegaven have beneficial effects on a rat model of ovarian ischemia/reperfusion? *Eur J Obstet Gynecol Reprod Biol* **2014**; 181: 240-245
8. Sengul O, Ferah I, Polat B, et al. Blockade of endothelin receptors with bosentan limits ischaemia/reperfusion-induced injury in rat ovaries. *Eur J Obstet Gynecol Reprod Biol* **2013**; 170: 458-463
9. Park ES, Kim J, Ha TU, et al. TDAG51 deficiency promotes oxidative stress-induced apoptosis through the generation of reactive oxygen species in mouse embryonic fibroblasts. *Exp Mol Med* **2013**; 45: 35
10. Kohen R, Nyska A. Oxidation of biological systems: oxidative stress phenomena, antioxidants, redox reactions, and methods for their quantification. *Toxicol Pathol* **2002**; 30: 620-650
11. Yapca OE, Borekci B, Suleyman H. Ischemia-reperfusion damage. *Eurasian J Med* 2013; **2013**; 45:126-137
12. Erel O. A new automated colorimetric method for measuring total oxidant status. *Clin Biochem* **2005**; 38: 1103-1111
13. Karhausen J, Qing M, Gibson A, et al. Intestinal mast cells mediate gut injury and systemic inflammation in a rat model of deep hypothermic circulatory arrest. *Crit Care Med* **2013**; 41: 200-210
14. Zhuang P, Wan Y, Geng S, et al. Salvianolic Acids for Injection (SAFI) suppresses inflammatory responses in activated microglia to attenuate brain damage in focal cerebral ischemia. *J ethnopharmacol* **2017**; 198: 194-204
15. Van Antwerpen P, Boudjeltia KZ, Babar S, et al. Thiol-containing molecules interact with the myeloperoxidase/H2O2/chloride system to inhibit LDL oxidation. *Biochemical and biophysical research communications* **2005**; 337:82-88
16. Eraslan E, Tanyeli A, Polat E, et al. 8-Br-cADPR, a TRPM2 ion channel antagonist, inhibits renal ischemia-reperfusion injury. **2019**; *J Cell Physiol* 234: 4572-4581
17. Eraslan E, Tanyeli A, Polat E, et al. Evodiamine alleviates kidney ischemia reperfusion injury in rats: A biochemical and histopathological study. **2019**; *J Cell Biochem* 120: 17159-17266
18. Ozturk D, Erdogan DG, Tanyeli A, et al. The protective effects of urapidil on lung tissue after intestinal ischemia-reperfusion injury. **2019**; 44: 539-548
19. Tanyeli A, Guler MC, Eraslan E, et al. Barbaloin attenuates ischemia reperfusion-induced oxidative renal injury via antioxidant and anti-inflammatory effects. *Med Sci* **2020**; 9: 246-250
20. Dogan C, Halici Z, Topcu A, et al. Effects of amlodipine on ischaemia/reperfusion injury in the rat testis. **2016**; *Andrologia* 48: 441-452
21. Han Q, Yuan Q, Meng X, Huo J, Bao Y, et al. 6-Shogaol attenuates LPS-induced inflammation in BV2 microglia cells by activating PPAR-γ. *Oncotarget* **2017**; 8: 42001-42006
22. Na JY, Song K, Lee JW, et al. Pretreatment of 6-shogaol attenuates oxidative stress and inflammation in middle cerebral artery occlusion-induced mice. **2016**; *Eur J Pharmacol* 788:241-257
23. Moon M, Kim HG, Choi JG, et al. 6-Shogaol, an active constituent of ginger, attenuates

neuroinflammation and cognitive deficits in animal models of dementia. *Biochem Biophys Res Commun* **2014**; 449: 8-13

24. Celik M, Aksoy AN, Aksoy H, et al. Sildenafil Reduces Ischemia-Reperfusion Injury in Rat Ovary: Biochemical and Histopathological Evaluation. *Gynecologic and Obstetric Investigation* **2014**; 78:162-167

25. Hassan SM, Hassan AH. The possibility of using shogaol for treatment of ulcerative colitis. *Iran J Basic Med Sci* **2018**; 21:943-949

26. Ohkawa H, Ohishi N, Yagi K. Assay for Lipid Peroxides in Animal-Tissues by Thiobarbituric Acid Reaction. *Anal Biochem* **1979**; 95:351-358

27. Sun Y, Oberley LW, Li Y. A Simple Method for Clinical Assay of Superoxide-Dismutase. *Clin Chem* **1988**; 34: 497-500

28. Bradley PP, Priebat DA, Christensen RD, et al. Measurement of cutaneous inflammation: estimation of neutrophil content with an enzyme marker. *J Invest Dermatol* **1982**; 78: 206-209

29. McWilliams GD, Hill MJ, Dietrich CS. Gynecologic emergencies. *Surg Clin North Am* **2008**; 88: 265-283

30. Houry D, Abbott JT. Ovarian torsion: a fifteen-year review. *Ann Emerg Med* **2001**; 38: 156-169

31. Ugurel V, Cicek AC, Cemek M, et al. Antioxidant and antiapoptotic effects of erdosteine in a rat model of ovarian ischemia-reperfusion injury. *Iran J Basic Med Sci* **2017**; 20: 53-68

32. Zimmerman BJ, Granger DN. Reperfusion injury. *Surg Clin North Am* **1992**; 72: 65-83

33. Borekci B, Gundogdu C, Altunkaynak BZ, et al. The protective effect of dehydroepiandrosterone on ovarian tissues after torsion-detorsion injury: a stereological and histopathological study. *Eurasian J Med* **2009**; 41: 22-27

34. Wu MY, Yiang GT, Liao WT, et al. Current Mechanistic Concepts in Ischemia and Reperfusion Injury. *Cell Physiol Biochem* **2018**; 46: 1650-1667

35. Pınar N, Soylu Karapınar O, Özcan O, et al. Protective effects of tempol in an experimental ovarian ischemia-reperfusion injury model in female Wistar albino rats. *Can J Physiol Pharmacol* **2017**; 95: 861-875

36. Tanyeli A, Güzel D. Investigation into the Biochemical Effects of Barbaloin on Renal Tissue in Cecal Ligation and Puncture-Induced Polymicrobial Sepsis Model in Rats. *Southern Clinics of Istanbul Eurasia* **2019**; 30: 285-299

37. Tanyeli A, Güzel D. Alliin mitigates Cecal Ligation Puncture (CLP)-induced lung injury through antioxidant and antiinflammatory effects. *Turh J Sci* **2019**; 4: 46-59

38. Ekinci Akdemir FN, Tanyeli A. The Antioxidant Effect of Fraxin against Acute Organ Damage in Polymicrobial Sepsis Model induced by Cecal Ligation and Puncture. *Turk J Sci* **2019**; 4: 22-29

39. Tanyeli A, Eraslan E, Guler MC, Sebin SO, et al. Investigation of biochemical and histopathological effects of tarantula cubensis D6 on lung tissue in cecal ligation and puncture-induced polymicrobial sepsis model in rats. *Med Sci* **2019**; 8: 644-650

40. Refaie MMM, El-Hussieny M. Protective effect of pioglitazone on ovarian ischemia reperfusion injury of female rats via modulation of peroxisome proliferator activated receptor gamma and heme-oxygenase 1. *Int Immunopharmacol* **2018**; 62:7-14

41. Erkanli Senturk G, Erkanli K, Aydin U, et al. The protective effect of oxytocin on ischemia/reperfusion injury in rat urinary bladder. *Peptides* **2013**; 40: 82-88

42. Gough DR, Cotter TG. Hydrogen peroxide: a Jekyll and Hyde signalling molecule. *Cell Death Dis* **2011**; 2: 213

43. Tang Y, Li S, Zhang P, et al. Soy Isoflavone Protects Myocardial Ischemia/Reperfusion Injury through Increasing Endothelial Nitric Oxide Synthase and Decreasing Oxidative Stress in Ovariectomized Rats. *Oxid Med Cell Longev* **2016**; 2016; (14 pages) doi: 10.1155/2016/5057405

44. Yazici S, Demirtas S, Guclu O, et al. Using oxidant and antioxidant levels to predict the duration of both acute peripheral and mesenteric ischemia. *Perfusion* **2014**; 29: 450-465

45. Erel O. A novel automated method to measure total antioxidant response against potent free radical reactions. *Clin Biochem* **2004**; 37: 112-129

46. Eltzschig HK, Collard CD. Vascular ischaemia and reperfusion injury. *BrMed Bul* **2004**; 70: 71-86

47. Dinarello CA. Proinflammatory cytokines. *Chest* **2000**; 118: 503-518

48. Tanyeli A, Ekinci Akdemir FN, Eraslan E, et al. Role of p-Coumaric acid in Alleviating of the Intestinal Ischemia/Reperfusion Injury. *Kocaeli Med J* **2020**; 9: 166-173

49. Topdagi O, Tanyeli A, Ekinci Akdemir FN, et al. Preventive effects of fraxin on ischemia/reperfusion-induced acute kidney injury in rats. *Life Sci* **2020**; 242: in press 117217.

50. Güzel D, Tanyeli A. Investigation of Chlorogenic Acid (Cga) as An Antioxidant in Renal Ischemia-Reperfusion Injury: An Experimental Study. *Sakarya Med J* **2018**; 8: 410-415

51. Güzel D, Tanyeli A. Investigation of Oxidative Damage of Lung Tissue in Experimental Renal Ischemia Reperfusion Model and The Protective Effects of Chlorogenic Acid (CGA). *Sakarya Med J* **2018**; 8:260-265

52. Topdağı O, Tanyeli A, Ekinci Akdemir FN, et al. Higenamine decreases testicular damage injured by ischemia reperfusion: A biochemical study *Turk J Sci* **2019**; (4)2: 92-99

53. Mascolo N, Jain R, Jain SC, et al. Ethnopharmacologic investigation of ginger (Zingiber officinale). *J Ethnopharmacol* **1989**; 27: 129-140

54. Suekawa M, Ishige A, Yuasa K, et al. Pharmacological studies on ginger. I. Pharmacological actions of pungent constitutents,

(6)-gingerol and (6)-shogaol. *J Pharmacobiodyn* **1984**; 7: 836-848
55. Park G, Kim HG, Ju MS, et al. 6-Shogaol, an active compound of ginger, protects dopaminergic neurons in Parkinson's disease models via anti-neuroinflammation. *Acta Pharmacol Sin* **2013**; 34: 1131-1139
56. Shim S, Kim S, Kwon YB, et al. Protection by [6]-shogaol against lipopolysaccharide-induced toxicity in murine astrocytes is related to production of brain-derived neurotrophic factor. *Food Chem Toxicol* **2012**; 50: 597-602
57. Ha SK, Moon E, Ju MS, et al. 6-Shogaol, a ginger product, modulates neuroinflammation: a new approach to neuroprotection. *Neuropharmacol* **2012**; 63: 211-223
58. Butt MS, Sultan MT. Ginger and its health claims: molecular aspects. *Crit Rev Food Sci Nutr* **2011**; 51: 383-393
59. Kim MO, Lee MH, Oi N, et al. [6]-shogaol inhibits growth and induces apoptosis of non-small cell lung cancer cells by directly regulating Akt1/2. *Carcinogen* **2014**; 35: 683-691

Authors' ORCID
Mustafa Can Güler
http://orcid.org/0000-0001-8588-1035
Ayhan Tanyeli
http://orcid.org/0000-0002-0095-0917
Ersen Eraslan
https://orcid.org/0000-0003-2424-2269
Fazile Nur Ekinci Akdemir
https://orcid.org/0000-0001-9585-3169

NTMS New Trends in Medicine Sciences
https://dergipark.org.tr/tr/pub/ntms

ISSN:XXXX-XXXX CASE REPORT

New Trend Med Sci 2020; 1(1): 35-37 https://dergipark.org.tr/tr/pub/ntms

Perineal Hernia Causing Intestinal Obstruction After Abdominoperineal Resection and Permanent Colostomy

Afak Durur Karakaya[1*], Derya Salim Uymaz[2], Emre Altınmakas[1], Emre Balık[2], Bengi Gürses[1]

[1] Department of Radiology, Faculty of Medicine, Koc University, İstanbul, Turkey
[2] Department of General Surgery, Faculty of Medicine, Koc University, İstanbul, Turkey

Article History
Received 23 May 2020
Accepted 06 June 2020
Published Online 15 June 2020

[*]***Corresponding Author***
Afak Durur Karakaya
Department of Radiology
Faculty of Medicine
Koc University
İstanbul, Turkey
Phone: +905337111996
E-mail: afkarakaya@kuh.ku.edu.tr
ORCID:http://orcid.org/0000-0003-3604-6791

Abstract: Internal hernia is a rare condition. It has different etiology according to the anatomical region encountered. In this paper we present a case of intestinal obstruction due to herniation of the small intestine to the perineal area after permanent colostomy with resection of the abdominoperineal colon, rectum and anüs. © 2020 NTMS.

Keywords: Perineal Hernia.

1. Introduction

Perineal hernia (PH) is defined as protrusion of intraabdominal structures through a pelvic floor defect into the perineum. Small intestines, colon, bladder, omentum, and uterus can be involved (1,2). It is a rare complication of some surgeries including abdominoperineal resection, pelvic exenteration, and prostatectomy (3-6) and usually occurs within 4-12 weeks following operation. Minimally invasive methods are used for treatment.

2. Material and Methods

2.1. Case

A 46-year-old male patient underwent robotic abdominoperineal resection and permanent colostomy for locally advanced rectal cancer. On postoperative 6th day, he developed lack of bowel sounds, abdominal distension, and pain.

Computerized tomography (CT) of abdomen with intravenous (IV) and oral contrast material was performed for further assessment. CT showed herniation of the small bowel loops through a posterior pelvic floor defect into the perineum. Small bowel loops were diffusely dilated, and passage of oral contrast media was prolonged. Thickening of the hernia wall and increased enhancement were also noted (Figure 1a, 1b and 2). Subsequently, the patient underwent surgery which confirmed the diagnosis (Figure 3).

3. Discussion

Perineal hernia is a rare complication of major pelvic surgeries. The incidence of post-pelvic surgery is 7%, whereas the need for additional surgery is 0.2-0.6% (7-9). It has been attributed to weakness of levator muscle in pelvic floor.

Cite this article as: Durur Karakaya A, Uymaz DS, Altınmakas E, Balık E, Gürses B. Perineal Hernia Causing Intestinal Obstruction After Abdominoperineal Resection and Permanent Colostomy. *New Trend Med Sci* **2020**;1 (1): 35-37.

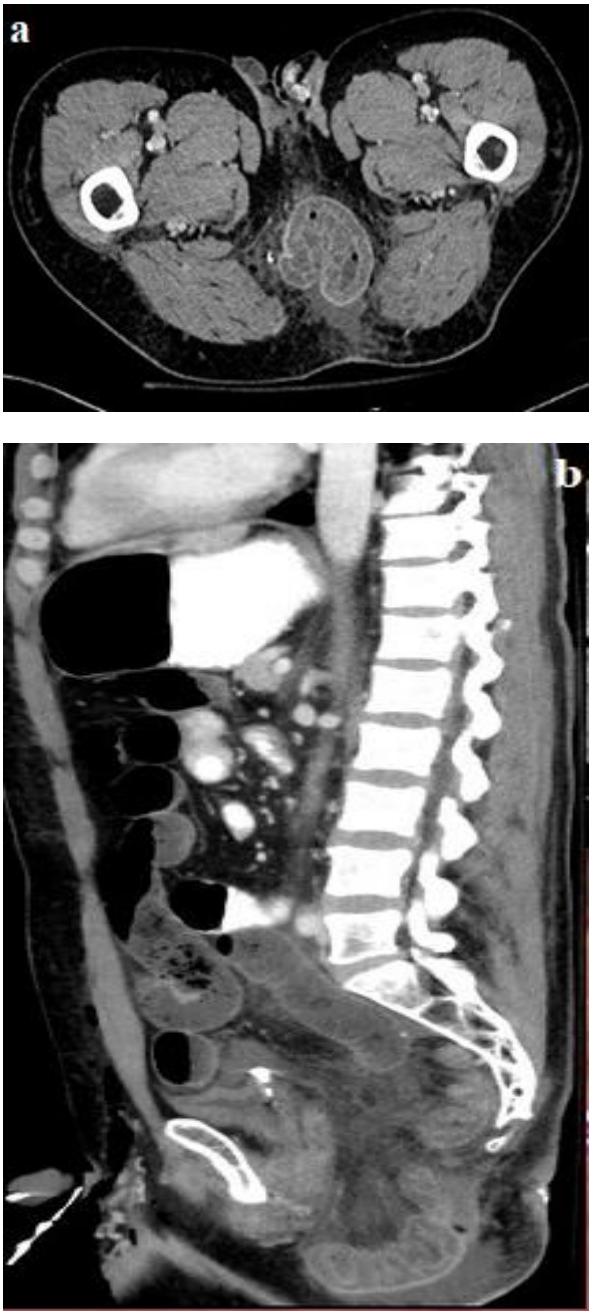

Figure 1a-b: Axial and coronal images of contrast-enhanced CT of abdomen shows herniation of the small bowel loops through a defect in the posterior pelvic floor into the perineum with thickening and increased enhancement of the hernia wall.

Figure 2: Dilatation of small bowel loops with air-liquid levels.

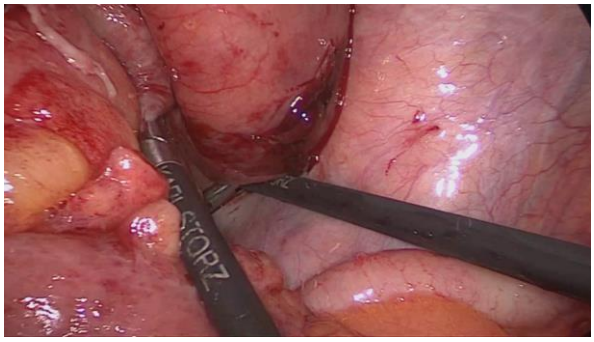

Figure 3: Herniated intestinal loops on laparoscopic images.

It has been reported that PH usually occurs within 4-12 weeks following surgery with no clinical symptoms. In our case, it developed on 6th day of the operation with symptoms of bowel obstruction. This condition can be repaired laparoscopically with transabdominal, perineal or combined abdominoperineal approach when necessary.

4. Conclusion

In our case, diagnostic laparoscopy was performed, and herniated bowel loops were reduced. In conclusion, diagnosis of PH should be considered in patients who are in early or late postoperative period of a major abdominopelvic surgery.

Conflict of interest statement

No conflict of interest.

References

1. Melich G, Lim DR, Hur H, Min BS, Baik SH, Arena GO, Gordon PH, Kim NK. Prevention of perineal hernia after laparoscopic and robotic abdominoperineal resection: review with illustrative case series of internal hernia through pelvic mesh. *Can J Surg* **2016**; 59(1): 54-58.
2. Maurissen J, Schoneveld M, Van Eetvelde E, Allaeys M. Robotic-assisted repair of perineal hernia after extralevator abdominoperineal resection. *Tech Coloproctol* **2019**; 23(5): 479-482.
3. Skipworth RJE, Smith GHM, Anderson DN. Secondary perineal hernia following open abdominoperineal excision of the rectum: report of a case and review of the literature. *Hernia* **2007**; 11: 541-545.
4. Rayhanabad J, Sassani P, Abbas MA. Laparoscopic repair of perineal hernia. *JSLS* **2009**; 13: 237-241.
5. Stephen R, Kavanagh DO, Neary PC. Laparoscopic repair of post- operative perineal hernia. *Case Rep Med* **2010**;10.1155
6. Dulucq JL, Wintringer P, Mahajna A. Laparoscopic repair of post-operative perineal hernia. *Surg Endosc* **2006**; 20: 414-418.
7. George 10 So JB, Palmer MT, Shellito PC. Postoperative perineal hernia. *Dis Colon Rectum* **1997**; 40: 954-957.
8. Aboian E, Winter DC, Metcalf DR, et al. Perineal hernia after proctectomy: prevalence, risks, and management. *Dis Colon Rectum.* **2006**; 49: 1564-1568.
9. Yokoyama Y, Kawai K, Kazama S, et al. A case of extraperitoneal stoma-associated internal hernia after abdominoperineal resection. *World J Surg Onc*ol **2014**: 6; 12: 141.

Authors' ORCID

Afak Durur Karakaya
http://orcid.org/0000-0003-3604-6791
Derya Salim Uymaz
http://orcid.org/0000-0002-2590-5872
Emre Altınmakas
http://orcid.org/0000-0002-0727-9230
Emre Balık
http://orcid.org/0000-0001-5751-1133
Bengi Gürses
http://orcid.org/0000-0002-2482-3445

NTMS New Trends in Medicine Sciences
https://dergipark.org.tr/tr/pub/ntms

ISSN:XXXX-XXXX CASE REPORT

New Trend Med Sci 2020; 1(1): 38-41 https://dergipark.org.tr/tr/pub/ntms

Ultrasound-Guided Infraclavicular Block for Closed Reduction Procedures on Pediatric Forearm Fractures: A Report of Ten Cases

Erdal Tekin[1], Muhammed Enes Aydin[2,3], Mehmet Cenk Turgut[4], Selahattin Karagoz[1], Habip Burak Ozgodek[2], Elif Oral Ahiskalioglu[2*]

[1]Department of Emergency Medicine, Atatürk University School of Medicine, Erzurum, Turkey
[2]Department of Anesthesiology and Reanimation, Atatürk University School of Medicine, Erzurum, Turkey
[3]Clinical Research, Development and Design Application and Research Center, Atatürk University, Erzurum, Turkey
[4]Department of Orthopedic Surgery, Atatürk University School of Medicine, Erzurum, Turkey

Article History
Received 27 May 2020
Accepted 03 June 2020
Published Online 15 June 2020

[*]***Corresponding Author***
Dr. Elif Oral Ahiskalioglu,
Ataturk University,
School of Medicine,
Department of Anesthesiology and Reanimation,
25070, Erzurum/Turkey
Phone: + 90 0442 344 87 96
Fax: +90 0442 2361301
E-mail: drelforl@hotmail.com
ORCID:http://orcid.org/0000-0003-1234-5973

Abstract: Procedural sedoanalgesia is a frequently used method in the emergency departments during pediatric interventional procedures and reductions. However, the method has some disadvantages such as respiratory and cardiac depression. Following the usage of ultrasonography in emergency medicine practice, the upper extremity nerve blocks have particularly gained popularity. However, the use of these blocks for pediatric cases is limited. With this series of ten cases, we aimed to share our successful ultrasound-guided infraclavicular block experiences in patients who had undergone forearm fracture for closed reduction. © 2020 NTMS.

Keywords: Pediatric, Fracture, Infraclavicular Block, Ultrasound, Anesthesia, Regional, Emergency Departments.

1. Introduction

Pediatric upper extremity traumas are one of the most common causes for emergency admission, and forearm traumas constitute majority of those admissions (1). Closed reduction has become the preferred treatment method for forearm fractures in pediatric patients (2). Similar to all extremity fractures, severe pain is experienced during forearm fracture reduction. Pain control is essential for comfort of both patient and practitioner during painful procedures, such as forearm fracture reduction. In the emergency department (ED), procedural sedoanalgesia (PSA) is most commonly used for this purpose. In most of the sedative and analgesic drugs used for PSA, serious side effects such as hypotension, cardiac, and respiratory depression are observed.

Furthermore, patients who have undergone sedoanalgesia must return to their previous consciousness status to be discharged from the ED; this results in late discharge of patients from the ED, thus increasing the associated workload of orthopedist and other physicians.

The perioperative analgesia and ultrasound-guided (UG) nerve blocks, which are used in anesthesia, are being used in the ED (3). The literature has demonstrated the performance and efficacy of brachial plexus block that has been performed for shoulder and elbow dislocation and fracture reduction in adult patients (4).

Cite this article as: Tekin E, Aydin ME, Turgut MC, Karagoz S, Ozgodek HB, Ahiskalioglu EO. Ultrasound-Guided Infraclavicular Block for Closed Reduction Procedures on Pediatric Forearm Fractures: A Report of Ten Cases. *New Trend Med Sci* **2020**; 1 (1): 38-41.

Pediatric ultrasound-guided infraclavicular brachial plexus block is frequently used in routine anesthesia practice for surgeries of hand and forearm. This block provides effective postoperative analgesia, and it is easy to use and safe. There are no case reports on brachial plexus block in the ED for children.
In this case series, we present UG infraclavicular block performance for closed reduction in ten patients with forearm fractures in the ED.

2. Material and Methods

2.1. Report of the cases

We decided to perform closed reduction under infraclavicular block in ten patients who were admitted to the ED with deformity and pain in the forearm due to falling down. Consent for publication has been obtained from closest relatives of patients. The ten patients were taken to the observation room and standard monitoring was performed (SpO_2, blood pressure, and electrocardiogram); subsequently, vascular access was entered and 0.09% NaCl was infused at the rate of 6 ml/kg/h.
The site to be intervened and the ultrasound probe were prepared in a sterile condition. When the patient was in a supine position, the head was reversed from the fractured side. The sterile USG probe was inserted into the lateral infraclavicular fossa, and the brachial plexus cords located around the axillary artery were monitored. After skin infiltration with local anesthetic, in-plane technique was used to enter the cranial to caudal direction. Between the posterior cord and the axillary artery, the probe was inserted at seven o'clock direction; no blood or air was detected by negative aspiration, and local anesthetic solution (0.5 ml/kg 1% lidocaine) was infused. After the blocks, sensory examination was performed within 20 minutes, and median, ulnar, and radial nerves were evaluated by hot and cold test. Sufficient anesthesia level was achieved, closed reduction was performed by orthopedic surgeon with traditional method. Wong Baker Scale (WBS) was used to evaluate pain before and after the procedure.
Data related to the case series block are shown in Table 1. For the ten patients (age, 10–14 years; WBS score, 6–10), WBS scores were recorded between 0 and 2 after UG infraclavicular block and during the reduction procedure. Block performance time ranged from 1 to 3 minutes. There were no complications or side effects during the procedures. It was observed that orthopedic practitioner and patient satisfaction were extremely good. The patients were discharged from the emergency department within 15–30 minutes after the forearm fracture reduction and after the control charts were constructed.

3. Discussion

In pediatric patients who undergo forearm fracture reduction at the ED, adequate analgesia levels are achieved with UG infraclavicular brachial plexus block. This helps avoid the potential risks associated with PSA.
Peripheral nerve blocks are frequently used by anesthesiologists for surgeries of upper extremity. Brachial plexus blocks of different levels, such as interscalene, supraclavicular, infraclavicular, and axillary blocks, have been defined for upper extremity procedures. It has been reported that infraclavicular block can be used in a shorter time and patient satisfaction is better in terms of pain.(5). Luftig J et al. demonstrated that the need for sedoanalgesia in the upper extremity procedures can be reduced by infraclavicular block in ED, and these blocks can be an alternative to PSA (6). In another case report of an adult patient, it was reported that infraclavicular block for wrist dislocation in the ED provided effective, rapid, and safe analgesia.(7) Many pediatric infraclavicular blocks have been reported to be used in anesthesia practice (8); however, in the monitoring of pediatric patients who undergo infraclavicular block, there were no reports on patients in the ED. In this case series, because pain was reduced after forearm fracture reduction, lidocaine -a short-acting local anesthetic- was used to prepare the analgesic solution for the block. The masking potential of infraclavicular block can delay the diagnosis of compartment syndrome particularly in pediatric population. We did not prefer using long-acting local anesthetic for early detection of complications after the reduction procedure. Therefore, we believe that lidocaine is a suitable drug in emergency procedures for rapid and early discharge of patients. In addition, all parents were informed about the compartment syndrome and discharged from the emergency room.
In this case series, the block was used to suitable and cooperative patients who aged 10 years and older.

Table 1: Demographic and procedural datas of cases. M:Male, F:Female, WBF: Wong Baker Faces Score , * Before Procedure, ** During and After Procedure.

	Age	*Sex*	*Weight*	*Fracture Localization*	*Block Performing Time (second)*	*WB** Score*	*WBF* Score*	*Duration of Analgesia (min)*	*Length of Stay ED (min)*
Case 1	10	M	40	Radius+Ulna	60	8	0	60	15
Case 2	13	F	55	Radius+Ulna	180	10	0	45	20
Case 3	10	F	35	Radius	75	8	0	75	30
Case 4	14	M	42	Radius+Ulna	90	6	0	90	30
Case 5	12	M	36	Radius+Ulna	125	8	2	70	25
Case 6	13	M	30	Radius+Ulna	150	10	0	80	30
Case 7	11	M	51	Radius+Ulna	160	7	0	90	30
Case 8	10	M	35	Radius+Ulna	120	9	2	120	30
Case 9	10	F	36	Radius	60	9	2	45	25
Case 10	14	M	44	Radius+Ulna	75	9	0	60	30

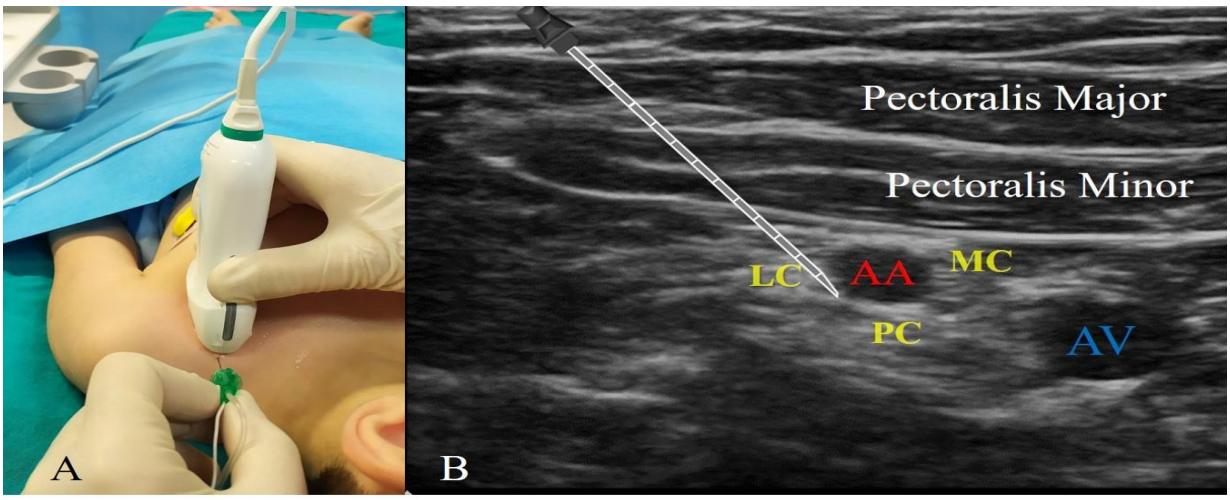

Figure 1. A) Patient and ultrasound probe orientation for infraclavicular block. **B)** Sonographic image of pediatric infraclavicular block, LC: Lateral cord, PC: Posterior cord, MC: Medial Cord, AA: Axillary Artery, AV: Axillary vein.

Although during blockade, pain was attempted to be alleviated by subcutaneous local anesthetic infiltration, it was obvious that in preschool children, mild sedoanalgesia support is needed to form the blocks. Therefore, we believe that use of this indication may be limited in preschool children. Although better results with multiple injections have been reported, we performed the block with a single-injection technique. We aimed to reduce block performance time and block-related pain by reducing the number of redirections. In the literature, it has already been reported that the same efficacy can be achieved with a single injection. Marie-Christine D et al. observed that the success rate was same regardless of the number of UG infraclavicular block injections (9). Additionally, single-injection technique was easier, faster, and more practical and reliable than multiple-injection technique (9, 10). In our study, we achieved successful and rapid effect with single-injection technique.

In conclusion, we suggest that ultrasound-guided UG infraclavicular block can be used as an effective, fast, and reliable method in selected pediatric patients with dislocation-reduction procedures in ED. Large randomized controlled studies with different pediatric age groups are required to validate these results.

Conflict of interest statement

The authors declare that they have no conflict of interest.

References

1. Hosseinzadeh P, Rickert KD, Edmonds EW. What's New in Pediatric Orthopaedic Trauma: The Upper Extremity. *J Pediatr Orthop* **2020**; 40: 283-286.
2. Zhu YL, Hu W, Yu XB, Wu YS, Sun LJ. A comparative study of two closed reduction methods for pediatric supracondylar humeral fractures. *J Orthop Sci* **2016**; 21: 609-613.
3. Frenkel O, Liebmann O, Fischer JW. Ultrasound-guided forearm nerve blocks in kids: a novel method for pain control in the treatment of hand-injured pediatric patients in the emergency

department. *Pediatr Emerg Care* **2015**; 31: 255-259.
4. Heflin T, Ahern T, Herring A. Ultrasound-guided infraclavicular brachial plexus block for emergency management of a posterior elbow dislocation. *The American journal of emergency medicine* **2015**; 33: 1321-1324.
5. Klein SM, Evans H, Nielsen K, Tucker M, Warner D, S S. Peripheral Nerve Block Technique for Ambulatory Surgery. *Anesthesia & Analgesia* **2005**; 101:1663–1676.
6. Luftig J, Mantuani D, Herring AA, A N. Ultrasound-Guided Retroclavicular Approach İnfraclavicular Brachial Plexus Block for Upper Extremity Emergency Procedures. *Am J Emerg Med* **2017**; 35: 773-777.
7. Akay S, Eksert S, Kaya M, Keklikci K, Kantemir A. Case Report: Ultrasound-Guided Infraclavicular Brachial Plexus Block for a Case with Posterior Elbow Dislocation. *J Emerg Med* **2017**; 53: 232-235.
8. Ponde V, Shah D, Johari A. Confirmation of local anesthetic distribution by radio-opaque contrast spread after ultrasound guided infraclavicular catheters placed along the posterior cord in children: a prospective analysis. *Paediatr Anaesth* **2015**; 25: 253-257.
9. Marie-Christine D, Simon L, Nicolas D et al. A Comparison of a Single or Triple Injection Technique for Ultrasound-Guided Infraclavicular Block: A Prospective Randomized Controlled Study. *Anesth Analg* **2009**; 109: 668-672.
10. Tran DQ, Bertini P, Zaouter C, Munoz L, RJ F. A Prospective, Randomized Comparison Between Single- and Double-İnjection Ultrasound-Guided İnfraclavicular Brachial Plexus Block. *Reg Anesth Pain Med* **2010** 35: 16-21.

Authors' ORCID
Erdal Tekin
http://orcid.org/0000-0002-6158-0286
Muhammed Enes Aydin
http://orcid.org/0000-0001-8491-6566
Mehmet Cenk Turgut
http://orcid.org/0000-0002-8642-6824
Selahattin Karagoz
http://orcid.org/0000-0002-0111-4347
Habip Burak Ozgodek
http://orcid.org/0000-0003-3042-9505
Elif Oral Ahiskalioglu
http://orcid.org/0000-0003-1234-5973

https://dergipark.org.tr/tr/pub/ntms

ISSN:XXXX-XXXX CASE REPORT

New Trend Med Sci 2020; 1(1): 42-45 https://dergipark.org.tr/tr/pub/ntms

Case of Calcaneus Fracture with Anderson-Fabry Disease; Anesthetized by Ultrasound Guided Popliteal Block

Muhammet Ahmet Karakaya[1]*, Belitsu Salgın[1], Kamil Darçın[1], İlker Eren[2], Ömür Erçelen[1]

[1] Department of Anesthesiology and Reanimation, Faculty of Medicine, Koc University, İstanbul, Turkey
[2] Department of Orthopedics and Traumatology, Faculty of Medicine, Koc University, İstanbul, Turkey

Article History
Received 24 May 2020
Accepted 30 May 2020
Published Online 15 June 2020

Corresponding Author
Muhammet Ahmet Karakaya
Koc University Hospital
Zeytinburnu/İstanbul, Turkey
Phone: +905332375730
E-mail: akarakaya@kuh.ku.edu.tr
ORCID:http://orcid.org/0000-0001-8026-4783

Abstract: Anderson-Fabry disease is a rare hereditary disease. It affects the entire body. Globotriacylceramide accumulates especially in the kidneys, myocardium, pancreas and lungs. All this accumulation can increase the risks of general anesthesia. Therefore, regional anesthesia methods can be used. We aimed to share with our anesthesia experience in a patient with Anderson-Fabry disease who was operated due to calcaneus fracture with ultrasound-guided popliteal block and sedation. © 2020 NTMS.

Keywords: Anderson-Fabry Disease, Nerve Blockade, Calcaneus fracture.

1. Introduction

Anderson-Fabry disease (FD) is a multisystemic, X-linked, hereditary disease that presents with vascular, endothelial and smooth muscle lysosomal glycosphingolipid accumulation caused by α-galactosidase A deficiency (in women) and absence (in men). It affects the whole body and causes progressive multiorgan dysfunction in childhood and early adulthood (1-3). Globotriacylceramide accumulates specifically in kidneys, the myocardium, pancreas and lungs. Among its many symptoms, the fact that it affects renal and respiratory functions and peripheral nervous system and causes cerebrovascular disease to hold clinical importance (2). There are only a few case reports on operations performed under general anesthesia in FD patients. In this report, we aim to share our anesthesia experience in a patient with FD undergoing operation for a calcaneal fracture surgery with a sciatic block and sedoanalgesia.

2. Material and Methods

2.1. Case

25 years-old male patient with FD and widespread angiokeratoma (Figure 1) presents with a calcaneus fracture following a fall-from-height. His previous medical history is remarkable for chronic neuropathic pain and myofascial pain with dizziness, day-time fatigue and tendency to over-sleep. He did not suffer from any heart failure symptoms and his echocardiography did not show any signs of heart failure also. His chest X-Ray was unremarkable. His diuresis was sufficient with BUN: 6 mg/dL, serum creatinine: 0,54 mg/dL and Urea: 12 mg/dL. However, his urine analysis revealed protein: 30 mg/dL and RBC: 62/µL. No pathology was detected after urological assessment. The patient was using agalsidaz alfa 0.2 mg/kg enzyme replacement therapy once every two weeks (Replagal®; Shire Human Genetic Therapies, Inc) and had no other regular medications.

Cite this article as: Karakaya MA, Salgın B, Darçın K, Eren İ, Erçelen Ö Case of Calcaneus Fracture with Anderson-Fabry Disease; Anesthetized by Ultrasound Guided Popliteal Block, *New Trend Med Sci* **2020**;1 (1): 42-45.

As premedication, he was given 2 mg midazolam. Sciatic nerve was visualized 5 cm above the popliteal fossa with an ultrasound (USG) device (Acuson Freestyle®, Siemens Medical Solutions USA, Inc.) lineer probe (5-13 MHz) in prone position. Peripheral block was applied in in-plane method with a USG compatible 50 mm, 22 gauge, short-bevel stimulating needle (Stimuplex D 50® ; B. Braun, Melsungen AG, Germany) with a 20 mL local anesthethic combination consisting of 200 mg lidocain (Aritmal® %2, Osel Inc.) and 50 mg bupivacaine (Marcaine®, Astrazeneca Inc.). (Figure 2). Blockage level was confirmed after 15 minutes with the pin-prick test and the patient was sedated with 50 µcg fentanyl (Talinat®, Vem Ilac Inc.) and 40 mg propofol (Propofol® %2, Fresenius Inc.) for the operation to proceed afterwards. 50 µcg fentanyl was added in the 70. minute of the operation. The operation lasted approximately 150 minutes. For post-operative analgesia management, the patient was prescribed intravenous patient-controlled analgesia (PCA) with a 10 µcg/mL fentanyl concentration, 10 µcg/h infusion rate, 15 µcg bolus dose and 15-minute lock period. The effect of the motor block at the postoperative 6th hour and the effect of the sensory block at the 7th hour disappeared. The patient defined pain at the end of post-operative 8th hour; however, his visual analogue score (VAS) remained below 3 throughout. In total, in the first 24 hours, 406 µcg fentanyl was given. His fentanyl infusion was stopped after 24 hours, and he received 180 µcg and 30 µcg in the second and third 24 hours, respectively.

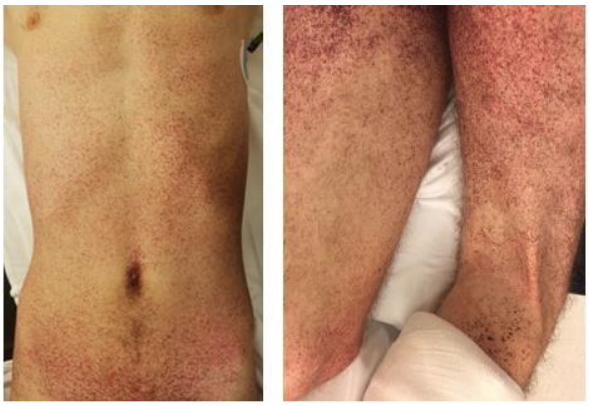

Figure 1: Fabry disease and widespread angiokeratoma.

3. Discussion

FD is a hereditary, X-linked, lysosomal storage disease with a multisystemic presentation. Galactosidase alpha (GLA) gene mutation, that codes for α-galactosidase A, results in glycolipid, especially globotriacylceramide (GL-3), accumulation in various cell types, especially in vascular endothelial and smooth muscle cells (1). It causes cellular dysfunction not only in skin, renal, heart, lung and brain cells but also in the gastrointestinal system and the cornea. Injured endothelial cells in large and small vessels and pathologic vascular smooth muscle cells cause early-onset hypertension, left ventricular hypertrophy, cardiac coronary disease and vertebrobasillar artery signs and symptoms with headache and tendency to over-sleep. Small fiber neuropathy may start early and presents with acroparesthesia of the hands and feet. FD includes a variety of symptoms, like acroparesthesia, cornea verticillata and stomach aches in childhood, angiokeratomes, renal failure, electrocardiography (ECG) anomalies in teenage years, and sleepiness, obstructive sleep apnea, hypertension, cardiomyopathy, kidney failure and strokes in adulthood. The most common first sign towards a diagnosis is the early onset renal failure (3). Given that it is a multisystemic disease, the preoperative evaluation should be individualized and careful. Those with FD are under great risk for surgery because of their renal and respiratory dysfunction, cerebrovascular and cardiovascular disease incidence and their intra-operative management may prove to be challenging. Pre-, intra-, and post-operatively, hypertension, cardiac valvular problems, arrhythmias, cardiac conduction pathologies, obstructive lung disease, hyperalgesia, proteinuria, renal damage and nausea-vomiting and malabsorption constitute the primary base of problems that can arise (3, 4). FD shows a variety of signs and symptoms that change with sex, severity and age that should be monitored and evaluated carefully pre-operatively (3). In addition, extra effort should be made to preserve organ functions in milder cases. In comparison with similar patient demographics without FD, chronic neuropathic and myofascial pain, dizziness, daytime fatigue, neurological signs like excessive sleeping and renal impairment were problems we had to manage with this case. No invasive monitoring was needed in our case; however, this could change with more intense symptoms. Dizziness was considered as a neurological symptom and therefore regional anesthesia was preferred over general anesthesia.

Renal pathologies are among the distinguishing signs of FD and usually are the cause of death between 30-50 years old. Polyuria because of concentrating incapacity might be the first sign and is always followed by rapidly progressing proteinuria (4). Therefore, the proteinuria in our patient was probably a sign of fore coming renal failure.

Spheric concentric ventricular hypertrophy, valvular anomalies, cardiac conduction defects are seen commonly in men with FD over 30 years old. In addition, lung and airway diseases are significantly worse in men and smokers. It is known that many patients with FD have explicit airway obstructions and intrinsic airway diseases (2, 4). This was one of the most important reason of why we chose regional anesthesia in this case.

None of the medications used were contraindications in enzyme replacement therapy. As a result, agalsidase alfa treatment should be prescribed as usual after regional anesthesia.

Using USG guidance for peripheral nerve blocks is a considerably new method in anesthesia but has grown rapidly over the past years. Of its reported benefits, faster initiation of block effect, higher success rates and longer operative and post-operative analgesia management can be counted. Better pain management, quicker return of gastrointestinal motility, lesser opioid use and resulting decreased nausea, decreased hospitalization times, better preservation of respiratory functions and easier involvement in physical therapy made regional anesthesia extremely popular in recent times (5, 6). In addition to there being very few case reports on general anesthesia and FD patients on literature, we did not come across one that has performed a peripheral block. Additionally, there is little information on peripheral blocks and post-operative analgesia. Planning of peri-operative pain management is of top-most importance for the patient. However, there is still no specific protocol to follow and both the patient and the surgeon's individual circumstance and preferences make it challenging to construct one (5, 6).

We preferred opioids instead of non-steroid anti-inflammatory drugs in post-operative analgesia to prevent renal damage. Recently, intravenous lidocaine has been used successfully to manage pain-episodes in FD patients (1). Therefore, we chose lidocaine to be the half of our local anesthesia in the peripheral block. Lastly, opioids are shown as effective in pain episode' management; however, it should be kept in mind that chronic use of opioids may result in constipation, addiction and drowsiness (3, 4). Additionally, if renal functions are compromised, wanted and unwanted effects of opioids may be prolonged and stressed. Accumulation of morphine and its metabolites may cause post-operative delayed respiratory depression. Fentanyl was chosen since it's metabolized in liver and has no toxic metabolite and is therefore safe to use in renal damage (7).

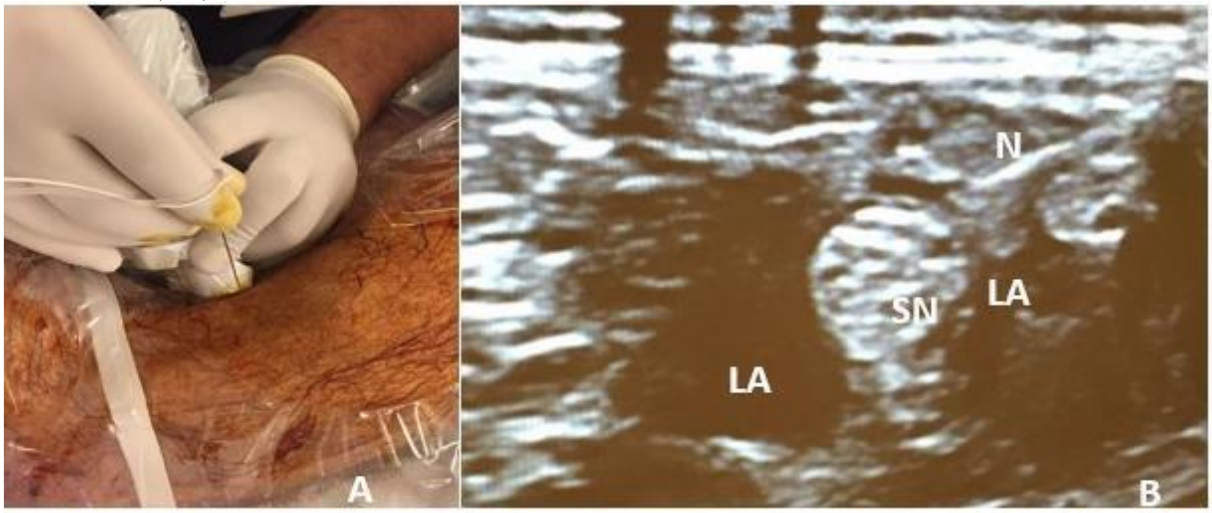

Figure 2: A. Sciatic Nerve block, USG guided in in-plane method. **B.** Sciatic Nerve USG view. LA: Local anesthetic, SN: Sciatic Nerve, N:Needle.

4. Conclusions

In conclusion, Anderson-Fabry disease' preoperative evaluation should focus on heart, brain, lung and renal organ damage assessment. Extra caution should be taken to preserve these organ functions. Our clinical experience showed peripheral blocks can be used in FD patients. We think careful post-operative pain management is additionally important in these patients who are inclined for chronic pains. We believe regional anesthesia practices are extra advantageous in these favored patients whom airway management is unpredicted.

Conflict of interest statement

No conflict of interest.

References

1. Politei JM, Bouhassira D, Germain DP, et al. Pain in Fabry disease: practical recommendations for diagnosis and treatment. *CNS Neurosci Ther* **2016**; 22: 568–576
2. Woolley J, Pichel AC. Peri-operative considerations for Anderson-Fabry disease. *Anaesthesia* **2008**; 63: 101–102.
3. Krüger S, Nowak A, Müller T, General Anesthesia and Fabry Disease: A Case Report. *Cases-Anesthesia-Analgesia* **2017**; 8: 247-249
4. Sorbello M, Veroux M, Cutuli M, et al. Anaesthesiologic protocol for kidney transplantation in two patients with Fabry disease: a case series. *Cases J* **2008**; 1: 321.

5. Fredrickson MJ, Kilfoyle DH, Neurological complication analysis of 1000 ultrasound guided peripheral nerve blocks for elective orthopaedic surgery: a prospective study. *Anaesthesia* **2009**; 64: 836-844.
6. Liu Q, Chelly JE, Williams JP, Gold MS. Impact of peripheral nerve block with low dose local anesthetics on analgesia and functional outcomes following total knee arthroplasty: a retrospective study. *Pain Med* **2015**; 16: 998-1006
7. Murtagh FE, Chai MO, Donohoe P, Edmonds PM, Higginson IJ. The use of opioid analgesia in end-stage renal disease patients managed without dialysis: recommendations for practice. *J Pain Palliat Care Pharmacother* **2007**; 21: 5–16.

Authors' ORCID
Muhammet Ahmet Karakaya
http://orcid.org/0000-0001-8026-4783
Belitsu Salgın
http://orcid.org/0000-0003-3134-3447
Kamil Darçın
http://orcid.org/0000-0002-0004-8392
İlker Eren
http://orcid.org/0000-0003-2965-7690
Ömür Erçelen
http://orcid.org/0000-0002-5508-1077

https://dergipark.org.tr/tr/pub/ntms

ISSN:XXXX-XXXX CASE REPORT

New Trend Med Sci 2020; 1(1): 46-50 https://dergipark.org.tr/tr/pub/ntms

Stomach Glomus Tumor

Fatma Altıntaş Güzel[1]*, Mustafa Göksu[2], Ayşegül Örmeci[3]

[1] Department of Pathology, Tunceli State Hospital, Tunceli, Turkey
[2] Department of General Surgery, T. R. Ministry of Health Adıyaman University Education and Research Hospital, Adıyaman, Turkey
[3] Department of Pathology, T. R. Ministry of Health Adıyaman University Education and Research Hospital, Adıyaman, Turkey

Article History
Received 03 June 2020
Accepted 11 June 2020
Published Online 15 June 2020

Corresponding Author
Fatma Altıntaş Güzel
Department of Pathology
Tunceli State Hospital
Tunceli Turkey
Phone: +905300689768
E-mail: faltintasguzel@gmail.com
ORCID:http://orcid.org/0000-0003-1142-9366

Abstract: A glomus tumor is a benign mesenchymal tumor developing either from the neuromuscular glomus cells or from the glomus bodies of the smooth muscle cells. While the gastrointestinal system is rarely the location for glomus tumors, extracutaneous glomus tumors are often encountered in the stomach. This study presents a 36-year-old male patient who applied to the hospital with complaints of nausea and vomiting accompanied by a stomach pain that gradually increased over two days and the endoscopic inspections have revealed a subepithelial lesion, which was removed with partial gastrectomy. Histopathological evaluations have shown that the tumor is based on the submucosal layer and had infiltrated into the muscular mucosa. Histopathologic evaluations and immunohistochemical staining had revealed the tumor as a glomus tumor. © 2020 NTMS.

Keywords: Stomach Mesenchymal Tumors, Glomus Tumor, Pathology.

1. Introduction

A glomus tumor (GT) is a benign mesenchymal tumor developing either from the neuromyoarterial glomus cells located in the arteriovenous intersection points or from the glomus bodies of the smooth muscle cells (1-3). GT's represent approximately 1.5% of all soft tissue tumors (4). There are two different forms for GT's, namely the sporadic form in which the lesions are solitary and the familial form which is often encountered in children and in which the lesions are multifocal. GT sporadic form is predominantly encountered in women between the ages 50 and 60 (5-7).

GT's are generally located in the skin or subcutaneous tissues. In young adults, GT's are often encountered in soft tissues and distal extremity nail folds and occur as painful lesions (4, 6, 8-10). While the stomach is rarely the target location for them, extracutaneous GT's are still most commonly encountered in the stomach and represent approximately 2% of all benign stomach tumors. Gastric glomus tumors (GGT) often localize into the submucosa of the antrum and are solitary, round-shaped lesions. These tumors are either asymptomatic or are accompanied by bleeding and epigastric pain when they cause ulcerations (8, 11-13). Tumor sizes vary between 1 and 7 cm, and their mitotic activities are usually low. Malignant behaviors are unexpected for GGT's (14). GGT's are commonly mistaken for gastrointestinal stromal tumors (GIST), leiomyomas, and carcinoid tumors (15). The definitive diagnosis for GGT is based on the pathological and immunohistochemical evaluations of the resected material (5, 16, 17).

2. Material and Methods

2.1. Case

The case in the present study is a 36-year-old male patient who applied with complaints of increasing stomach pain for two days accompanied by nausea and vomiting. Physical inspection revealed sensitivity in the epigastric region and upper gastrointestinal endoscopy has shown the presence of a sub-epithelial lesion of 3-4 cm size, located in the large curvature of

the antrum and covered with normal epithelial tissue. There is no Computer Tomography (CT) information regarding the stomach or any stomach mass for the case.

The patient was surgically operated and the lesion located in the large curvature of the antrum was palpated first and then was removed with stomach wedge resection.

A tumoral lesion was observed during the inspection of the partial gastrectomy material, which was 1.8x1.5x0.6 cm in size and started from the submucosa and infiltrated into the muscular mucosa. The section surface of the tumor was grey-white and the tumor was solid in structure with point-like focal bleeding spots. The distance of the tumor to the surgical border was 0.4 cm.

The inspection of HE sections has shown that the tumoral lesion starts from the lamina propria and infiltrates through the muscular mucosa. The tumor consists of monotonous cells that form large nodules separated from each other with thick bands and with eosinophilic cytoplasms that sometimes contain 1-2 nucleoles with dispersed chromatins. Inside the tumor nodules, vascular gaps surrounded with glomus cells with round-shaped nucleus were observed along with neural bundles and perineural invasion was present. Lymphovascular invasion was also present, while no atypical mitosis or necrosis was observed. Similarly, there was no serosal infiltration.

The mucosa at the tumor surface is intact and no tumor tissue was observed along the surgical border (Figure 1A-F). Neuroendocrine tumors, small round blue cell tumors and GIST's were considered for the differential diagnosis. AE1/AE3, CD45, Chromogranin A, Synaptophysin, CD56, Ki67, CD117, CD34, SMA and Caldesmon stainings were applied as part of immunohistochemical evaluations and the tumor cells represented strong SMA and Caldesmon positivities, along with pale Synaptophysin positivity. AE1/AE3, CD117, CD56, S100, CD34 and Chromogranin A were all negative. Ki67 proliferation index was around 2-3% (Figure G-K). The fact that CD117 was negative reduced GIST potential. Considering all of these findings, the case was evaluated as a glomus tumor case.

3. Discussion

In histomorphological terms, benign GT's are localized in dilated vein walls and have a uniform nucleus and they consist of small, uniform, round glomus cells. These cells are localized around the vein walls in the form of nests.

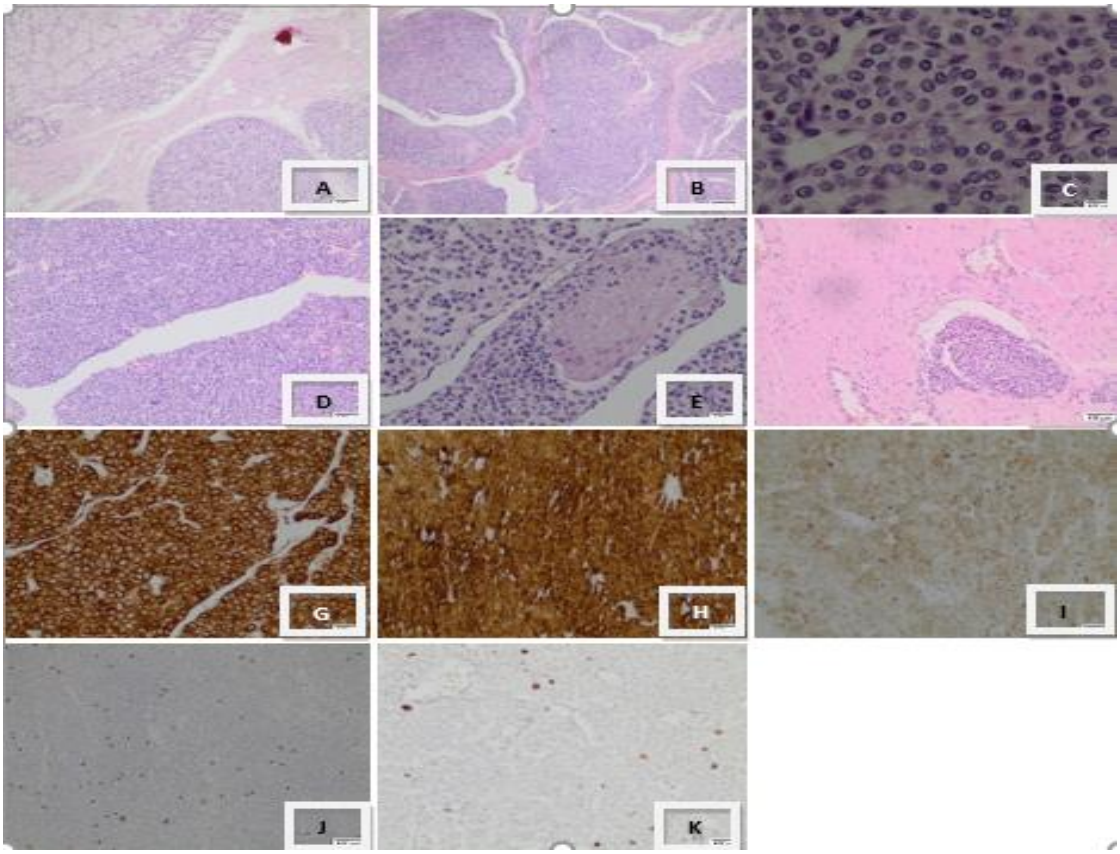

Figure 1: A. Tumor-mucosa relation, B. Nodular structure, C. Tumor cells, D. Vascular structures, E. Perineural invasion, F. Lymphovascular invasion, G. S100 positive, H. Caldesmon positive, I. Weak synaptophysin positive, J. CD117 negative, K. Ki67 (2-3%).

GT's can be separated into two groups as glomangioma and glomangiomyoma tumors based on the glomus cells, the vascular structures and the smooth muscle intensity involved. The most frequent variant is the solid glomus tumor which displays glomus cell islets surrounded by capillary veins and hyalinised stroma or stroma with myxoid changes. In glomangioma, a vein proliferation surrounded by with glomus cell nests with irregular borders can be observed, similar to that of cavernous hemangioma. Glomangiomyoma, on the other hand, is characterized by elongated glomus cells that are similar to mature smooth muscle cells (14-18). GT's have been defined by French researchers Barre and Manson in 1924 and by Russian researchers Markelov in 1934 and Liveschin in 1936. Histopathological findings of the tumor have been defined by Murray in 1942 (19). The first identification of GT in the stomach was performed by Key et al. in 1951 (20). GT's are often localized in the antrum or prepyloric region, are solitary and usually display submucosal nodule formations accompanied by gastrointestinal bleeding. Disturbances in the epigastric region, nausea and vomiting can also accompany these findings (3, 13). In the case of this study, an increasing sense of stomach pain and accompanying nausea and vomiting were present.

Gastric submucosal tumors (GMT) are neoplasms localized in the submucosa of the stomach wall or to the muscularis propria and are usually benign, but sometimes can become malignant. The most frequent malignant GMT is the GIST which 100 times more frequent than the GGT's. Unlike GIST's, GGT's are benign tumors that are c-Kit negative (6).

GT's are often seen as sub-epithelial masses during the endoscopic inspections, making endoscopic biopsy somewhat less effective in diagnosis (12, 17). The endoscopy performed in the present case has shown a submucosal mass of 3-4 cm size covered with regular mucosa and a mass of 2 cm size was found during the surgery. This is also indicative that endoscopic biopsy is not very accurate for the diagnosis and determination of lesion size.

It is thereby necessary to perform differential diagnosis on GT's to separate them from GIST's and other mesenchymal tumors. The pre-surgery diagnosis of GGT is relatively challenging. Endoscopic biopsies are unable to provide ample amounts of sample to represent the whole lesion in cases where the lesion is located deep in or is submucosal (11). Studies performed with barium usually reveal submucosal masses with either smooth mucosal surfaces or with ulcerations located in the large quarter of the antrum. Endoscopic USG and CT's are important for the diagnosis of gastric submucosal tumors, where findings of heterogenous hypoechoic round-shaped masses support the GT diagnosis.

In CT, GT's show up as submucosal masses of homogenous density with regular and smooth borders. In contrast viewing, the arterial phase shows strong enhancement, while the portal venous phase shows persistent enhancements. These viewing techniques can differentiate GT's from other stromal or mesenchymal tumors and can provide information regarding the tissue the tumor is based upon (17, 21-23). In the case of the present study the endoscopic biopsy failed to provide a definitive diagnosis and only revealed the presence of a submucosal mass. In CT, no information was provided for the stomach or any masses within it. The diagnosis of the detected mass could only be provided with the histopathological inspection of the surgery material. These events show that radiological scanning methods can fail to accurately diagnose GT's, and the resection and histopathological evaluation of the tissue are essential for a correct diagnosis.

From the histopathological perspective, GGT's consist of monotonous small round cell layers and vascular gaps (24, 25). While stomach GT's are often benign, they can nevertheless be malignant in rare cases. Felope et al. have defined certain criteria for malignant glomus tumors and have stated that a size larger than 2 cm, a deep localization (subfascial or organ), atypical mitosis, atypical nuclei and the presence of more than 5 mitoses' in 50 BBA's are findings that support malignity (3, 13, 18, 25). In the case of the present study, the only malignancy criteria is the fact that the lesion is located in an organ and none of the other criteria are met.

In differential diagnosis, leiomyomas, carcinoid tumors and paragangliomas should be considered.

Immunohistochemical staining is important for the differential diagnosis of the tumor. The tumor cells are SMA, calponin, vimentin, collagen type-IV and synaptophysin (dot-like) positive, while they are desmin, cytokeratin (AE1/AE3b), EMA, creatinine kinase, chromogranin A, p53, NSE, DOG1, s100, c-Kit negative. Gastrointestinal endocrine tumors are actin negative, but half of the GIST's are positive for it. The fact that GIST's lack dilated capillaries and are c-Kit and DOG-1 positive help differentiate them from GT's (13, 24). Leiomyomas and leiomyosarcomas are differentiated from GIST's with their desmin and SMA positivities and c-Kit and CD34 negativities (23).

While morphologically GT's can be confused with grade-1 neuroendocrine tumors, the presence of nest structures surrounded by thin veins and trabecular pattern in the neuroendocrine tumors, along with synaptophysin, chromogranin, cytokeratin, CD56 and NSE positivity and SMA and CD34 negativity, helps with their differentiation (26). GT differentiation with paraganglioma, on the other hand, is performed considering the chromogranin A and S-100 positivities and SMA negativity, along with histopathological findings of thin-wall organoid pattern that is rich in vein structures, presence of Zellballen pattern, nucleomegaly, hyperchromasia and wide eosinophilic cytoplasma (24,26).

GGT's are rarely encountered benign tumors and the results show that endoscopic biopsy has limited value in their diagnosis. Endoscopic USG and CT are important for accurate diagnosis, but the definitive

diagnosis requires resection of the mass and the histopathological evaluation of the sample.

Conflict of interest statement
No conflict of interest.

References

1. Batra RB, Mehta A, Rama Mohan PV, Singh KJ. Glomus tumor of the stomach. *Indian J Pathol Microbiol* **2009**; 52:77-9.
2. Liu KL, Wang HP, Tseng WY, Shun CT, Chen SJ, Tsang YM. Glomus tumor of the stomach: MRI findings. *AJR Am J Roentgenol* **2005**; 185: 1190-1192.
3. Dong LL, Chen EG, Sheikh IS, Jiang ZN, Huang AH, Ying KJ. Malignant glomus tumor of the lung with multiorgan metastases: case report and literature review. *OncoTargets Ther* **2015**; 8: 1909-1914.
4. Essia Saïji M, Guillou L, Hornick JL. Epithelioid and Epithelial-like Tumors; Glomus Tumor. Practical soft tissue pathology: a diagnostic approach. Hornick JL (Ed). 1600 John F. Kennedy Blvd. Ste 1800 Philadelphia, PA 19103-2899: by Saunders, an imprint of Elsevier Inc. **2013**. pp. 162-165.
5. Lee HW, Lee JJ, Yang DH, Lee BH. A clinicopathologic study of glomus tumor of the stomach. J Clin Gastroenterol 2006; 40: 717-720.
6. Miettinen M, Paal E, Lasota J, Sobin LH. Gastrointestinal glomus tumors: a clinicopathologic, immunohistochemical, and molecular genetic study of 32 cases. Am J Surg Pathol 2002; 26: 301-311.
7. Wang LM, Chetty R. Selected unusual tumors of the stomach: a review. Int J Surg Pathol 2012; 20: 5-14.
8. Fang HQ, Yang J, Zhang FF, Cui Y, Han AJ. Clinicopathological features of gastric glomus tumor. World J Gastroenterol 2010; 16: 4616-4620.
9. Orellana F, Onetto C, Balbontin P, et al. Gastric glomus tumor: report of one case and review. Endoscopy 2011; 43(2): 71-72.
10. Tsuneyoshi M, Enjoji M. Glomus tumor: a clinicopathologic and electron microscopic study. Cancer 1982; 50: 1601-1607.
11. Vassiliou I, Tympa A, Theodosopoulos T, Dafnios N, Fragulidis G, Koureas A, Kairi E: Gastric glomus tumor: a case report. World J Surg Oncol 2010, 8: 19.
12. Nascimento EF, Fonte FP, Mendonca RL, Nonose R, de Souza CA, Martinez CA. Glomus tumor of the stomach: a rare cause of upper gastrointestinal bleeding. Case Rep Surg 2011; 2011: 371082.
13. Nagtegaal I, Odze R, Klimstra D, et al. The 2019 WHO classification of tumours of the digestive system - Glomus tumor. Histopathol 2019: 473-474.
14. Miettinen M. Glomus Tumor, Sinonasal Hemangiopericytoma, and Myopericytoma - Glomus Tumor. Modern soft tissue pathology: tumors and non-neoplastic conditions Miettinen M.(Ed) 32 Avenue of the Americas, New York, NY 10013-2473, USA: Cambridge University Press, 2010; 648-649.
15. Campbell MJ, Irani S, Olgac S, Chang LC: Laparoscopic resection of a gastric glomus tumor. Indian J Surg 2011; 73: 230-232.
16. Bauerova L, Gabris V, Honsova E, Povysil C. Glomus tumor of the stomach: a case report and review of the literature. Cesk Patol 2011, 47: 128-129.
17. Kang G, Park HJ, Kim JY, Choi D, Min BH, Lee JH, Kim JJ, Kim KM, Park CK, Sohn TS, Kim S: Glomus tumor of the stomach: a clinicopathologic analysis of 10 cases and review of the literature. Gut and liver 2012; 6: 52-57.
18. Folpe AL, Fanburg-Smith JC, Miettinen M, Weiss SW: Atypical and malignant glomus tumors: analysis of 52 cases, with a proposal for the reclassification of glomus tumors. Am J Surg Pathol 2001; 25: 1-12.
19. Chabowski M, Paszkowski A, Skotarczak J, et al. Glomus Tumor of the Stomach - A Case Report and A Literature Review. Pol Przegl Chir 2016; 88: 356-358.
20. Kay S, Callahan WP, Jr., Murray MR, Randall HT, Stout AP: Glomus tumors of the stomach. Cancer 1951; 4: 726-736.
21. Yan SL, Yeh YH, Chen CH, Yang CC, Kuo CL, Wu HS. Gastric glomus tumor: a hypervascular submucosal tumor on power Doppler endosonography. J Clin Ultrasound 2007; 35: 164-168.
22. Imamura A, Tochihara M, Natsui K, et al. Glomus tumor of the stomach: endoscopic ultrasonographic findings. Am J Gastroenterol 1994; 89: 271-272.
23. Agawa H, Matsushita M, Nishio A, Takakuwa H. Gastric glomus tumor. Gastrointest Endosc 2002; 56: 903.
24. Lin YM, Chiu NC, Li AFY, Liu CA, Chou YH, Chiou YY. Unusual gastric tumors and tumor-like lesions: Radiological with pathological correlation and literature review. World J Gastroenterol 2017; 23: 2493-2504.
25. Lindberg MR, Lucas D, Gardner JM, Cassarino DS, Stallings-Archer K. Glomus Tumors (and Variants). Dıagnostıc Pathology: Soft Tıssue Tumors, Second Edıtıon. Edited by Lindberg MR. 2 ed. Philadelphia, PA 19103-2899: Elsevier, 2016: 338-43.
26. Vig T, Bindra MS, Kumar RM, Alexander S. Gastric Glomus Tumour Misdiagnosed as Gastric Carcinoid: An Unfamiliar Entity with Aids to Diagnosis and Review of Literature. J Clin Diagn Res 2017; 11:32-33.

Authors' ORCID
Fatma Altıntaş Güzel
http://orcid.org/0000-0003-1142-9366
Mustafa Göksu

http://orcid.org/0000-0002-1807-6957
Ayşegül Örmeci
http://orcid.org/0000-0002-4426-9787

NTMS New Trends in Medicine Sciences
https://dergipark.org.tr/tr/pub/ntms

ISSN:XXXX-XXXX LETTER TO THE EDITOR

New Trend Med Sci 2020; 1(1): 51-52 https://dergipark.org.tr/tr/pub/ntms

The Effect of Coronavirus on the Liver and Histopathological Findings

Sevilay Özmen[1*], Onur Ceylan[1]

[1] Department of Pathology, School of Medicine, Atatürk University, Erzurum, Turkey

Article History
Received 03 June 2020
Accepted 08 June 2020
Published Online 15 June 2020

Keywords: Coronavirus, Liver, Histopathological Findings.

[*]***Corresponding Author***
Dr Sevilay Özmen
Department of Pathology,
School of Medicine,
Atatürk University,
Erzurum, Turkey
Phone: +905337254072
E-mail: ertekozmen@gmail.com
ORCID:http://orcid.org/0000-0002-1973-6101

Letter to the Editor

Coronavirus is a single-stranded large RNA virus that infects humans (1). According to the World Health Organization (WHO), the cause of SARS-CoV-2 is called disease COVID-19. Similar to SARS-CoV, SARS-Cov-2 mainly attacks the respiratory system. Symptomatic conditions indicate clinical symptoms of the disease, symptoms of fever, cough, fatigue and other respiratory infections (2). Although the main clinical findings of COVID-19 are associated with lung injury, which is the main cause of mortality, findings related to the involvement of other organs such as cardiac and liver have also been reported (3).

No evidence of isolated acute liver failure has been observed in COVID-19 patients, but there are articles on autopsy cases on histopathological data of liver damage during the disease. Zhang Y and colleagues from Wuhan University Zhongnan Hospital reported that they did not determine a definite change in the macroscopic appearance of the liver in the autopsy results of COVID-19 related deaths (1). In histopathological analysis, they stated that there was mild sinusoidal dilatation and minimal lymphocytic infiltration and no other special damage was observed (1).

Li Y et al. also found that mild sinusoidal lymphocytic infiltration and sinusoidal dilatation were the main pathological findings in histopathological examination of the liver. There were also mild steatosis and multifocal hepatic necrosis in some patients. In addition, hyperinflammatory reactions were associated with COVID-19 and COVID-19 may contribute to liver damage in pre-existing chronic liver disease (4).

In addition to other studies, Xu Z et al. reported that portal inflammation was not prominent .They observed mild lobular and portal activity, moderate microvesicular steatosis (5). Tian S et al. also observed hepatic necrosis foci in the liver zone 1 and zone 3 areas. They reported that they did not find out any serious inflammatory cell infiltration, cytoplasmic balloon degeneration, mallory hyaline or fibrosis. They emphasized that the current findings were consistent with the pattern of acute liver injury, and no more serious histological changes such as coagulative necrosis and severe cholestasis occured (6). Yao et al. reported that they rarely observed canalicular cholestasis (7).

Chai X et al. stated that angiotensin converting enzyme 2 (ACE2), which is the default receptor for SARS-CoV-2, is expressed more intensely in bile duct epithelial cells, can be directly attached to these cells except hepatocytes. For this reason, they thought that the liver abnormalities of the patients might be caused by cholangiocyte dysfunction, not hepatocyte damage (8). They emphasized that sinusoidal dilatation was due to cardiogenic venous outflow slowing, however, other histological described findings were probably related to the patient's primary disease, namely COVID-19. Drugs used in the treatment of COVID-19 (hydroxychloroquine and azithromycin) can also cause liver injury.

Cite this article as: Özmen S, Ceylan O. The Effect of Coronavirus on the Liver and Histopathological Findings, *New Trend Med Sci* **2020**;1 (1): 51-52.

These drugs have been shown to cause various degrees of hepatotoxicity. Also, the hypoxic condition commonly associated with COVID-19 pneumonia may make hepatocytes more susceptible to toxic injuries (6). Decreased perfusion to the liver due to heart failure in these patients may also exacerbate this process (4). These studies in the literature show that during the clinical course of COVID-19, cell injury due to direct viral origin and potential hepatotoxicity caused by therapeutic drugs occur. Especially in patients with serious or critical disease, liver damage has been observed to be significant. The underlying mechanisms of hepatic injury can be multifactorial and may vary individually. There are many factors related to this condition, including direct viral attack, hepatotoxicity of therapeutic drugs, hyper-inflammatory reactions, pre-existing chronic liver disease and hypoxemic state (4). As a result, in patients with COVID-19, mild increase in sinusoidal lymphocytic infiltration, sinusoidal dilatation, mild steatosis and multifocal hepatic necrosis are the main histopathological abnormalities. Liver failure is not a prominent feature of the disease (9). Therefore, biopsy in this process is not recommended as it may cause greater harm than possible benefit.

References

1. Zhang Y, Zheng L, Liu L, Zhao M, Xiao J, Zhao Q. Liver impairment in COVID-19 patients: A retrospective analysis of 115 cases from a single centre in Wuhan city, China. *Liver International* **2020**.
2. Chen N, Zhou M, Dong X, Qu J, Gong F, Han Y, et al. Epidemiological and clinical characteristics of 99 cases of 2019 novel coronavirus pneumonia in Wuhan, China: a descriptive study. *Lancet* **2020**; 395(10223): 507-513.
3. Zhu N, Zhang D, Wang W, Li X, Yang B, Song J, et al. A novel coronavirus from patients with pneumonia in China, 2019. *New Engl J Med* **2020**.
4. Li Y, Xiao SY. Hepatic involvement in COVID-19 patients: pathology, pathogenesis and clinical implications. *J Medical Virol* **2020**.
5. Xu Z, Shi L, Wang Y, Zhang J, Huang L, Zhang C, et al. Pathological findings of COVID-19 associated with acute respiratory distress syndrome. *Lancet Resp Med* **2020**; 8(4): 420-422.
6. Tian S, Xiong Y, Liu H, Niu L, Guo J, Liao M, et al. Pathological study of the 2019 novel coronavirus disease (COVID-19) through postmortem core biopsies. *Modern Pathol* **2020**: 1-8.
7. Yao X, Li T, He Z, Ping Y, Liu H, et al. A pathological report of three COVID-19 cases by minimally invasive autopsies. Zhonghua bing li xue za zhi= *Chi J Pathol* 2020; 49: 009
8. Chai X, Hu L, Zhang Y, Han W, Lu Z, Ke A, et al. Specific ACE2 expression in cholangiocytes may cause liver damage after 2019-nCoV infection. *BioRxiv* **2020**.
9. Humar A, McGilvray I, Phillips MJ, Levy GA. Severe acute respiratory syndrome and the liver. *Hepatol (Baltimore, Md)* **2004**; 39(2): 291.

Authors' ORCID
Sevilay Özmen
http://orcid.org/0000-0002-1973-6101
Onur Ceylan
https://orcid.org/0000-0001-7025-0521

https://dergipark.org.tr/tr/pub/ntms